The Berriasian–Valanginian boundary in the Mediterranean Province of the Tethyan Realm: Ammonite and calcareous nannofossil biostratigraphy of the Vergol section (Montbrun-les-Bains, SE France), candidate for the Valanginian GSSP

Samer Kenjo, Stéphane Reboulet, Emanuela Mattioli, Kayed Ma'Louleh

Green text = corrections related to the comments made by Dr. Ottilia Szives (1st reviewer).

Blue text = corrections related to the comments by Miguel Company (2nd reviewer); he contacted us to say that "he forgot to sign his report".

Red text = other corrections.

The Berriasian–Valanginian boundary in the Mediterranean Province of the Tethyan Realm: ammonite and calcareous nannofossil biostratigraphy of the Vergol section (Montbrun-les-Bains, SE France), candidate for the Valanginian GSSP

Samer Kenjo[1], Stéphane Reboulet[2], Emanuela Mattioli[2,3], Kayed Ma'louleh[1]

[1] Laboratory of Geology, department of Geology, Faculty of Sciences, Damascus University, Syria

[2] Univ Lyon, Univ Lyon 1, ENSL, CNRS, LGL-TPE, F-69622, Villeurbanne, France

[3] Instituit Universitaire de France (IUF)

Corresponding author

E-mail address: stephane.reboulet@univ-lyon1.fr (S. Reboulet)

Abstract

The Vergol locality (Montbrun-les-Bains, South-East France), a candidate section for the Valanginian GSSP (Global Stratotype Section and Point), was studied in detail for ammonites and calcareous nannofossils. A bed-by-bed sampling and a quantitative approach were carried out on this expanded succession presenting a continuous record of calcareous-marl

alternations covering the uppermost Berriasian and lowermost Valanginian. The ammonite distribution observed allows a precise characterization of the Berriasian–Valanginian boundary with the recognition of the *Tirnovella alpillensis* (latest zone of the Berriasian) and "*Thurmanniceras*" *pertransiens* (earliest zone of the Valanginian) standard zones. The base of the Valanginian is here defined by the First Appearance Datum of "*T.*" *pertransiens*; this boundary can be well-characterized by ammonite assemblages and by using various calcareous nannofossil bioevents, like the First Occurrence of *Calcicalathina oblongata*. A tidy comparison with previous works on the Vergol section is made in order to integrate data on calpionellids. A discussion on the choice of the primary marker (ammonites *versus* calpionellids) for the Valanginian GSSP is proposed.

Keywords

Ammonite, Calcareous nannofossil, Biostratigraphy, Valanginian, GSSP, France

1. Introduction

Since five decades (Cretaceous Symposium, Lyon 1963, Barbier and Thieuloy, 1965a,b; Busnardo and Le Hégarat, 1965), vigorous discussions on the definition of the Berriasian–Valanginian boundary have taken place in the different groups of the IUGS Subcommission on Cretaceous Stratigraphy (Birkelund et al., 1984; Bulot et al., 1996). For the Mediterranean Province of the Mediterranean–Caucasian Subrealm (Tethyan Realm), many biostratigraphic studies were achieved for the interval around the boundary in South–East France and South–East Spain in order to establish a zonation based on ammonites (Le Hégarat, 1973; Allemann et al., 1975; Busnardo and Thieuloy, 1979; Hoedemaeker, 1981; 1982; 1983; Company and Tavera, 1982; Tavera, 1985; Company, 1987). Due to some differences in taxonomic concepts (i.e., misidentifications of some species) and biostratigraphic methodologies (i.e.,

heterogeneous zonations and problems with their reproductibility), it was difficult to reach a consensus on the basis of previous works. Thus the establishement of an ammonite standard zonation is needed; this was already the aim of the Lower Cretaceous Cephalopod Team (LCCT; Hoedemaeker et al., 1990). Concerning the base of the Valanginian, the LCCT correlated it with the base of the "*Thurmanniceras" otopeta* Ammonite Zone (AZ; see Appendix A), as proposed by Busnardo and Thieuloy (1979), as also recommended by Birkelund et al. (1984); in the zonal scheme of Le Hégarat (1973), such a solution corresponds (approximatively) to the base of "*Thurmanniceras" pertransiens* Ammonite Subzone of the author (ASZ; his *Kilianella roubaudiana* AZ) as its lower part includes the interval corresponding to the *"T." otopeta* AZ *sensu* Busnardo and Thieuloy (1979). The LCCT (Hoedemaeker et al., 1990; 1993) rejected the suggestion of Hoedemaeker (1982) who defined the base of Valanginian with the base of his *Tirnovella alpillensis* ASZ that roughly corresponds to the *Berriasella calisto* ASZ of Le Hégarat (1973).

In order to define effective chronostratigraphic subdivisions based upon biostratigraphy, the main trend was to develop a homogeneous Valanginian ammonite zonation based on the recognition of successive faunal turnovers and by using interval zones of index-species, defined by the First Appearance Datums (FAD), and characterized by their association (for SE France see: Reboulet et al., 1992; Bulot et al., 1993a, b; Bulot, 1995; Bulot and Thieuloy, 1995; Reboulet, 1996; Reboulet and Atrops, 1999). According to this approach, Bulot and Thieuloy (1993) and Bulot et al. (1993a, b) preferred to place the base of the Valanginian at the base of the "*T." pertransiens* AZ. This horizon corresponds (approximatively) to the historical definition of the Berriasian–Valanginian boundary *sensu* Kilian (1910; base of his *Holplites* (*K.) roubaudiana* AZ) and Mazenot (1939; base of his *Neocomites neocomiensis* AZ; for complete correlation between different zonal schemes established for over a century, see tables 2 and 3 in Busnardo and Thieuloy, 1979; tables 2 and 5 in Bulot, 1995; fig. 2 in

Aguado et al., 2000). This position of the boundary was adopted by the IUGS Lower Cretaceous Ammonites Working Group (the Kilian Group) and the *"T." otopeta* AZ was downgraded to the rank of a subzone of the *Fauriella boissieri* AZ (Hoedemaeker et al., 2003); this scheme was maintained in the successive meetings of the group (Reboulet et al., 2006; 2009; 2011; 2014). Based on the PhD thesis of Kenjo (2014), the Kilian Group agreed to change the standard zonation around the boundary as follows: for the uppermost Berriasian the *T. alpillensis* AZ, subdivided in *T. alpillensis* and "*T.*" *otopeta* ASZ, and for the lowermost Valanginian, the "*T.*" *pertransiens* AZ with the *Neocomites premolicus* ASZ (Reboulet et al., 2018).

Two candidates sections have been proposed for the Valanginian GSSP, namely Vergol (Montbrun-les-Bains, SE France; Blanc et al., 1994) and Barranco de Cañada Luenga (Cehegin, Caravaca, SE Spain; Aguado et al., 2000). As classical sections of the Vocontian basin (for example Berrias, Ardèche; Angles, Alpes-de-Haute-Provence; Barret-le-Bas, Hautes-Alpes; see Le Hégarat, 1973 and Busnardo and Thieuloy, 1979) are characterized by reworked sediments or hiatus or paucity in ammonites for the uppermost Berriasian–lowermost Valanginian interval, Blanc et al. (1994) selected the well-developed succession of Montbrun-les-Bains (see also Blanc, 1996). These authors mainly described the calpionellid succession; data on ammonites are less abundant and their distribution is discontinuous. However, as they observed that the First Occurrences (FOs) ~~FADs~~ of *Calpionellites darderi* and "*T.*" *pertransiens* are almost synchronous, they confirmed the suggestion of Bulot and Thieuloy (1993) and Bulot et al. (1993a, b) to define the base of the Valanginian Stage using an ammonite as primary marker, namely the FAD of "*T.*" *pertransiens*. Aguado et al. (2000) established an integrated stratigraphy for SE Spain (Caravaca–Cehegin region) by using ammonites, calpionellids and calcareous nannofossils; their biostratigraphy was plotted against the magnetic scale. These latter authors defined the Berriasian–Valanginian boundary

101 on the basis of the FAD of *C. darderi* following the provisional recommendation of the
102 Valanginian Working Group to use calpionellids as primary marker (base of the
103 *Calpionellites* zone E, Bulot et al., 1996).
104 Calcareous nannofossils have been also used for characterizing the Berriasian–Valanginian
105 boundary (Thierstein, 1971; Manivit, 1979; Perch-Nielsen, 1979; Bralower et al., 1989;
106 Mutterlose, 1992; Bown, 1998; 2005; Aguado et al., 2000). This boundary is characterized by
107 several bioevents of calcareous nannofossils, like the ~~First Occurrences~~ FO of *Calcicalathina*
108 *oblongata*, which identifies the base of *C. oblongata* Nannofossil Zone (NZ) in the lower
109 Valanginian, and *Tubodiscus jurapelagicus, Tubodiscus verenae*, *Eiffellithus windii*
110 (Bralower et al., 1989; Bown, 1998). However, changes in nannofossil assemblages allowing
111 characterization of the Berriasian–Valanginian boundary have been comparatively less
112 studied.
113 The aims of our work is (1) to establish an integrated biostratigraphic scheme between
114 ammonites and calcareous nannofossils, useful for large-scale correlations; and to (2) discuss
115 the choice of the primary marker (ammonites *versus* calpionellids). The newly established
116 bio- and chrono-stratigraphic scheme should enable us to discuss the Berriasian–Valanginian
117 boundary at Vergol within the framework of a new GSSP.
118

119 **2. Geological setting of the Vergol section**

120 The Vergol section was palaeogeographically located in the central part of the epicontinental
121 Vocontian basin (South-East France), at a palaeolatitude of approximately 30°N (Savostin et
122 al., 1986; Fig. 1A). This basin was surrounded by carbonate platforms (Cotillon et al., 1980;
123 Gréselle and Pittet, 2010), such as the Jura platform to the North, and the Provence platform
124 to the South (Fig. 1B). The Vocontian basin belonged to the European Tethyan passive
125 margin and it was infilled by a sequence of sediments which were deposited in a hemipelagic

environment (Gréselle et al., 2011; Martinez et al., 2013). The Vergol section is composed of marl-limestone alternations that represent the typical sedimentary pattern of Mesozoic series in the Vocontian basin. As shown by Cotillon et al (1980), the Valanginian alternations are remarkably continuous within this basin; they are stacked in bundles becoming more calcareous stratigraphically upwards and can be correlated over a large area. Recently, the Vergol site was used by Reboulet et al. (2003), Gréselle et al. (2011) and Martinez et al. (2013) as a case study for the formation of marl-limestone alternations.

At Vergol (44°12'10''N; 5°25'06''E), three successive sites of observations were selected to provide a continuous log from the upper Berriasian (*T. alpillensis* AZ) to the middle part of the lower Valanginian ("*T.*" *pertransiens* AZ and *N. neocomiensiformis* AZ *p.p.*). Two long outcrops are located along the road D159 where the lithologic succession is easily and continuously followed. A third intermediate outcrop occurs laterally, along the small creek orthogonal at the road. Thus, a very careful observation and lateral correlation allowed us to complete the stratigraphic gap (a few meters in thickness) reported by Blanc (1996, fig. 62) in the upper Berriasian. The studied interval of the Vergol section consists of a succession of 87 meters (53 m from the bed VGL-B95 until the base of the slump and 34 m from the base of the slump until the bed VGL-V69; Fig. 1C). Small cycles formed of 4 to 6 calcareous beds can be recognized. The base of the studied interval (upper Berriasian) is characterized by thick limestone beds (as VGL-B100 and VGL-B101) alternating with thin marly beds. Limestone beds become thinner stratigraphically upwards while marl interbeds are thicker. The uppermost Berriasian is characterized by a limestone-dominated interval of 12 calcareous beds (calcareous bundle VGL-B118 to VGL-B129) named the "Otopeta bundle" that is located just below the Berriasian–Valanginian boundary (*sensu* Kenjo 2014, this work). Around this boundary and in the lowermost Valanginian, the limestone beds tend to be thinner while marlstones are thicker, even if the marly interbeds remain generally thinner than

limestones. From bed VGL-V30 until the slump (VGL-V44), marly interbeds become generally thicker than limestones. Above the slump, marly interbeds are still generally thicker than limestones, except for beds VGL-V63 and 64. In the middle part of layer VGL-V48, marlstones are finely laminated with pyritous ammonites and nodules. The beds VGL-V61-62 are characterized by numerous bivalves (lumachelles); similar observations were made in the beds LPD-64-65 of the Les Prades section (Drôme; Reboulet, 1996) providing two characteristic layers for correlations between these two sections. Above the bed VGL-V69, litho-biostratigraphic data of the lower Valanginian and the lower part of the upper Valanginian have been published by Reboulet (1996), Reboulet et al. (2003) and Reboulet and Rard (2008). **-Fig. 1, here-**

3. Materials and Methods

3.1. Macrofauna

The selected interval of the Vergol section was studied for its content of pelagic and benthic macrofauna. 1623 specimens of ammonites were sampled. 113 aptychus, 7 rhyncholites, 35 belemnites, 227 bivalves, 15 gastropods, 3 brachiopods and 4 echinoids have been also found. Around one hour and one half was spent for the extraction of the macrofauna from every limestone bed of the Vergol section (122 beds). Concerning ammonites, only the preserved specimens for which the identification was possible (see Appendix A) were transferred to the laboratory where extraction was completed using a vibratory device, and determination effectuated (using the palaeontological worksheet). The specimens doubtfully identified are indicated by a question mark. When the identification was impossible, the ammonites were counted as undetermined species (420 specimens). Dissolution of shells is usual ~~the norm~~ and ammonites are preserved as internal calcareous moulds. Their fragmentation is relatively frequent and compaction is important, particularly for the phragmocones. Consequently, some

176 characteristics, such the whorl section and the strength of ribs and tubercules, and how they
177 change between the inner and outer whorls, cannot be correctly observed and compared for a
178 part of the material. The specimens are stored in the "Collections de géologie" of the
179 "Université Claude Bernard" (Lyon, France; collection of Kenjo and Reboulet).
180
181 **3.2. Calcareous nannofossils**
182 Eighty-two samples have been studied for calcareous nannofossils contents in the Vergol
183 section. Samples were systematically taken from adjacent marl-limestone couplets. Sample
184 spacing was quite large (every one meter) at the base of the section and much closer around
185 the Berriasian–Valanginian boundary (bed by bed). The method used for the preparation of
186 slides (Random Setting Technique) was first described by Beaufort (1991) and modified by
187 Geisen et al. (1999). This method is used to calculate the absolute abundance of nannofossils
188 (specimens per gram of rock). These slides were observed in optical microscope by using
189 immersion oil and polarized light with a magnification 1000X. Samples and calcareous
190 nannofossil slides are labelled with a FSL number and curated at the "Collections de
191 géologie" of the "Université Claude Bernard" (Lyon, France; collection of Kenjo, Mattioli
192 and Reboulet).
193 The absolute abundance and composition of the assemblage were studied through the
194 determination of nannofossils species. In each slide, 500 nannofossils were counted in a
195 variable number of fields of view. Such count provides us with a probability of 0.5-1% not to
196 record species as rare as representing 1% of the assemblage (Hay, 1972). Each sample was
197 then re-analyzed thoroughly in order to detect rare species potentially useful for
198 biostratigraphical purposes.
199 We calculate the absolute abundance using the following equation:
200 $X = (N * V) / (M * A * F * H);$

X: Number of nannofossils per gram of rock;

N: Total number of specimens counted;

V: Volume of water used (475 ml);

M: Mass of powder used;

F: Number of fields of view observed under the microscope;

A: Surface of a field of view ($3.14 * 10^{-4}$ cm^2);

H: height of the water column above the slide in the settling box (2.1 cm).

Principal Component Analysis (PCA) was used to treat nannofossil assemblages in order to interpret this complex data set and reduce the large data matrix, which is composed of several variables (78 taxa were recorded in 82 samples, see Appendix B) into a small number of factors representing the main modes of variations (Beaufort and Heussner, 2001). PCA was computed with the PAST software 3.01. Because of the presence of dominant taxa (e.g., *W. barnesiae*) and in order to reduce the impact of the closed-sum effect, the relative abundance was transformed in log using PAST before running the PCA. Some clusters were created by grouping the species belonging to the same genus and having significant correlations. Thus, all the species of the genus *Rhagodiscus* except *R. asper*, all the small *Zeugrhabdotus*, the *Biscutum*, the pentaliths, the *Cretarhabdus* plus *Retecapsa*, were lumped for PCA. The *Nannoconus* species were all grouped for the analysis. The matrix in our study consists of the relative abundances of 22 taxa representing more than 90% of the total counted nannofossils. The rare and discontinuously recorded taxa (i.e., less than 2% on average) were not integrated in the analysis.

As the values obtained for the various parameters are largely fluctuating according to the lithology, a LOESS smoothing with a 0.2 factor and a 9999 bootstrap was applied to the loading factor values, to absolute abundance data and to the Shannon diversity index by using

PAST. Such a smoothing allows a better appreciation of changes through time of different parameters.

4. Results

4.1. Ammonites

4.1.1. Systematic remarks

The ammonite fauna of the studied section (Fig. 2A, B) consists of twenty (sub-)genera grouped into seven families, using the supra-classification proposed by Klein (2005) and Klein et al. (2007, 2009; Appendix A). The systematic revision of all species was made during the PhD thesis of one of us (S. Kenjo, 2014). Here, only palaeontological comments are proposed for some taxa and quantitative data are also given. Further information on stratigraphy and taxonomy is available in the papers of Le Hégarat (1973), Company (1987), Reboulet et al. (1992), Bulot et al. (1993b), Bulot (1995), Reboulet (1996), Reboulet and Atrops (1999), Joly (2000), Busnardo et al. (2003), Busnardo (*in* Gauthier et al., 2006), Wippich (2001; 2003), Ettachfini (2004), and Company and Tavera (2015). -**Figs. 2A,2B, approximatively here (in the paper, it would be preferable that they are facing each other)-**

Neocomitids are represented by eight genera in the Vergol section. The species *B. calisto* (Fig. 3A), *Berriasella picteti* and *F. boissieri* (Fig. 3B) are overall rare. In agreement with Company's comments (personal communication, 2014), Kenjo (2014) discussed the possibility of a dimorphism between *B. calisto* (microconch) and *F. boissieri* (macroconch). If this dimorphism holds true, *F. boissieri* should be considered as a junior synonymy of *B. calisto*. The similarity between these two taxa was already suggested by Mazenot (1939; p. 108). The Berriasian interval is also well characterized by the occurrences of *T. alpillensis* (Fig. 3C-D), *Erdenella paquieri* (Fig. 3E), and *"T." otopeta* (Fig. 4A-B) that is relatively

abundant in beds VGL-B127-B128-B129 (Fig. 2A). -**Fig. 3, approximatively here-** The genus *"Thurmanniceras"* also occurs in the lower Valanginian with *"T." pertransiens* (Fig. 4C-H) and *"Thurmanniceras" gratianopolitense* (Fig. 4I) that are recorded as common and rare, respectively. The generic name *"Thurmanniceras"* is cited with inverted commas to indicate that the assignment of the species to that genus is provisional and they await revision (Kenjo, 2014; Reboulet et al., 2014; Company and Tavera, 2015). The taxonomy of *"T." gratianopolitense* is well discussed in Kenjo (2014), who acknowledged the point of view of Aguado et al. (2000). These latter authors support that *"Fauriella" kiliani* should be put in synonymy with *"T." gratianopolitense* because, in the neritic facies of the western High Atlas (Morocco), there are large specimens that very closely resemble to the type of *"T." gratianopolitense*; their juvenile stages are comparable to the small specimens characteristic of the Mediterranean (hemi-)pelagic facies for which Bulot (1995) created the species *"F." kiliani* (*nomen nudum*). Large specimens identified as *"T." gratianopolitense* have also been found by one of us in some neritic sections of western High Atlas (Morocco; S. Reboulet, work in progress). The good preservation of these Moroccan specimens allowed us to observe changes in the ornamentation: ribs are generally grouped in pairs at the umbilicus in the juvenile stage, while they are isolated in the adult stage. According to these observations, large Moroccan specimens identified as *"Thurmanniceras" thurmanni* by Wippich (2001; pl. 19, fig. 1; pl. 20, fig. 1) could correspond to *"T." gratianopolitense*, which is attributed to the genus *"Thurmanniceras"* and not to the genus *Fauriella* as suggested by Bulot (1995) and Klein (2005). -**Fig. 4, approximatively here-** The lower Valanginian assemblage (Fig. 2A, B) is also characterized by the occurrences of *N. premolicus* ~~(Fig. 5A)~~ and *Neocomites neocomiensiformis* (Fig. 5A,B) ~~found below and above the slumped interval, respectively (Fig. 2A, B)~~. Other neocomitids are represented by *Kilianella* (one *K. lucensis* Fig. 5C and

mainly *K. roubaudiana* Fig. 5D), and few specimens of *Luppovella* (*L. superba,* Fig. 5E) and *Sarasinella* (*S. ambigua* and *S. eucyrta* Fig. 5F). -**Fig. 5, approximatively here-**

Olcostephanids are mainly represented by *Olcostephanus* that is generally rare in the studied section but slightly more abundant in its uppermost part (Fig. 2A, B). Due to their poor preservation, as indicated by Bulot (1990) for lower Valanginian specimens of SE France, the identification at the specific level was very often impossible; only few specimens of *Olcostephanus* aff. *tenuituberculatus* (Fig. 6A) and *Olcostephanus josephinus* have been recognized in bed VGL-V62. One specimen has been identified as *Spiticeras multiforme* (bed VGL-B112; Fig. 6B).

Haploceratids, with *Neolissoceras*, are relatively common. Three species have been identified: *Neolissoceras grasianum*, *Neolissoceras* (*Vergoliceras*) *extracornutum* (Fig. 6C and *Neolissoceras* (*Vergoliceras*) *salinarium* (Fig. 6D). According to Reboulet et al. (2003) and Kenjo (2014), even if *Vergoliceras* is well characterized by a ventral keel, this taxon is here considered as a subgenus of *Neolissoceras*, and not as a separate genus as suggested by Klein et al. (2009).

Lytoceratids are rare to common. This family is represented by *Lytoceras honnoratianum* (Fig. 6E), that seems restricted to the Berriasian interval of the Vergol section, and *Lytoceras quadrisulcatum* (Fig. 6F).

Phylloceratids are common to frequent. Three species have been recognized: *Holcophylloceras silesiacum* (Fig. 6G), *Ptychophylloceras* (*Semisulcatoceras*) *semisulcatum* (Fig. 6H) and *Phylloceras* (*Hypophylloceras*) *tethys* (Fig. 6I).

Heteromorphs are represented by Bochianitids, with *Bochianites neocomiensis* (Fig. 6J) that is rare, and Protancyloceratids, with *Leptoceras* and *Protancyloceras* (Fig. 6K) that are very rare and poorly preserved. -**Fig. 6, approximatively here-**

4.1.2. Biostratigraphic implications

The analysis of the stratigraphic distribution of the species done by Kenjo (PhD thesis, 2014) allowed us to establish a new ammonite zonation of the Vergol section. This zonal scheme was presented by one of us (S. Reboulet) to the Kilian Group at the 2017 Vienna meeting (Reboulet et al., 2018). In order to follow the standard ammonite zonation built for the Mediterranean Province, only ammonite zones and subzones (respectively AZ and ASZ) adopted by the Kilian Group are presented here for the Vergol section. Thus, from bottom to top of the studied interval, the (sub-)zones are: the *T. alpillensis* AZ (latest zone of the Berriasian; with the *T. alpillensis* and "*T.*" *otopeta* ASZs), "*T.*" *pertransiens* AZ (earliest zone of the Valanginian; with the *N. premolicus* ASZ), and the *N. neocomiensiformis* AZ. In this work, ammonite zones are interval zones and they are defined by the interval between the FAD of two successive ammonite-indices (Hedberg, 1976). As it was proposed by Reboulet and Atrops (1999), who modified the zonal scheme for the uppermost lower Valanginian–lower Hauterivian to correlate more precisely biostratigraphic subdivisions with ammonite evolution, the boundaries of the interval zones of the uppermost Berriasian–lower Valanginian correspond to major changes in the ammonite fauna (Kenjo, 2014; Company and Tavera, 2015) allowing a better faunal characterization of the zones.

The *T. alpillensis* Ammonite Zone, and the *T. alpillensis* and *"T." otopeta* Ammonite Subzones

The *T. alpillensis* AZ used here is defined by the FAD of *T. alpillensis*, as proposed by Bulot et al. (1993a, b; see also Bulot, 1995) for the *T. alpillensis* ASZ. According to this definition, the *T. alpillensis* AZ replaces the upper part of the *Fauriella boissieri* AZ of Le Hégarat (1973). Consequently, the former late Berriasian *F. boissieri* AZ (composed of the *Malbosiceras paramimounum*, *B. picteti*, *T. alpillensis* and "*T.*" *otopeta* ASZs; Hoedemaeker

et al., 1993, 2003) has been modified and restricted to its lower part that corresponds now to the *F. boissieri* AZ *sensu* Kenjo (2014) with *M. paramimounum* and *B. picteti* ASZs *sensu* Le Hégarat (1973). Kenjo (2014, p. 103–106) provided a detailed discussion about the *F. boissieri* AZ and the choice of a new index-species for this interval.

The *T. alpillensis* ASZ is risen to the rank of zone for the following reasons: (1) the *T. alpillensis* ASZ, introduced by Hoedemaeker (1982), was already used in the standard zonation and adopted as an acme zone during the 1992 Mula meeting (Hoedemaeker et al., 1993); it corresponds to the "un-named association" evoked during the 1990 Digne meeting (Hoedemaeker et al., 1990); (2) *T. alpillensis* is easy to identify and has been well-described by Le Hégarat (1973), Tavera Benítez (1985), Company (1987), Bulot (1995), Kenjo (2014); (3) specimens of *T. alpillensis* are found in almost all the corresponding zone and it is abundant as reported by Company (1987), Aguado et al. (2000), and Kenjo (2014). According to Bulot (1995), this species disappeared in the lowermost part of the "*T.*" *pertransiens* AZ; (4) *T. alpillensis* occurs both in proximal (platform) and distal (basin) palaeoenvironments (Bulot, 1995); (5) it is a quite ubiquitous species in the Mediterranean Province (Company, 1987; see the synonymy of *T. alpillensis* in Klein, 2005); (6) in the *T. alpillensis* AZ (mainly in the "*T.*" *otopeta* ASZ), there is a characteristic ammonite assemblage of latest Berriasian and earliest Valanginian taxa (Bulot et al., 1993a, b; Bulot, 1995), which is very different with respect to the assemblages of ammonite subzones in the interval below (approximately *M. paramimounum* and *B. picteti* ASZs); an ammonite faunal turnover occurs at the top of the *B. picteti* ASZ (Bulot et al., 1993a, b); (7) the base of *T. alpillensis* AZ roughly corresponds to the base of the D3 calpionellid Zone (Bulot et al., 1993a, b; Bulot, 1995).

In the Vergol section (Fig. 2A), the *T. alpillensis* AZ is characterized by many species that are quite characteristic of the upper Berriasian like *B. picteti, B. calisto, F. boissieri, E. paquieri, "T." otopeta*, *S. multiformе, L. honnoratianum* and *Leptoceras* sp. ind. Other taxa which cross

the Berriasian–Valanginian boundary are also found in the uppermost Berriasian, like *N. grasianum, L. quadrisulcatum, P. (H.) tethys, P. (S.) semisulcatum, H. silesiacum*, *Protancyloceras* sp. ind. and *B. neocomiensis.*

The *T. alpillensis* AZ is subdivided into a lower *T. alpillensis* ASZ and an upper "*T.*" *otopeta* ASZ (Kenjo, 2014). The earliest specimen of *T. alpillensis* has been found from the base of the studied interval (VGL-B96; Fig. 2A); as no sampling has been made below this layer, ~~this FO cannot be considered as the FAD of the index-species and thus~~ it cannot be excluded that the *T. alpillensis* ASZ/AZ is partly represented in the studied interval. Lithologic correlations show that the bed VGL-B96 should correspond to bed COUR-96 of the Courchons section (Saint-André-les-Alpes, Alpes-de-Haute-Provence; Kenjo, 2014). In this last section, the FO of *T. alpillensis* is observed around one meter below (bed COUR-92), but this specimen was identified with doubt. The base of the "*T.*" *otopeta* ASZ, introduced by Busnardo and Thieuloy (1979) as a zone, is defined by the FAD of *"T." otopeta*; its FO is recorded in the bed VGL-B116; the consistent record of this index-species begins in the bed VGL-B121. Even if the specimen of bed VGL-B116 is doubtful, the base of the *"T." otopeta* ASZ can be maintained at the base of this bed. Indeed, in the Courchons section (~~Saint-André-les-Alpes, Alpes-de-Haute-Provence;~~ Kenjo, 2014), the base of the *"T." otopeta* ASZ is placed at the base of bed COUR-122 that is correlated to the bed VGL-B117 (less one meter above the base of the bed VGL-B116). The index-species, which is recorded in almost the entire corresponding subzone, is very commonly recorded in SE France, mainly in basinal sections ~~whilst it is rare in SE Spain~~ (~~Company, 1987~~ Bulot, 1995).

The "*T.*" *pertransiens* Ammonte Zone, and the *N. premolicus* Ammonite Subzone

The "*T.*" *pertransiens* AZ was created by Le Hégarat and Remane (1968) as a subzone of the *"K. roubaudiana"* AZ; their "*T.*" *pertransiens* ASZ included the interval corresponding to the

374 "*T.*" *otopeta* ASZ. More recently, the "*T.*" *pertransiens* ASZ has been elevated to the rank of
375 zone and its base is defined by the FAD of "*T.*" *pertransiens* (Company, 1987; Blanc et al.,
376 1994; Bulot, 1995; Aguado et al., 2000; Kenjo, 2014). The FO of this species is recorded in
377 the bed VGL-B136 (Fig. 2A). The assemblage of the "*T.*" *pertransiens* AZ is characterized by
378 many species belonging to *Neocomites*, *Neolissoceras (Vergoliceras)*, *Kilianella* and
379 *Sarasinella*. Other taxa which cross the Berriasian–Valanginian boundary are also found in
380 the "*T.*" *pertransiens* AZ like *N. grasianum, L. quadrisulcatum, P. (H.) tethys, P. (S.)*
381 *semisulcatum, H. silesiacum* and *B. neocomiensis*. *"T." gratianopolitense* and
382 *Protancyloceras* sp. ind. are only recorded in the lowermost part of this zone where latest
383 specimens of *Berriasella* sp. ind. occur.
384 Kenjo (2014) proposed to subdivide the "*T.*" *pertransiens* AZ into two parts, namely the *N.*
385 *premolicus* and *N.* (*V.*) *salinarium* ASZs. Only the earliest subzone was accepted by the
386 Kilian Group (Reboulet et al., 2018). The *N.* (*V.*) *salinarium* ASZ was not adopted as there
387 are some discrepancies with the ~~FAD~~ FO of the index-species (see Ettachfini, 2004; Kenjo,
388 2014 *versus* Company and Tavera, 2015), thus for the moment the upper part of the "*T.*"
389 *pertransiens* AZ of the standard zonation is not characterised by any subzone. Consequently,
390 the Kilian Group agreed to consider provisionally the *N. premolicus* ASZ as a total range
391 subzone. It starts at the base of the "*T.*" *pertransiens* AZ in order that their bases coincide, and
392 ends at the last occurrence (LO) of *N. premolicus*. In the Vergol section, the FO of *N.*
393 *premolicus* is recorded in the bed VGL-B141, just five beds above the FO of "*T.*"
394 *pertransiens* (Fig. 2A; Kenjo, 2014). This author also acknowledged that *N. premolicus* first
395 occurs in the basal part of the "*T.*" *pertransiens* AZ in the Courchons section ~~(Saint-André-~~
396 ~~les-Alpes, Alpes-de-Haute-Provence)~~. According to Bulot and Thieuloy (1995) and Bulot
397 (1995), the FOs of *N. premolicus* and "*T.*" *pertransiens* are very close to each other in other
398 sections of the SE France basin. *N. premolicus* first occurs in SE Spain at the base of the "*T.*"

399 *pertransiens* AZ and is reported as abundant in its lower part (Company, 1987; Aguado et al.,
400 2000; Company and Tavera, 2015). The FO of *N. premolicus* was used by Ettachfini (2004) to
401 recognize the base of the Valanginian in the Atlas-Atlantic of Morocco, due the (quasi-)
402 absence of *"T." pertransiens* in this region. Reboulet (work in progress) also uses *N.*
403 *premolicus* to put the base of this stage in the studied Moroccan sections. *N. premolicus* is
404 easy to identify and relatively frequent in France (Kenjo, 2014), Spain (Company and Tavera,
405 2015) and Morocco (Ettachfini, 2004; Reboulet, work in progress); for a detailed
406 palaeobiogeographic distribution of this taxon, see Klein (2005, p. 309–310). Thus, the
407 introduction of the *N. premolicus* ASZ in the standard zonation allows a good characterisation
408 of the lowermost part of the Valanginian and the establishment of solid biostratigraphic
409 correlations between the sections of the northern and southern Mediterranean areas.
410
411 **The *N. neocomiensiformis* Ammonite Zone**
412 Company and Tavera (2015) proposed the *N. neocomiensiformis* AZ for the middle part of the
413 lower Valanginian. This proposal was accepted by the Kilian Group and introduced in the
414 standard zonation of the Lower Cretaceous (Reboulet et al., 2014). The base of this zone is
415 defined by the FAD of the species index. In the Vergol section, the FO of *N.*
416 *neocomiensiformis* is recorded in the bed VGL-V38 (Fig. 2B). This zone is characterized by
417 an assemblage of several taxa, like *K. roubaudiana*, *L. superba*, *O.* aff. *tenuituberculatus*, *N.*
418 *(V.) salinarium*, *N.* (*V.*) *extracornutum*, *L. quadrisulcatum*, *P.* (*H.*) *tethys*, *P.* (*S.*)
419 *semisulcatum*, and *B. neocomienis*. A single specimen of *O. josephinus* was recorded
420 (Fig.2B); according to Company and Tavera (2015), this species seems to be restricted to the
421 *N. neocomiensiformis* AZ. As observed by these authors for some Spanish sections, the basal
422 part of the range of *N. neocomiensiformis* can overlap the uppermost part of the range of "*T.*"
423 *pertransiens* in the Vergol section where both species co-occur in the bed VGL-V38.

Kenjo (2014) proposed to characterize the lower part of the *N. neocomiensiformis* AZ by the *L. superba* ASZ. However, this proposal was not validated by the Kilian Group as there are some discrepancies with the ~~FAD~~ FO of the index-species (see Bulot, 1995; Ettachfini, 2004; Kenjo, 2014 *versus* Company and Tavera, 2015).

4.2. Calcareous nannofossil distribution, events and zonation

In this work, taxonomy is based upon Bralower et al. (1989), Bown (1998), Aguado (1994) and Aguado et al. (2000). The zonation of calcareous nannofossils is based on interval zones, which are identified by the FO and LO of marker species (in the rest of manuscript: Nannofossil Zone = NZ; Nannofossil Subzone = NSZ). Although preservation is commonly poor to moderate with specimens severely overgrown (Figs. 7 and 8), many bioevents are recorded across the Berriasian–Valanginian boundary of the Vergol section (Fig. 9; Table 1).

-**Figs 7; 8; 9, approximatively here - Table 1 in supplementary data/material-**

The presence of *Retecapsa angustiforata* (previously considered as *Cretarhabdus angustiforatus*) is observed from the base of the section (bed VGL-B95). This record allows recognition of the *C. angustiforatus* NZ, NK-2 that is subdivided into two nannofossil subzones, namely *Assipetra infracretacea* NK-2A and *Percivalia fenestrata* NK-2B. The NK-2A/NK-2B boundary was originally draft by Bralower et al. (1989) within the *F. boisseri* AZ, *B. picteti* ASZ (Fig. 10). The top of *A. infracretacea* NSZ is placed in the bed VGL-B112M (M = Marlstones) because of the FO of *P. fenestrata*; in the same sample, ~~also first occurs~~ the FO of *Ethmorhabdus hauterivianus* is observed (Fig. 9). This subzone boundary is placed within the *T. alpillensis* ASZ of the present work. Our record is consistent with Aguado et al. (2000; Fig. 11). The species *Haqius circumradiatus* first occurs shortly afterwards, in the sample VGL-B113c M (Fig. 9). This event is however documented earlier by Bown (1998) in the basal part of the *F. boisseri* AZ (Fig. 10). It is possible that the discontinuous record of

449 this species accounts for the inconstistency of the event. Following this event, *Retecapsa*
450 *surirella* first occurs in the bed VGL-B117M (Fig. 9). *Tubodiscus frankiae* is recorded from
451 bed 134 M. This species, which is the earliest known of the genus, has been recently
452 introduced by Bown (2005) and attributed to the NK-2A NSZ. Our record ~~if confirmed by~~
453 ~~other studies, would~~ allows to place the onset of *Tubodiscus* genus in the "*T.*" *otopeta* ASZ of
454 the Vergol section. The species *Zeugrhabdotus trivectis* was found in the bed VGL-B136M at
455 the base of the *"T."pertransiens* AZ. This record is shortly earlier than previously reported
456 (uppermost part of the former *Busnardoites campylotoxus* AZ, early Valanginian by Bown,
457 1998, Fig. 10); uppermost part of *"T." pertransiens* AZ of the Angles section by Duchamp-
458 Alphonse et al., 2007; Fig. 11). The FO of *Staurolithites crux* is recorded at the base of *"T."*
459 *pertransiens* AZ, in the bed VGL-B143L (L = Limestone; Fig. 9). This species was already
460 reported in the upper part of ~~early~~ lower Valanginian of the Vergol section (Mattioli et al.,
461 2014), as well as in the "*T.*" *otopeta* ASZ Zone of the Cañada Lengua section (Subbetic area,
462 Spain; Aguado, 1994; considered as a zone in his work), and in a single Berriasian sample
463 from Crimea (Gradstein et al., 2019). Our record at the base of the Valanginian ~~is a very~~
464 confirms therefore a new datum; in fact this species was previously reported as occurring in
465 the upper Hauterivian by Bown (1998; p. 102). *Tubodiscus jurapelagicus* first occurs in the
466 bed 145M. This event was reported slightly earlier by Bralower et al. (1989; at the top of the
467 *B. calisto* ASZ; Fig. 10) and Aguado et al. (2000; *F. boissieri* AZ, *T. alpillensis* ASZ; Fig.
468 11). The FO of *Calcicalathina oblongata* is recorded in the bed VGL-B146M that
469 corresponds to the lowermost part of *"T." pertransiens* AZ (Fig. 9). This record is consistent
470 with previous biostratigraphic data; in fact Bown (1998) in its synthesis of Tethyan
471 nannofossil data report it at the base of the *"T." pertransiens* AZ and Bralower et al. (1989) at
472 the lowermost part of their *K. roubaudiana* AZ by means of indirect correlation of calcareous
473 nannofossil bio-horizons, magnetostratigraphy and ammonite zones (Fig. 10). Duchamp-

Alphonse et al. (2007) record consistently the FO of *C. oblongata* in the lowermost part of *"T." pertransiens* AZ of the Angles section (Fig. 11); it should be noted that the base of this zone is questionably identified at Angles (see Busnardo and Thieuloy, 1979). Conversely, Aguado et al. (2000) reported the FO of *C. oblongata* from the uppermost part of the *"T." pertransiens* AZ, but in their plates they showed ~~a~~ forms with a smaller average size and a thicker rim, *C. praeoblongata* occurring in the *F. boissieri* AZ, *T. alpillensis* ASZ. However, the pictures they illustrate of *C. praeoblongata* rather figure out a large *Rhagodiscus asper* (Erba, personal communication 2019). The FO of *C. oblongata* allows the identification of the top of the *C. angustiforatus* NZ. The *C. oblongata* NZ spans the entire *"T." pertransiens* AZ to the top of studied interval (Fig. 9). The FO of *Eiffellithus windii* is noticed in the bed VGL-B150 (basal part of *"T." pertransiens* AZ). This bioevent occurs later in other sections: in the middle part of *K. roubaudiana* AZ for Bralower et al. (1989), in the former *B. campylotoxus* AZ for Bown (1998) (Fig. 10), and in the *Olcostephanus stephanophorus* AZ (= current *N. neocomiensiformis* AZ) of the Angles section studied by Duchamp-Alphonse et al. (2007) (Fig. 11). The FO of *Tubodiscus verenae* is also recorded at Vergol in the *"T." pertransiens* AZ (VGL-V1b M; Fig. 9). This event was reported in the Angles section in the "alpillensis/callisto subzone" by Bergen (1994; cf. text-figure 2), but later Duchamp-Alphonse et al. (2007) do not show this event in the same section. Other discrepancies are observed in the ranking of nannofossil events when looking at these two papers reporting on the same section. The FO of T. verenae is reported by Aguado et al. (2000) in the *T. alpillensis* ASZ (Fig. 11). ~~but~~ Bralower et al. (1989) placed it ~~at~~ in an interval time-equivalent of the lowermost part of *K. roubaudiana* AZ (Fig. 10). These latter authors thoroughly discussed the ranking of the FOs of *T. jurapelagicus*, *T. verenae* and *C. oblongata*. They acknowledge the biostratigraphic value of these three events although their respective FOs is slightly controversial. This inconsistency might be also due to the presence of early specimens

(likely corresponding to *T. frankiae*) in some of their studied sites. The FO of *Micrantholithus speetonensis* is noticed in the bed VGL-V4M (*"T." pertransiens* AZ; Fig. 9). This species has a very short range, disappearing in the bed VLG-V31M within the *"T." pertransiens* AZ. A similar pattern is reported for the ~~Boreal Realm by Bown (1998)~~ north-western Europe by Crux (1989), where *M. speetonensis* is used to define a total range zone spanning the *Paratollia* spp. and *Polychtichites* spp. AZs of England (Fig. 10). According to the inter-regional correlation of zonal schemes for north-west Europe and south-east France proposed by Kemper et al. (1981), these two ammonite zones would cover the uppermost Berriasian (current "*T.*" *otopeta* ASZ) and nearly the whole lower Valanginian ("*T.*" *pertransiens* AZ and a large part of the former *B. campylotoxus* AZ of the Mediterranean area). More recently, the lower Valanginian of England has been subdivided into three ammonite zones: *Peregrinoceras albidum*, *Paratollia* spp. and *Polyptychites* spp. (Rawson, 2006). Gardin in Bulot et al. (1996) as well as Lakova et al. (1999) noticed this boreal, early Valanginian species within the late Berriasian of the Mediterranean region. However, Duchamp-Alphonse et al. (2007) reported sporadic occurrence of *M. speetonensis* in the "*T.*" *pertransiens* AZ of the Angles section. ~~The FO of~~ *Staurolithites mutterlosei* is recorded in the bed VGL-V31M (*"T." pertransiens* AZ; Fig. 9). ~~This record allows us~~ If this record corresponded to a real FO, it would allows us to precise the ~~FO~~ distribution of the species, which was previously reported from an ?early Valanginian age by Bown (1998; p. 102). The LO of *Rhagodiscus nebulosus* is recorded in the bed VGL-V36M. This species, which is reported to have a mid Berriasian–Valanginian range by Bralower et al. (1989) has been recorded very discontinuously in the Vergol section, but never observed from the interval above the *"T." pertransiens* AZ (Mattioli, personal observation). Aguado et al. (2000) report the last consistent record of *Percivalia nebulosa* (the basionym is *Rhagodiscus nebulosus*) in the upper part of *T. alpillensis* ASZ, but very sporadic occurrences are recorded in the *"T." otopeta* ASZ.

Duchamp-Alphonse et al. (2007) report *R. nebulosus* in the lowermost part of the *"T." otopeta* ASZ (Fig. 11). The LO of *Helenea quadrata* is in the sample VGL-V38M (Fig. 9). Although Bergen (1994) notice the LO of *Grantarhabdus quadratus* (synonym of *H. quadrata*) in the upper Hauterivian of Angles, and Bown (1998) report a Berriasian–Hauterivian range for this species, it has never been recorded later in the Valanginian of the Vergol section (Mattioli, personal observation). In the uppermost part of the studied section (VGL-V42M), two other distinctive *Zeugrhabdotus*, namely *Z. diplogrammus* and *Z. xenotus*, are recorded in the lower part of the *N. neocomiensiformis* AZ. These two taxa are consistent components of the nannofossil assemblages of the upper part of the Vergol section (upper part of lower Valanginian to upper Valanginian) studied by Mattioli et al. (2014). The record of *Z. diplogrammus* is quite consistent with the Angles section, where its FO is reported in the ~~early~~ lower part of the *O. stephanophorus* AZ (Duchamp-Alphonse et al., 2007; Fig. 11). *Z. diplogrammus* and *Z. xenotus* FOs are both reported by Bown (1998) in the former *B. campylotoxus* AZ (Fig. 10).

In synthesis, nineteen bioevents have been recorded (Fig. 11) in the studied interval of Vergol, mainly first occurrences. The majority of these bioevents occur around the Berriasian–Valanginian boundary ~~allowing its precise characterization~~. In spite of the fact that these events may have in some cases a local extent, they allow the boundary characterization at Vergol. -**Figs. 10 and 11, approximatively here-**

4.3. Abundances, species richness and principal component analysis of calcareous nannofossil assemblages

In order to check if calcareous nannofossil assemblages ~~did~~ significantly changed across the Berriasian–Valanginian boundary, a PCA using the PAST software 3.01 was applied and the Shannon diversity index was calculated (Fig. 12; Table 2). PCA factor 1 receives loading on

549 positive values by *Watznaueria fossacincta*, *Biscutum constans/ellipticum*, and
550 *Diazomatolithus lehmanii* and by *W. barnesiae* on negative values. PCA factor 2 shows
551 positive loadings of *Nannoconus* and pentaliths (*Micrantholithus hoschulzii* and *M. obtusus*).
552 PCA factor 3 has *B. constans/ellipticum*, *Rhagodiscus asper* and *D. lehmanii* on positive
553 loading and *W. britannica-W. fossacincta* on negative loading.
554 PCA factorial scores show significant trends (Fig. 13). A temporary decrease of factor 1
555 scores occurred at the Berriasian–Valanginian boundary. A significant decrease of PCA 1 is
556 observed later in the upper part of *"T." pertransiens* AZ. PCA factor 2 shows fluctuating
557 values across the studied interval but wihout any significant shift. For PCA factor 3, a net
558 decrease of values precisely starts at the Berriasian–Valanginian boundary. This trend mirrors
559 a parallel increase of absolute abundance values starting at the base of Valanginian. Absolute
560 abundances are largely fluctuating according to the lithologies: low abundances are recorded
561 in limestones and higher values in marlstones. In spite of this already known pattern
562 (Reboulet et al., 2003), a trend can be observed with lower values in the upper Berriasian
563 (0.01 to 0.45 * 10^9 specimens per gram of rock) and higher values being recorded starting
564 from the *"T." pertransiens* AZ (0.01 – 1.1 * 10^9 specimens per gram of rock). Shannon
565 diversity index displays a relevant decrease from 2.2 to 1.3 within the *T. alpillensis* ASZ,
566 followed by a return to values around 2.1 in the "*T." otopeta* ASZ. -**Figs. 12 and 13,**
567 **approximatively here- Table 2 in supplementary data/material-**
568
569 **5. Discussion**
570 **5.1. Characterization of the Berriasian–Valanginian boundary by an integrated**
571 **biostratigraphy of ammonites and calcareous nannofossils**
572 Blanc et al. (1994) used the integrated zonation of ammonites and calpionellids for the
573 characterization of the Berriasian–Valanginian boundary in the Vergol section. This boundary

574 has been identified by the authors at the base of the bed 210 that is marked by the FO of "*T.*"
575 *pertransiens* which is quasi-synchronical with respect to the FO of *C. darderi* recorded in the
576 bed 209. According to these authors, few meters below this bed, ammonite assemblage is
577 characterized by a Berriasian fauna (*F. boissieri* AZ, "*T.*" *otopeta* ASZ) in which occur some
578 taxa as *F.* gr. *boissieri*, *T. alpillensis,* "*T.*" *otopeta* and *E. paquieri.* However, taking into
579 account our new biostratigraphic data (FO of "*T.*" *pertransiens* in VGL-B136; Fig. 2A) and
580 the lithological correlations suggested in Figure 14 (bed 210 = bed VGL-V1b), the interval
581 considered by Blanc et al. (1994) as Berriasian should be dated as ~~lower~~ early Valanginian
582 ("*T.*" *pertransiens* AZ, *N. premolicus* ASZ, see faunal assemblage in Fig. 2A). Indeed, they
583 observed the ~~Last Occurrence~~ LO of "*T*". *otopeta* in their bed 206 that corresponds to bed
584 VGL-B150 of our new log. Conversely, in our work this event is recorded in bed VGL-B135
585 (Figs. 2; 14). Thus, the stratigraphic correlation with the work of Blanc et al. (1994) indicates
586 two different ammonite assemblages for the same interval in the Vergol section. This
587 discrepancy cannot be clairly explained, but a misidentification of some taxa cannot be
588 excluded. However, most of the ammonite species, such as *T. alpillensis*, "*T.*" *otopeta* or *E.*
589 *paquieri* are relatively easy to identify, thus the risk for a misidentification of all the species
590 of this assemblage is limited. As an alternative explanation, an error in the stratigraphic
591 correlations of the Vergol sections *sensu* Kenjo (2014; this work) and *sensu* Blanc et al.
592 (1994) might have occurred. However, a 6-metre offset in the bed-by-bed correlation from
593 VGL-B135 (= LO of "*T.*" *otopeta sensu* Kenjo, 2014 and this work) to bed 206 (= LO of "*T.*"
594 *otopeta sensu* Blanc et al., 1994) cannot be probably supported. A miscalculation in the
595 construction of the section *sensu* Blanc et al. (1994) could be also invoked as different points
596 of observation are needed in the field in order to establish a continuous succession. According
597 to our correlations (Fig. 14), the bed in which Blanc (1996) recorded the FO of "*T.*" *otopeta*
598 would be the equivalent of bed VGL-B135 that corresponds in our work to the end of the

range of this species. As the ammonite distribution is not precisely documented by Blanc et al. (1994) and Blanc (1996; where the FO of few species are only indicated), it is likely that they did not make a bed-by-bed sampling for macrofauna (but this does not explain the occurrence of *"T." otopeta* above bed VGL-B135 up to bed VGL-B150 observed by these authors). Moreover, the highest probability to find this species during its acme (VGL-B128-129; Figs. 2; 14) was not possible for these authors as their log of the Vergol section is not continuous (gap) around this event. -**Fig. 14, approximatively here-**

The analysis of calcareous nannofossils seems to confirm that the interval just below the bed 210 (= VGL-V1b), can be dated as ~~lower~~ early Valanginian (Kenjo, 2014, this work) and not as ~~upper~~ late Berriasian as proposed by Blanc et al. (1994). Indeed, the FO of *C. oblongata* is observed in the bed VGL-B146M (Figs. 7, 14) and its appearance is typical for the lower part of Valanginian. This species has systematically been recorded in the basal Valanginian (Thierstein, 1971; Sissingh, 1977; Perch-Nielsen, 1985; Bralower et al., 1989; Bown, 1998), even though Aguado et al. (2000) reported a *C. praeoblongata* from the upper Berriasian and *C. oblongata* from the upper part of the "*T.*" *pertransiens* AZ of SE Spain.

Few papers present a detailed comparison between ammonite and nannofossil biostratigraphy for the Berriasian–Valanginian boundary. A comparison is made here (Fig. 11) between the Vergol section and other sections located in the Vocontian basin (Angles, Duchamp-Alphonse et al., 2007) and in SE Spain (several localities, Aguado et al., 2000). The ammonite zonation used by Duchamp-Alphonse et al. (2007) comes from Bulot and Thieuloy (1995; it is noticeable that, in the Angles section, these latter authors only provide biostratigraphic data around the lower (*Karakaschiceras inostranzewi* AZ)–upper (*Saynoceras verrucosum* AZ) Valanginian boundary interval); this zonation presents some differences with respect to the one used in the present work. In ~~their paper~~ Duchamp-Alphonse et al. (2007), the uppermost Berriasian is characterized by the *T. alpillensis* and "*T.*" *otopeta* ASZ (*F. boissieri* AZ *p.p.*)

624 that have been recognized in our *T. alpillensis* AZ. Even if the *Kilianella thieuloyi* ASZ
625 ~~Ammonite Horizon (*sensu* Bulot and Thieuloy, 1995); presented as an Ammonite Subzone in~~
626 ~~the Angles section by Duchamp-Alphonse et al., 2007)~~ has not been recognized in the upper
627 part of the "*T.*" *otopeta* ASZ in the Vergol section, the conception of the base of this latter
628 ammonite subzone is not changed as it is an interval subzone defined by the ~~FO~~ FAD of the
629 index-species. Duchamp-Alphonse et al. (2007) placed the base of the Valanginian stage at
630 the base of the "*T.*" *pertransiens* AZ in the Angles section, using the same criteria as those
631 applied to the Vergol section (Kenjo, 2014; this work). The base of the *O. stephanophorus* AZ
632 (Bulot and Thieuloy, 1995) can be correlated with the base of the *N. neocomiensiformis* AZ
633 (see explanations in Reboulet et al., 2014). Aguado et al. (2000) also used the *T. alpillensis*
634 and "*T.*" *otopeta* ASZ (*F. boissieri* AZ *p.p.*) and the "*T.*" *pertransiens* AZ to establish the
635 zonal schemes in the sections they studied in Spain. These authors supported the proposal of
636 the 1995 Brussels meeting (Bulot et al., 1996) to define the base of the Valanginian Stage at
637 the FAD of *C. darderi*; they observed that the FO of this index-species practically coincides
638 with the FO of "*T.*" *pertransiens*. Consequently, the zonal schemes used by Aguado et al.
639 (2000) and Duchamp-Alphonse et al. (2007) can be easily correlated with the zonal scheme of
640 the Vergol section (Kenjo, 2014; this work). The distributions of species having a
641 biostratigraphic interest in the Vergol (Kenjo, 2014; this work) and Spanish (Aguado et al.,
642 2000) sections are very similar as far as the interval around the Berriasian–Valanginian
643 boundary is concerned. In both areas, the disappearances of "*T.*" *otopeta*, *F. boissieri*, *B.*
644 *callisto*, *E. paquieri*, *T. alpillensis* and *Leptoceras* occur in the "*T.*" *otopeta* ASZ (mainly in
645 its upper part); also the appearances of "*T.*" *pertransiens*, "*T.*" *gratianopolitense*, *N.*
646 *premolicus*, *K. roubaudiana* occur in the lowermost part of the "*T.*" *pertansiens* AZ.
647 Ammonite distribution is not shown for Angles by Bulot and Thieuloy (1995) and Duchamp-
648 Alphonse et al. (2007) for the interval around the Berriasian–Valanginian boundary.

649 Concerning the nannofossil zones, Duchamp-Alphonse et al. (2007) and Aguado et al. (2000)
650 used the Bralower et al. (1989) biostratigraphical scheme, which was also applied in the
651 present work. The uppermost Berriasian corresponds in the three papers to the *C.*
652 *angustiforatus* NZ. The lower boundary of *C. oblongata* NZ corresponds to the lower part of
653 the "*T.*" *pertransiens* AZ in Vergol (this work) and Angles sections (Duchamp-Alphone et al.,
654 2007), but *C. oblongata* is recorded later in the upper part of the "*T.*" *pertransiens* AZ in SE
655 Spain (Aguado et al., 2000). This difference is probably related to the introduction of a new
656 form (Aguado et al., 2000) morphologically similar to *C. oblongata* but with more primitive
657 characters; this new species has been named *C. praeoblongata*. Aguado et al. (2000) found *C.*
658 *praeoblongata* in the lower part of their *T. alpillensis* ASZ. The pictures of *C. praeoblongata*
659 shown by Aguado et al. (2000, fig. 8, pictures 28-33) look like overgrown specimens of *R.*
660 *asper* (Erba, personal communication 2019). Thus, the discrepant range of *C. oblongata* in SE
661 France and SE Spain could be related to different taxonomical concepts.
662 Some discrepancies have been observed between these three works. The FO of *T.*
663 *jurapelagicus* has been placed in the upper Berriasian (*T. alpillensis* ASZ, *A. infracretacea*
664 NSZ) in SE Spain, but in Vergol this species appears just below *C. oblongata*. The same
665 pattern has been observed for *T. verenae* recorded in the basal Valanginian ("*T.*" *pertransiens*
666 AZ; *C. oblongata* NZ) in Vergol and, conversely, reported from the upper Berriasian (*T.*
667 *alpillensis* ASZ) and matching with the FO of *P. fenestrata* in Aguado et al. (2000). The
668 relationships between the FOs of *T. jurapelagicus*, *C. oblongata* and *T. verenae* have been
669 thoroughly discussed by Bralower et al. (1989) who observed some discrepancies in the
670 sections/cores they studied. A part of the problem is the occurrence of earlier transitional
671 forms (Bralower et al., 1989), which likely correspond to *T. frankiae* (a slightly smaller form)
672 which was introduced by Bown (2005) and considered in the present work.

673 Another difference between the present paper and previous literature is the occurrence of *P.*
674 *nebulosa/R. nebulosus*, which last occurred in the *P. fenestrata* NSZ in the Angles section
675 (Duchamp-Alphonse et al., 2007) and SE Spain (Aguado et al., 2000), but its LO is recorded
676 much later in the *C. oblongata* NZ (early Valanginian) in Vergol. Likely, this later record has
677 related to the very discontinuous and rare occurrence of *R. nebulosus*.
678 The comparison between our work with earlier similar works, like Aguado et al. (2000) or
679 Duchamp-Alphonse et al. (2007), indicates that calcareous nannofossil bioevents recorded in
680 the present work characterize very finely the interval Berriasian–Valanginian, because a
681 number of calcareous nannofossil events have recorded around the Berriasian–Valanginian
682 boundary in Vergol section (Fig. 9).
683 Furthermore, the PCA analysis compared to absolute abundance and Shannon diversity index
684 point to an important change in nannofossil assemblage composition and abundance starting
685 at the biostratigraphic boundary as defined by ammonites. PCA factors indicate a prominent
686 change occurring in correspondence of the Berriasian–Valanginian boundary, with factor 1
687 showing an excursion encapsulating the boundary, while factor 3 reveals a longer-term
688 decrease and steady values in the rest of Valanginian. Assemblages from the lower
689 Valanginian are richer both in terms of diversity and of absolute abundances. Following such
690 an enrichment, values stay quite steady although fluctuating for the rest of the lower
691 Valanginian (this work; Mattioli et al., 2014). The understanding of the palaeoenvironmental
692 reasons explaining such a change in calcareous nannofossil assemblage are behind the scope
693 of the present work, because other independent proxies (such as carbon or oxygen stable
694 isotopes, total organic matter content, etc.) are not yet available to discriminate between the
695 influence of palaeoenvironmental parameters, such as surface water fertility or temperature
696 controlling nannofossil assemblages. Also, the observed changes might be due to evolutionary
697 patterns, as the Berriasian–Valanginian saw the new entry of several coccolith species.

However, if confirmed in other areas this lower Valanginian change in nannofossil assemblages may represent a further argument to differentiate the Berriasian from the Valanginian as proposed in the present work.

5.2. Discussion on the choice of the primary marker and the candidate section for the Valanginian GSSP

As previously stated, in Spain (Company and Tavera, 1982; Aguado et al., 2000) and France (Blanc et al., 1994; Blanc, 1996) the base of *Calpionellites* zone E (FO of *C. darderi*) coincides with the base of the "*T.*" *pertransiens* AZ (FO of this index-species). However, Aguado et al. (2000) noticed some discrepancies in the compared distribution of these ammonite and calpionellid species as the FO of *C. darderi* reported at a much higher stratigraphic level in the Miravetes succession (Rio Argos area, SE Spain, see Hoedemaeker and Leereveld, 1995); according to Aguado et al. (2000), this could be due to problems of preservation of calpionellids in this section. Biostratigraphic remarks on the compared distribution of both these species could be also made for two classical sections of the Vocontian basin, namely Barret-le-Bas and Angles sections (for the Vergol section, see part 5.1). According to Blanc (1996), *C. darderi* first occurs just two beds above the FO of "*T.*" *pertransiens* in the Barret-le-Bas section; however, just below these both events there is a slump of 15 m thick that does not allow to have data on ammonite and calpionellid distributions. It should be also noted that the specimen identified as "*T.*" *pertransiens* by Busnardo and Thieuloy (1979, fig. 13) and occurring in bed number "-1" (bed below the slump) was not indicated in Bulot (1995, fig. 3). In the Angles section, Allemann and Remane (1979, fig. 29) observed the FO of *C. darderi* slightly above the bed number 220; this event was noticed lower in the succession by Bulot (1995, fig. 53) who put the FO of this species in bed number 207. In this section, the distribution of "*T.*" *pertransiens* was not given (Busnardo

723 and Thieuloy, 1979; Bulot, 1995); as noted by Blanc (1996), the interval around the
724 Berrisian–Valanginian boundary is very poor in ammonites. Consequently, ~~there is not a good~~
725 ~~continuous~~ the fossil record is not well documented in this interval of the Barret-le-Bas (cf.
726 slump) and Angles (cf. rarity of ammonites) sections ~~this~~ which do not allow to provide
727 robust results for the discussion on the synchronism of *C. darderi versus* "*T.*" *pertransiens*.
728 As far as the Vergol section is concerned, the ~~FADs~~ FOs of *C. darderi* and *"T." pertransiens*
729 are considered as being almost synchonous, occurring in beds 209 and 210, respectively
730 (Blanc et al., 1994) or beds MB210 and MB211, respectively (Blanc, 1996). Blanc et al.
731 (1994) proposed the Montbrun-les-Bains (Vergol) section as a potential boundary stratotype
732 between the Berriasian and Valanginian stages, and they proposed to put the golden spike at
733 the base of bed 210 in which they recorded the FO of *"T." pertransiens.* However, the
734 provisional recommandation of the Valanginian Working Group (Bulot et al., 1996) was to
735 place the boundary at the base of *Calpionellites* Zone E (FAD of *C. darderi*, bed 209 in the
736 candidate section, Blanc et al., 1994). Compared to the ammonite *"T." pertransiens*, the
737 working group emphasized the broader geographic distribution of the calpionellid index-
738 species (recorded from Mexico to Turkey). In the Geologic Time Scale 2016 (Ogg et al.,
739 2016), the proposed Valanginian GSSP marker is the FAD of *C. darderi* (base of
740 *Calpionellites* Zone E). However, if *C. darderi* has a wider palaeogeographic distribution than
741 "*T.*" *pertransiens*, it seems that the occurrence and abundance of this calpionellid species is
742 more dependant on the preservation effect, as observed by Aguado et al. (2000) for some
743 Spanish sections ~~and reiterated in the Geologic Time Scale 2012 (Ogg et al., 2012)~~. In SE
744 France, Allemann and Remane (1979) reported that Valanginian calpionellid faunas of the
745 Vocontian basin were impoverished compared to that of "South Mediterranean area" (see also
746 Le Hégarat *in* Cotillon et al., 1984) and they stressed out the scarcity of *C. darderi* although
747 its earliest occurrence can be recorded if numerous fields of view are studied. When Bulot et

748 al. (1993a) described the evolution of calpionellids, they stated that no important turnovers
749 occurred at the Berriasian–Valanginian boundary and that "*Lorenziella hungarica*, whose first
750 appearance defines the base of D3, remains always rare. The same is true as for *C. darderi*
751 (base of zone E)".
752 Taking into account the ammonite data and the correlations proposed in this work (Fig. 14),
753 the FO of *"T." pertransiens* (VGL-B136) occurs around 7 m below the FO of *C. darderi*
754 (VGL-V1). Contrarily to the observations of Blanc et al. (1994; see also Blanc, 1996), these
755 two bioevents are not synchonous in the Vergol section. If priority is given to the FAD of *C.*
756 *darderi* to define the base of the Valanginian, then the base of the *"T." pertransiens* AZ
757 (currently considered as the earliest zone of the Valanginian) would be placed in the upper
758 Berriasian. Two options stay possible.
759 First, it can be considered that it is not problematic to have the lower part of the historical
760 Valanginian *"T." pertransiens* AZ in the late Berriasian and that the earliest zone of the
761 Valanginian overlaps the Berriasian–Valanginian boundary, because this would be defined by
762 another group, namely the calpionellids. A similar case can be cited with the Albian–
763 Cenomanian boundary. The base of the Cenomanian stage (ratified GSSP at Mont Risou,
764 Hautes-Alpes, France, Kennedy et al., 2004) is defined by the FAD of *Rotalipora*
765 *globotruncanoides* (foraminifera). This event occurs in the upper part of the former
766 *Arrhaphoceras briacensis* ASZ, now considered as a zone (Reboulet et al., 2011). Thus, this
767 last unit of the Albian zonal scheme is Albian in age for its lower part and Cenomanian in age
768 for its uppermost part.
769 As a second solution, adopted here, the base of the Valanginian is defined by the FAD of "*T.*"
770 *pertransiens*. This species has a large distribution and it is relatively well represented in the
771 Mediterranean Province of the Mediterranean–Caucasian Subrealm (Tethyan Realm;
772 Company, 1987; Bulot, 1995; Klein, 2005; Kenjo, 2014). The base of the "*T.*" *pertransiens*

AZ coincides with a significant ammonite faunal renewal (further details in Kenjo, 2014; Company and Tavera, 2015; this work). According to ammonite and calcareous nannofossil data provided by Kenjo (2014) and this work, the Berriasian–Valanginian boundary is also well-characterized by the FO of the ammonite *N. premolicus* (bed VGL-B141; Fig. 2A) and the FO of the calcareous nannofossil *C. oblongata* (VGL-B146M, Fig. 9). Both bioevents are recorded respectively only 2 and 4 m above the FO of "*T.*" *pertransiens* (bed VGL-B136) in the candidate section. *N. premolicus* was used to recognize and/or characterize the base of the Valanginian in some areas of the Mediterranean Province (Ettachfini, 2004; Kenjo, 2014; Company and Tavera, 2015) and *C. oblongata* is consistently recorded in the lowermost part of *"T." pertransiens* AZ (Bralower et al., 1989; Bulot et al., 1996; Bown, 1998; Duchamp-Alphonse, 2007; Kenjo, 2014; this work). The choice of an ammonite index-species is also motivated by a pragmatic approach. The base of Phanerozoic stages is often defined by biologic markers (GSSP table of ICS, http://www.stratigraphy.org/index.php/ics-gssps) that are ammonites for all stages of the Jurassic System ~~Period~~ (ratified GSSPs or proposals in progress for other stages). Indeed, for this period and also for Cretaceous, studies on ammonites generally provides the highest biostratigraphical resolution of stages to establish their subdivision and define their base. Consequently, taking into acccout that "*T.*" *pertransiens* has a large palaeogeographic distribution allowing a good correlation, a priority is given here to ammonite biostratigraphic data in order to make a good and workable correspondence in the subdivision of the Valanginian Stage (ammonite (sub-)zones) and the definition of its base (the base of the Valanginian corresponds to the base of the earliest zone, namely the "*T.*" *pertransiens* AZ).

Taking into account previous synthetic studies (Birkelund et al., 1984; Bulot et al., 1996; Ogg et al., 2016), ammonites, calpionellids and calcareous nannofosssils, are the three main groups that can be used to define the Berriasian–Valanginian boundary. According to Ogg et al.

798 (2012), the age model for the Berriasian–Barremian ammonite zonal scheme is mainly
799 derived from correlations to the M-sequence of marine magnetic anomalies, linearization of
800 strontium isotope trends, and/or cycle stratigraphy. Concerning the magnetostratigraphy, the
801 previous sampling made on the Vergol section has not allowed to provide significant
802 geomagnetic reversals (Blanc, 1996; Bulot et al., 1996). For the other candidate GSSP section
803 at Barranco de Cañada Luenga (south of Cehegın, SE Spain), a direct calibration of
804 magnetostratigraphic reversals against biostratigraphic scales was proposed. In order to
805 recognize and characterize the Valanginian Weissert Event in SE France, stable isotopic data
806 (oxygen and carbon isotope curves) are relatively abundant for the Vergol section from the
807 middle part of the lower Valanginian (*N. neocomiensiformis* AZ) to the middle part of the
808 upper Valanginian (*Neocomites peregrinus* AZ; McArthur et al., 2007; Gréselle et al., 2011;
809 Kujau et al., 2012). However, data are scarcer for the interval around the Berriasian–
810 Valanginian boundary (McArthur et al., 2007). These last authors also provided $^{87}Sr/^{86}Sr$
811 trends that enable global correlation and relative dating, but the curve was also built with
812 isotopic data coming from different sections. In Vergol, the interval from the uppermost
813 Berriasian (*T. alpillensis* AZ) to the middle part of the upper Valanginian (*N. peregrinus* AZ)
814 has been scaled using astronomically-forced cycle stratigraphy, especially using the long-term
815 eccentricity cycles (medium-scale sequences to 405-kyr) and short-term eccentricity cycles
816 (small-scale sequences to 100-kyr; Gréselle et al., 2011; Martinez et al., 2013). Based on an
817 integrated stratigraphy of the Vergol-la Charce (Drôme) and Reynier-Angles (Alpes-de-Haute
818 Provence) composite sections from the Vocontian basin, Martinez et al. (2013) suggested a
819 duration of 5.08 Ma for the Valanginian stage. After an astrochronological study of the
820 Hauterivian Stage and using new radiometric ages extracted from tuff levels in the middle
821 Hauterivian in the Neuquén Basin (Argentina), Martinez et al. (2015) calculated an age of
822 137.05 ± 1.0 Ma for the base of the Valanginian Stage.

The interest of these studies on the Vergol locality is mainly due to a very good sedimentary record for the uppermost Berriasian–lowermost Valanginian interval (Fig. 2). This succession made of a calcareous-marl alternation is more expanded than the Cañada Luenga section, at least for the interval around the Berriasian–Valanginian boundary. Indeed, in this Spanish section, the stratigraphic interval dated from the "*T.*" *otopeta* ASZ is composed of 5 beds for a 2-m-thick interval (see fig. 5 in Aguado et al., 2000); in the Vergol section (Fig. 2A), the interval corresponding to the "*T.*" *otopeta* ASZ is composed by 20 beds for a 8-m-thick interval (or at least 15 beds for 6 m, if the specimen from bed VGL-B116 identified with doubt as "*T.*" *otopeta* is not considered as the FO of this index-species). In the Cañada Luenga section, the stratigraphic interval dated from the "*T.*" *pertransiens* AZ is composed of 20 beds for a 13-m-thick interval (see fig. 2 in Company and Tavera, 2015); in the Vergol section (Fig. 2A), the interval corresponding to the "*T.*" *pertransiens* AZ is composed by 53 beds (and most of them are composed of 2 or 3 layers) for a 30-m-thick interval. Thus, as far as these intervals are concerned, the Vergol section is around 2.5 times thicker than the Cañada Luenga section. The limited thickness of the Cañada Luenga section with respect to Vergol might explain the co-occurrence of "*T.*" *pertransiens* and *C. darderi* in the same layer. A similar assumption can be made to explain their co-occurrence in Bulgaria (Petrova et al., 2011) in the Barlya section for which the whole lower Valanginian is around 30 m thick with respect to Vergol where the substage is represented by a succession of 108 m thick. It cannot be excluded that *C. darderi* occurred lower in the Vergol section (from bed VGL-B136 to VGL-B151) along with the earliest "*T.*" *pertransiens*. However, as previously discussed for some Spanish sections, the lack of *C. darderi* in this interval might also be related to a preservation effect.

For the purposes of the Valanginian GSSP proposal (chairs M. Company and S. Reboulet), a new study on calpionellid distribution is in preparation on the Vergol section in order to check

the hypothesis evoked previously. Concerning the magnetostratigraphy, a second attempt using a different method should be made in order to calibrate magnetic reversals against biostratigraphy.

6. Conclusions

A quantitative palaeontological study of ammonites and calcareous nannofossils was performed in the Vergol reference section (Montbrun-les-Bains, SE France, Vocontian basin), in order to refine the previously proposed biostratigraphic frame for the interval around the Berriasian–Valanginian boundary. The analysis of the ammonite distributions shows a major turnover and allowed the establishment of a detailed zonal scheme; it corresponds to the standard zonation built for the Mediterranean Province of the Mediterranean–Caucasian Subrealm (Tethyan Realm) that is partly based on ammonite data from the Vergol section (Kenjo, 2014; Reboulet et al., 2018; this work). The FAD of *T.alpillensis* allows the definition of the base of the latest Berriasian zone that is subdivided into *T. alpillensis* and *"T." otopeta* ASZs. The earliest Valanginian zone is defined by the FAD of "*T.*" *pertransiens*; the appearance of *N. premolicus* can also be used to recognize the base of this zone. The lower boundary of *C. oblongata* NZ corresponds to the lower part of the "*T.*" *pertransiens* AZ. The interval around the Berriasian–Valanginian boundary is also characterized by other bioevents of calcareous nannofossil species, mainly first occurrences, but also by a prominent change in the assemblage composition and an increase in absolute abundance.

The comparison with the work of Blanc et al. (1994) and Blanc (1996) points to some discrepancies in ammonite bioevents and the lower boundary of "*T.*" *pertransiens* AZ must therefore be moved downwards in the section (around 7 m below) with respect to the boundary proposed by these authors. So, contrarily to their assertion, it seems that the FO of "*T.*" *pertransiens* is not synchronous with the FO of *C. darderi* that is the index-species for

873 the base of the Valanginian Stage as provisionally recommended by the Valanginian Working
874 Group (Bulot et al., 1996). Taking into account that ammonite and calcareous nannofossil
875 bioevents allow a precise characterization of the Berriasian–Valanginian boundary (*sensu*
876 Kenjo, 2014; this work) and that some studies are still in progress on the Vergol candidate
877 section for the Valanginian GSSP (cf. proposal), the choice has been made to ~~identify~~ define
878 the base of the stage by using the FAD of "*T.*" *pertransiens,* index-species of the first current
879 Valanginian AZ. ~~that~~ This corresponds to the historical definition of the boundary *sensu*
880 Kilian (1910) and Mazenot (1939).
881
882 **Acknowledgements**
883 We thank Ghislaine Broillet for slide preparation for the study of nannofossil samples. The
884 authors are grateful to the reviewers Miguel Company (University of Granada, Spain) and
885 Ottilia Szives (Hungarian Natural History Museum, Hungary) for their valuable comments
886 which greatly improved the overall quality of the paper. We also thank Eduardo Koutsoukos
887 for his editorial assistance.
888
889 **References**
890
891 Aguado, R., 1994. ~~Nannofosiles del Cretacico de la cordillera betica (sur de Espana)~~.
892 Nannofósiles del Cretácico de la Cordillera Bética (sur de España). Bioestratigrafia. Ph.D.
893 Thesis, University of Granada, 1994, 413 pp.
894
895 Aguado, R, Company, M., Tavera, J.M., 2000. The Berriasian/Valanginian boundary in the
896 Mediterranean region: new data from the Caravaca and Cehegín sections, SE Spain.
897 Cretaceous Research 21, 1–21.

Allemann, F., Remane, J., 1979. Les faunes de calpionelles du Berriasien supérieur/Valanginien. In: Busnardo, R., Thieuloy, J. P., Moullade, M. (Eds), Hypostratotype mésogéen de l'étage Valanginien (sud-est de la France). Edition C.N.R.S (Paris), Les stratotypes français 6, 99–109.

Allemann, F., Grün, W., Wiedmann, J., 1975. The Berriasian of Caravaca (Prov. of Murcia) in the subbetic zone of Spain and its importance for defining this stage and the Jurassic–Cretaceous boundary. Colloque sur la limite Jurassique–Crétacé, Lyon-Neuchâtel, 1973. Mémoires du Bureau de Recherches Géologiques et Minières 86, 14–22.

Barbier, R., Thieuloy, J.P., 1965a. Etage Berriasien. In: Colloque sur le Crétacé inférieur (Lyon, 1963). Mémoires du Bureau de Recherches Géologiques et Minières 34, 69–77.

Barbier, R., Thieuloy, J.P., 1965b. Etage Valanginien. In: Colloque sur le Crétacé inférieur (Lyon, 1963). Mémoires du Bureau de Recherches Géologiques et Minières 34, 79–84.

Beaufort L., 1991. Adaptation of the random settling method for quantitative studies of calcareous nannofossils. Micropaleontology 37, 415–418.

Beaufort, L., Heussner, S., 2001. Seasonal dynamics of calcareous nannoplankton on a west European continental margin: The Bay of Biscay, Marine Micropaleontology 43, 27–55.

921 Bergen, J. A., 1994. Berriasian to early Aptian calcareous nannofossils from the Vocontian
922 Trough (SE France) and Deep Sea Drilling Site 534: new nannofossil taxa and a summary of
923 low- latitude biostratigraphic events. Journal of Nannoplankton Research 16, 59–69.
924
925 Bergen, J. A., 2000 ~~1998~~. Calcareous nannofossils from the lower Aptian historical stratotype
926 at Cassis-La Bedoule (SE France). Géologie Méditerranéenne 25 (3-4) (1998), 227–255.
927
928 Birkelund, T., Hancock, J.M., Hart, M.B., Rawson, P.F., Remane, J., Robaszynski, F.,
929 Schmid, F., Surlyk, F., 1984. Cretaceous stage boundaries – proposals. Bulletin of the
930 Geological Society of Denmark 33, 3–20.
931
932 Blanc, E., 1996. Transect plateforme - bassin dans les séries carbonatées du Berriasien
933 supérieur et du Valanginien inférieur (domaines jurassien et nord-vocontien).
934 Chronostratigraphie et transferts des sédiments. Géologie Alpine, Mémoire Hors Série 25,
935 312 pp.
936
937 Blanc, E., Bulot, L.G., Paicheler, J.C., 1994. La coupe de référence de Montbrun-les-Bains
938 (Drôme, SE France) : un stratotype potentiel pour la limite Berriasien–Valanginien. Comptes
939 Rendus de l'Académie des Sciences de Paris 318 (sér. II), 101–108.
940
941 Bornemann, A., Mutterlose, J., 2006. Size analyses of the coccolith species *Biscutum*
942 *constans* and *Watznaueria barnesiae* from the Late Albian "Niveau Breistroffer" (SE France):
943 taxonomic and palaeoecological implications. Geobios 39, 599–615.
944

945 Bown, P.R., 2005. Early to mid-Cretaceous calcareous nannoplankton from the northwest Pacific
946 Ocean, ODP Leg 198, Shatsky Rise. In Bralower, T.J., Premoli Silva, I., and Malone, M.J. (Eds.),
947 Proceedings of the Ocean Drilling Program, Scientific Results 198, 1–82.
948
949 Bown, P.R. (Ed.), 1998. Calcareous nannoplankton Biostratigraphy. British
950 Micropaleontological Society Publication Series. Kluver Academic Publishers, 314 pp.
951
952 Bralower, T. J., Monechi, S., Thierstein, H. R., 1989. Calcareous nannofossil zonation of the
953 Jurassic–Cretaceous boundary interval and correlation with the geomagnetic polarity
954 timescale. Marine Micropaleontology 14, 153–235.
955
956 Bulot, L.G., 1990. Evolution des Olcostephaninae (Ammonitina, Cephalopoda) dans le contexte
957 paléo-biogéographique du Crétacé inférieur (Valanginien–Hauterivien) du Sud-Est de la France.
958 Diplôme Etude Supérieur (unpublished), Université de Bourgogne, 177 pp.
959
960 Bulot, L.G., 1995. Les formations à ammonites du Crétacé inférieur dans le Sud-Est de la
961 France (Berriasien à Hauterivien) : biostratigraphie, paléontologie et cycles sédimentaires.
962 Unpublished PhD thesis, Muséum National d'Histoire Naturelle, Paris, 398 pp.
963
964 Bulot, L.G., Thieuloy, J.-P., 1993. Implications chronostratigraphiques de la révision de l'échelle
965 biostratigraphique du Valanginien supérieur et de l'Hauterivien du Sud-Est de la France.
966 Comptes rendus de l'Académie des Sciences de Paris 317 (sér. II), 387–394.
967

968 Bulot, L.G., Thieuloy, J.-P., 1995. Les biohorizons du Valanginien du Sud-Est de la France : un
969 outil fondamental pour les corrélations au sein de la Téthys occidentale. Géologie Alpine,
970 Mémoire Hors Série 20 (1994), 15–41.
971
972 Bulot, L.G., Blanc, E., Thieuloy, J.-P., Remane, J., 1993a. La limite Berriasien–Valanginien
973 dans le Sud-Est de la France : données biostratigraphiques nouvelles. Compte Rendus de
974 l'Académie des Sciences de Paris 316 (sér. II), 1771–1778.
975
976 Bulot, L.G., Thieuloy, J.-P., Blanc, E., Klein, J., 1993b. Le cadre stratigraphique du
977 Valanginien supérieur et de l'Hauterivien du Sud-Est de la France : définition de
978 biochronozones et caractérisation de nouveaux biohorizons. Géologie Alpine 68 (1992), 13–
979 56.
980
981 Bulot, L.G. (reporter), Blanc, E., Company, M., Gardin, S., Hennig, S., Hoedemaeker, P.J.,
982 Leereveld, H., Magniez-Jannin, F., Mutterlose, J., Pop, G., Rawson, P.F., 1996. The
983 Valanginian Stage. In: Rawson, P.F., Dhondt, A.V., Hancock, J.M., Kennedy, W.J. (Eds.),
984 "Proceedings of the Second International Symposium on Cretaceous Stage Boundaries",
985 Brussels, 1995. Bulletin de l'Institut Royal des Sciences Naturelles de Belgique, Sciences de
986 la Terre 66-supp., 11–18.
987
988 Busnardo, R., Le Hégarat, G. 1965. Le stratotype du Berriasien - IV. Conclusions. In:
989 Colloque sur le Crétacé inférieur (Lyon, 1963). Mémoires du Bureau de Recherches
990 Géologiques et Minières 34, 25–33.
991

992 Busnardo, R., Thieuloy, J.P., 1979. Les zones d'ammonites du Valanginien. In: Busnardo, R.,
993 Thieuloy, J.P., Moullade, M. (Eds.), Hypostratotype mésogéen de l'étage Valanginien (sud-
994 est de la France). Edition C.N.R.S (Paris), Les stratotypes français 6, 58–68.
995
996 Busnardo, R., Charollais, J., Weidmann, M., Clavel, B., 2003. Le Crétacé inférieur de la
997 Veveyse de Châtel (Ultrahelvétique des Préalpes externes ; canton de Fribourg, Suisse).
998 Revue de Paléobiologie 22, 1–174.
999
1000 Company, M., 1987. Los ammonites del Valanginiense del sector oriental de las Cordilleras
1001 Béticas (SE de España). Tesis Doctoral, Universidad de Granada, Granada, 294 pp.
1002
1003 Company, M., Tavera, J.M., 1982. Los ammonites del tránsito Berriasense–Valanginiense en
1004 la región de Cehegín (prov. De Murcia, SE de España). Cuadernos de Geología Ibérica 8,
1005 651–664.
1006
1007 Company, M., Tavera, J.M., 2015. Lower Valanginian ammonite biostratigraphy in the
1008 Subbetic Domain (Betic Cordillera, southeastern Spain). Carnets de Géologie 15 ~~(8)~~, 71–88.
1009
1010 Cotillon, P. (reporter), Arnaud-Vanneau, A., Arnaud, H, Boisseau, T., Busnardo, R.,
1011 Charollais, B., Clavel, B., Combémorel, R., Conrad, M.-A., Darsac, C., Demay, J.-L., Ferry,
1012 S., Jardine, S., Le Hégarat, G., Magniez-Jannin, F., Manivit, H., Masse, J.-P., Medioni, R.,
1013 Moullade, M., Oertli, H.-J., Peybernès, B., Raynaud, J.-F., de Reneville, P., Salvini, G.,
1014 Sornay, J., Steinhauser, N., Thieuloy, J.-P., Tronchetti, G., Vieban, F., 1984. Chapitre 6,
1015 Crétacé inférieur, *in* Debrand-Passard, S., Courbouleix, S., Lienhardt, M.-J., Synthèse

géologique du Sud-Est de la France. Mémoire du Bureau de Recherches Géologiques et Minières 125, 287–338.

Cotillon, P., Ferry, S., Gaillard, C., Jautée, E., Latreille, G., Rio, M., 1980. Fluctuation des paramètres du milieu marin dans le domaine vocontien (France Sud-Est) au Crétacé inférieur : mise en évidence par l'étude des formations marno-calcaires alternantes. Bulletin de la Société Géologique de France (7) 22, 735–744.

Crux, J.A., 1989. Biostratigraphy and palaeogeographical application of Lower Cretaceous nannofossils from north-western Europe. *In*: J.A. Crux and S.E. van Heck (Eds.) Nannofossils and their aplications, Ellis Howrwood Chichester, 143–211.

Duchamp-Alphonse, S., Gardin, S., Fiet, N., Bartolini, A., Blamart, D., Pagel, M., 2007. Fertilization of the northwestern Tethys (Vocontian basin, SE France) during the Valanginian carbon isotope perturbation: Evidence from calcareous nannofossils and trace element data. Palaeogeography, Palaeoclimatology, Palaeoecology 243, 132–151.

Ettachfini, M., 2004. Les ammonites néocomiennes dans l'Atlas atlantique (Maroc) : biostratigraphie, paléontologie, paléobiogéographie et paléoécologie. Strata 2 (43), 225 pp.

Gauthier, H. (Ed.), Busnardo, R., Combémorel, R., Delanoy G., Fischer, J.-C., Guérin-Franiatte, S., Joly, B., Kennedy, W.J., Sornay, J., Tintant, H., 2006. Révision critique de la Paléontologie française d'Alcide d'Orbigny. Volume IV. Céphalopodes crétacés. Backhuys Publisher, Leiden, 292 pp.

Geisen, M., Bollmann, J., Herrle, J.O., Mutterlose, J., Young, J. R., 1999. Calibration of the random settling technique for calculation of absolute abundances of calcareous nannoplankton, Micropaleontology 45, 437–442.

Gradstein, F.M., Waskowska, A., Kopaevich, L., Watkins, D.K, Friis, H., Pérez Panera, J., 2019. Berriasian planktonic foraminifera and calcareous nannofossils from Crimea Mountains, with reference to microfossil evolution. Swiss Journal of Palaeontology 138, 213–236.

Gréselle, B., Pittet, B., 2010. Sea-level reconstructions from the Peri–Vocontian Zone (SE France) point to Valanginian glacio–eustasy. Sedimentology 57, 1640–1684.

Gréselle, B., Pittet, B., Mattioli, E., Joachimski, M., Barbarin, N., Riquier, L., Reboulet, S., Pucéat, E., 2011. The Valanginian isotope event: A complex suite of palaeoenvironmental perturbations. Palaeogeogeography, Palaeoclimatology, Palaeoecology 306 ~~/1–2~~, 41–57.

Hay, W.W., 1972. Probabilistic stratigraphy. Eclogae Geologicae Helveticae 65, 255–266.

Hedberg, H.D., 1976. International stratigraphic guide. A Guide to Stratigraphic Classification, Terminology, and Procedure. Wiley J. and Sons, New York, 200 pp.

Hoedemaeker, Ph.J., 1981. The Jurassic–Cretaceous boundary near Miravetes (Caravaca, SE Spain); arguments for its position at the base of the Occitanica Zone. Cuadernos de Geologiá ~~Geologicos~~ 10 (1979), 235–247.

1066 Hoedemaeker, Ph.J., 1982. Ammonite biostratigraphy of the uppermost Tithonian, Berriasian,
1067 and lower Valanginian along the Río Argos (Caravaca, SE Spain). Scripta Geologica 65, 1–
1068 81.
1069
1070 Hoedemaeker, P.J., 1983. Reconsideration of the stratigraphic position of the boundary
1071 between the Berriasian and the Nemausian (= Valanginian *sensu stricto*). Zitteliana 10, 447–
1072 457.
1073
1074 Hoedemaeker, P.J., Leereveld, H., 1995. Biostratigraphy and sequence stratigraphy of the
1075 Berriasian–lowest Aptian (Lower Cretaceous) of the Río Argos succession, Caravaca, SE
1076 Spain. Cretaceous Research 16, 195–230.
1077
1078 Hoedemaeker, P.J., Bulot, L. (reporters), Avram, E., Busnardo, R., Company, M., Delanoy,
1079 G., Kakabadze, M., Kotetishvilli, E., Krishna, J., Kvantaliani, I., Latil, J.L., Memmi, L.,
1080 Rawson, P.F., Sandoval, J., Tavera, J.M., Thieuloy, J.-P., Thomel, G., Vašíček, Z.,
1081 Vermeulen, J., 1990. Preliminary ammonite zonation for the Lower Cretaceous of the
1082 Mediterranean region. Géologie Alpine 66, 123–127.
1083
1084 Hoedemaeker, P.J., Company, M., (reporters), Aguirre-Urreta, M.B., Avram, E., Bogdanova,
1085 T.N., Bujtor, L., Bulot, L., Cecca, F., Delanoy, G., Ettachfini, M., Memmi, L., Owen, H.G.,
1086 Rawson, P.F., Sandoval., J., Tavera, J.M., Thieuloy, J.-P., Tovbina, S.Z., Vašíček, Z., 1993.
1087 Ammonite zonation for the Lower Cretaceous of the Mediterranean region; basis for the
1088 stratigraphic correlation within IGCP-Project 262. Revista Española de Paleontologiá 8, 117–
1089 120.
1090

Hoedemaeker, P.J., Reboulet, S., (reporters), Aguirre-Urreta, M.B., Alsen, P., Aoutem, M., Atrops, F., Barragán, R., Company, M., González-Arreola, C., Klein, J., Lukeneder, A., Ploch, I., Raisossadat, N., Rawson, P.F., Ropolo, P., Vašíček, Z., Vermeulen, J., Wippich M.G.E., 2003. Report on the 1st International Workshop of the IUGS Lower Cretaceous Ammonite Working Group, the "Kilian Group" (Lyon, 11 July 2002). Cretaceous Research 24, 89–94, and erratum (p. 805).

Joly, B., 2000. Les Juraphyllitidae, Phylloceratidae, Neophylloceratidac (Phylloceratacеae, Phylloceratina, Ammonoidea) de France au Jurassique et au Crétacé. Geobios, Mémoire Spécial 23, and Mémoire de la Société Géologique de France 174, 204 pp.

Kemper, E., Rawson, P.F., Thieuloy, J.-P., 1981. Ammonites of Tethyan ancestry in the early Lower Cretaceous of north-west Europe. Palaeontology, 24: 251–311.

Kenjo, S., 2014. Biostratigraphie intégrée à nannofossiles calcaires et ammonoïdes : développement et implications pour la définition et la valorisation des stratotypes d'unité et de limite. L'exemple des étages Berriasien et Valanginien et de leur limite (140 Millions d'années). Unpublished PhD thesis, Université de Lyon, 226 pp.

Kennedy, W.J., Gale, A.S., Lees, J.A., Caron, M., 2004. ~~Definition of a~~ The Global Boundary Stratotype Section and Point (GSSP) for the base of the Cenomanian Stage, Mont Risou, Hautes-Alpes, France. Episodes 27, 21–32.

Kilian, W. 1910. Valendis-Stufe (Valanginien). In: Lethaea geognostica. Unterkreide (Palaeocretacicum), pp. 169–202 (E. Schweizerbart'sche Verlagsbuchhandlung, Stuttgart).

Klein, J., 2005. Lower Cretaceous Ammonites I, Perisphinctaceae 1: Himalayitidae, Olcostephanidae, Holcodiscidae, Neocomitidae, Oosterellidae. In: Riegraf, W. (Ed.), Fossilium Catalogus I: Animalia. Backhuys Publishers, Leiden, Netherlands, Pars 139, 484 pp.

Klein, J., Busnardo, R., Company, M., Delanoy, G., Kakabadze, M., Reboulet, S., Ropolo, P., Vašíček, Z., Vermeulen, J., 2007. Lower Cretaceous Ammonites III. Bochianitoidea, Protancyloceratoidea, Ancyloceratoidea, Ptychoceratoidea. In: Riegraf, W. (Ed.), Fossilium Catalogus I: Animalia. Backhuys Publishers, Leiden, Netherlands, Pars 144, 381 pp.

Klein, J., Hoffmann, R., Joly, B., Shigeta, Y., Vašíček, Z., 2009. Lower Cretaceous Ammonites IV. Boreophylloceratoidea, Phylloceratoidea, Lytoceratoidea, Tetragonitoidea, Haploceratoidea including the Upper Cretaceous representatives. In: Riegraf, W. (Ed.), Fossilium Catalogus I: Animalia. Backhuys Publishers, Leiden, Netherlands, Pars 146, 416 pp.

Kujau, A., Heimhofer, U., Ostertag-Henning, C., Gréselle, B., Mutterlose, J., 2012. No evidence for anoxia during the Valanginian carbon isotope event – an organic - geochemical study from the Vocontian Basin, SE France. Global and Planetary Change 92–93, 93–104.

Lakova, I., Stoykova, K., Ivanova, D., 1999. Calpionellid, nannofossil and calcareous dinocyst bioevents and integrated biochronology of Tithonian to Valanginian in the Western Balkanides, Bulgaria. Geologica Carpathica 50, 151-168.

1141 Le Hégarat, G., 1973. Le Berriasien du Sud-Est de la France. Documents des Laboratoires de
1142 Géologie, Faculté des Sciences de Lyon 43 (1971), 576 pp.
1143
1144 Le Hégarat, G., Remane, J., 1968. Tithonique supérieur et Berriasien de l'Ardèche et de
1145 l'Hérault. Corrélation des ammonites et des calpionelles. Geobios 1, 7–70.
1146
1147 Manivit, H., 1979. Les nannofossiles. In: Busnardo, R., Thieuloy, J.P., Moullade, M. (Eds.),
1148 Hypostratotype mésogéen de l'étage Valanginien (sud-est de la France). Edition C.N.R.S
1149 (Paris), Les stratotypes français 6: 87-98.
1150
1151 Martinez, M., Deconinck, J.-F., Pellenard, P., Reboulet, S., Riquier, L., 2013.
1152 Astrochronology of the Valanginian Stage from reference sections (Vocontian Basin, France)
1153 and palaeoenvironmental implications for the Weissert Event. Palaeogeographgy,
1154 Palaeoclimatology, Palaeoecology 376, 91–102.
1155
1156 Martinez, M., Deconinck, J-F., Pellenard, P., Riquier, L., Company, M., Reboulet, S.,
1157 Moiroud, M., 2015. Astrochronology of the Valanginian–Hauterivian stages (Early
1158 Cretaceous): chronological relationships between the Paraná–Etendeka large igneous province
1159 and the Weissert and the Faraoni events. Global and Planetary Change 131, 158–173.
1160
1161 Mattioli, E., Pittet, B., Riquier, L., Grossi, V., 2014. The mid–Valanginian Weissert Event as
1162 recorded by calcareous nannoplankton in the Vocontian Basin. Palaeogeography,
1163 Palaeoclimatology, Palaeoecology 414, 472–485.
1164

Mazenot, G., 1939. Les Palaehoplitidae tithoniques et berriasiens du Sud-Est de la France. Mémoire de la Société Géologique de France, Nouvelle Série~~, 18/~~ 41, 303 pp.

McArthur, J.M., Janssen, N.M.M., Reboulet, S., Leng, M.J., Thirlwall, M.F., van de Schootbrugge, B., 2007. Palaeotemperatures, polar ice-volume, and isotope stratigraphy (Mg/Ca, $\delta^{18}O$, $\delta^{13}C$, $^{87}Sr/^{86}Sr$): The Early Cretaceous (Berriasian, Valanginian, Hauterivian). Palaeogeography, Palaeoclimatology, Palaeoecology 248, 391–430.

Mutterlose, J., 1992. Biostratigraphy and palaeobiogeography of Early Cretaceous calcareous nannofossils. Cretaceous Research 13, 167–189.

Ogg, J.G., Hinnov, L.A., Huang, C., 2012. Chapter 27. Cretaceous. In: Gradstein, F.M., Ogg, J.G., Schmitz, M.D., Ogg, G.M. (Eds), The Geologic Time Scale 2012. Elsevier, Amsterdam, Netherlands, 793–853.

Ogg, J.G., Ogg, G.M., Gradstein, F.M., 2016. Chapter 13. Cretaceous. A Concise GeologicTime Scale 2016. Elsevier, Amsterdam, Netherlands, 167–186.

Petrova, S., Lakova, I., Ivanova, D., 2011. Berriasian–Valanginian boundary in Bulgaria. Review of the Bulgarian Geological Society 72 (1–3): 91–97.

Perch-Nielsen, K., 1979. Calcareous nannofossils from the Crelaceous between the North Sea and the Mediterranean. Aspekte der Kreide Europa, lUGS Series A, 6, 223-272.

1189 Perch-Nielsen, K., 1985. Mesozoic calcareous nannofossils. In: Bolli, H.M., Saunders, J.B.,
1190 Perch-Nielsen, K. (Eds.) Plankton Stratigraphy Volume 1, Planktic Foraminifera, Calcareous
1191 Nannofossils and Calpionellids, Cambridge Earth Science Series, 608 pp.
1192
1193 Rawson, P.F., 2006. Chapter 15, Cretaceous: sea levels peak as the North Atlantic opens. In:
1194 Brenchley, P.J., Rawson, P.F. (eds), The Geology of England and Wales (second edition). The
1195 Geological Society, London, viii+559 pp.
1196
1197 Reboulet, S., 1996. L'évolution des ammonites du Valanginien-Hauterivien inférieur du
1198 bassin vocontien et de la plate-forme provençale (S-E de la France) : relations avec la
1199 stratigraphie séquentielle et implications biostratigraphiques. Documents des Laboratoires de
1200 Géologie, Lyon 137 (1995): 371 pp.
1201
1202 Reboulet, S., Atrops, F., 1999. Comments and proposals about the Valanginian–lower
1203 Hauterivian ammonite zonation of south-eastern France. Eclogae Geologicae Helvetiae 92,
1204 183–197.
1205
1206 Reboulet, S., Rard, A., 2008. Double alignments of ammonoid aptychi from the Lower
1207 Cretaceous of Southeast France: Result of a post–mortem transport or bromalites? Acta
1208 Palaeontologica Polonica 53 ~~(2)~~, 261–274.
1209
1210 Reboulet, S., Atrops, F., Ferry, S., Schaaf, A., 1992. Renouvellement des ammonites en fosse
1211 vocontienne à la limite Valanginien–Hauterivien. Géobios 25, 469–476.
1212

Reboulet, S., Mattioli, E., Pittet, B., Baudin, F., Olivero, D., Proux, O., 2003. Ammonoid and nannoplankton abundance in Valanginian (early Cretaceous) limestone–marl successions from the southeast France Basin: carbonate dilution or productivity? Palaeogeography, Palaeoclimatology, Palaeoecology 201, 113–139.

Reboulet, S., Hoedemaeker, P.J., (reporters), Aguirre-Urreta, M.B., Alsen, P., Atrops, F., Baraboshkin, E.Y., Company, M., Delanoy, G., Dutour, Y., Klein, J., Latil, J.L., Lukeneder, A., Mitta, V., Mourgues, F.A., Ploch, I., Raisossadat, N., Ropolo, P., Sandoval, J., Tavera, J.M., Vašíček, Z., Vermeulen, J., 2006. Report on the 2nd international meeting of the IUGS Lower Cretaceous ammonite working group, the "Kilian Group" (Neuchâtel, Switzerland, 8 September 2005). Cretaceous Research 27, 712–715.

Reboulet, S., Klein, J. (reporters), Barragán, R., Company, M., González-Arreola, C., Lukeneder, A., Raisossadat, S.N., Sandoval, J., Szives, O., Tavera, J.M., Vašíček, Z., Vermeulen, J., 2009. Report on the 3rd International Meeting of the IUGS Lower Cretaceous AmmoniteWorking Group, the "Kilian Group" (Vienna, Austria, 15th April 2008). Cretaceous Research 30, 496–502.

Reboulet, S., Rawson, P.F., Moreno-Bedmar, J.A. (reporters), Aguirre-Urreta, M.B., Barragán, R., Bogomolov, Y., Company, M., González-Arreola, C., Idakieva Stoyanova, V., Lukeneder, A., Matrion, B., Mitta, V., Randrianaly, H., Vašíček, Z., Baraboshkin, E.J., Bert, D., Bersac, S., Bogdanova, T.N., Bulot, L.G., Latil, J.-L., Mikhailova, I.A., Ropolo, P., Szives, O., 2011. Report on the 4th International Meeting of the IUGS Lower Cretaceous Ammonite Working Group, the "Kilian Group" (Dijon, France, 30th August 2010). Cretaceous Research 32, 786–793.

Reboulet, S., Szives, O. (reporters), Aguirre-Urreta, B., Barragán, R., Company, M., Idakieva, V., Ivanov, M., Kakabadze, M.V., Moreno-Bedmar, J.A., Sandoval, J., Baraboshkin, E.J., Çağlar, M.K., Főzy, I., González-Arreola, C., Kenjo, S., Lukeneder, A., Raisossadat, S.N., Rawson, P.F., Tavera, J.M., 2014. Report of the 5th International Meeting of the IUGS Lower Cretaceous Ammonite Working Group, the Kilian Group (Ankara, Turkey, 31st August 2013). Cretaceous Research 50, 126–137.

Reboulet, S., Szives, O. (reporters), Aguirre-Urreta, B., Barragán, R., Company, M., Frau, C., Kakabadze, M.V., Klein, J., Moreno-Bedmar, J.A., Lukeneder, A., Pictet, P., Ploch, I., Raisossadat, S.N., Vašíček, Z., Baraboshkin, E.J., Mitta, V.V., 2018. Report on the 6th International Meeting of the IUGS Lower Cretaceous Ammonite Working Group, the Kilian Group (Vienna, Austria, 20th August 2017). Cretaceous Research 91, 100–110.

Savostin, L., Sibuet, J.C., Zonenshain, L.P., Le Pichon, X., Roulet, M., 1986. Kinematic evolution of the Tethys belt from the Atlantic ocean to the Pamirs since the Triassic. Tectonophysics 123, 1–35.

Sissingh, W., 1977. Biostratigraphy of Cretaceous calcareous nannoplankton. Geologie en Mijnbouw 56, 37–65.

Tavera Benítez, J.-M., 1985. Los ammonites del Tithónico superior-Berriasense de la Zona Subbética (Cordilleras Béticas). Unpublished PhD thesis. Universidad de Granada, Granada, 381 pp.

1263 Thierstein, H. R., 1971. Tentative Lower Cretaceous calcareous nannoplankton zonation.
1264 Eclogae Geologicae Helvetiae 64, 459–488.
1265
1266 Wippich, M.G.E., 2001. Die tiefe Unter-Kreide (Berrias bis Unter-Hauterive) im
1267 südwestmarokkanischen Becken: Ammonitenfauna, Bio-und Sequenzstratigraphie.
1268 Unpublished PhD thesis, Universität Bochum, 142 pp.
1269
1270 Wippich, M., 2003. Valanginian (Early Cretaceous) ammonite faunas from the western High
1271 Atlas, Morocco, and the recognition of western Mediterranean "standard" zones. Cretaceous
1272 Research 24, 357–374.
1273

1274 **Appendix A - Taxonomic list of ammonites**

1275 Perisphinctoidea STEINMANN
1276 Neocomitidae SALFELD
1277 Berriasellinae SPATH
1278 *Berriasella* UHLIG; considered as a subgenus of *Berriasella* according to Klein
1279 (2005, p. 163)
1280 *Berriasella calisto* (D'ORBIGNY)
1281 *Berriasella picteti* (KILIAN)
1282 *Malbosiceras* GRIGORIEVA
1283 *Malbosiceras paramimounum* (MAZENOT)
1284 Neocomitinae SALFELD
1285 *Fauriella* NIKOLOV
1286 *Fauriella boissieri* (PICTET)
1287 *"Fauriella" kiliani* BULOT (*nomen nudum*)

Erdenella NIKOLOV

Erdenella paquieri (SIMIONESCU)

Tirnovella NIKOLOV

Tirnovella alpillensis (MAZENOT)

"Thurmanniceras" COSSMANN; the inverted commas indicate that the assignment of the species to that genus is provisional and they await revision (Kenjo, 2014; Reboulet et al., 2014; Company and Tavera, 2015)

"Thurmanniceras" gratianopolitense (SAYN); included in *Fauriella* according to Klein (2005, p. 262)

"Thurmanniceras" otopeta THIEULOY

"Thurmanniceras" pertransiens (SAYN)

"Thurmanniceras" thurmanni (PICTET & CAMPICHE)

Neocomites UHLIG; considered as a subgenus of *Neocomites* according to Klein (2005, p. 304)

Neocomites neocomiensiformis (UHLIG); included in *Busnardoites*? According to Klein (2005, p. 323)

Neocomites neocomiensis (D'ORBIGNY)

Neocomites peregrinus (RAWSON & KEMPER)

Neocomites premolicus SAYN

Kilianella UHLIG

Kilianella lucensis (SAYN)

Kilianella roubaudiana (D'ORBIGNY)

Kilianella thieuloyi BULOT (nomen nudum)

Sarasinella UHLIG

Sarasinella ambigua (UHLIG)

Sarasinella eucyrta (SAYN)

Luppovella NIKOLOV; considered as a subgenus of *Luppovella* according to Klein (2005, p. 294)

Luppovella superba (SAYN)

Busnardoites NIKOLOV

Busnardoites campylotoxus (UHLIG)

Karakaschiceras THIEULOY

K. inostranzewi (KARAKASCH)

Olcostephanidae HAUG

Spiticeratinae SPATH

Spiticeras UHLIG

Spiticeras multiforme DJANÉLIDZÉ

Olcostephaninae HAUG

Olcostephanus NEUMAYR

Olcostephanus josephinus (D'ORBIGNY)

Olcostephanus stephanophorus (MATHERON)

Olcostephanus tenuituberculatus BULOT

Saynoceras MUNIER-CHALMAS

Saynoceras verrucosum (D'ORBIGNY)

Polyptychitidae WEDEKIND

Paratollia CASEY

Peregrinoceras SAZONOVA

Peregrinoceras albidum CASEY

Polychtichites PAVLOW

Haploceratoidea VON ZITTEL

Haploceratidae VON ZITTEL

Neolissoceras SPATH

Neolissoceras grasianum (D'ORBIGNY)

Neolissoceras (*Vergoliceras*) ATROPS & REBOULET; *Vergoliceras* is considered as a genus according to Klein et al. (2009, p. 263)

Neolissoceras (*Vergoliceras*) *salinarium* (UHLIG)

Neolissoceras (*Vergoliceras*) *extracornutum* (CECCA)

Lytoceratoidea NEUMAYR

Lytoceratidae NEUMAYR

Lytoceratinae NEUMAYR

Lytoceras SUESS; as underlined by Klein et al. (2009, p. 134 and appendix n°18, p. 310), *Protetragonites* is probably a subjective synonym of *Lytoceras*)

Lytoceras honnoratianum (D'ORBIGNY); included in *Protetragonites* according to Klein et al. (2009, p. 139)

Lytoceras quadrisulcatum (d'ORBIGNY); included in *Protetragonites* according to Klein et al. (2009, p. 142)

Phylloceratoidea VON ZITTEL

Phylloceratidae VON ZITTEL

Phylloceratinae VON ZITTEL

Phylloceras (*Hypophylloceras*) SALFELD

Phylloceras (*Hypophylloceras*) *tethys* (D'ORBIGNY)

Ptychophylloceratinae COLLIGNON

Ptychophylloceras (*Semisulcatoceras*) JOLY

Ptychophylloceras (*Semisulcatoceras*) *semisulcatum* (D'ORBIGNY)

Calliphylloceratinae SPATH

Holcophylloceras SPATH

Holcophylloceras silesiacum (OPPEL)

Bochianitoidea SPATH

Bochianitidae SPATH

Bochianites LORY

Bochianites neocomiensis (D'ORBIGNY)

Protancyloceratoidea BREISTROFFER

Protancyloceratidae BREISTROFFER

Leptoceras UHLIG

Protancyloceras SPATH

Hoplitoidea DOUVILLÉ

Hoplitidae DOUVILLÉ

Hoplitinae DOUVILLÉ

Arrhaphoceras briacensis SCHOLZ

Appendix B - Taxonomic list and remarks on calcareous nannofossils

Axopodorhabdus dietzmannii Reinhardt, 1965

Anfractus harrisonii (Medd, 1979)

Assipetra terebrodentarius (Applegate et al. *in* Covington and Wise, 1987) Rutledge and Bergen *in* Bergen, 1994

Biscutum constans (Górka, 1957) Black *in* Black and Barnes, 1959

Biscutum ellipticum (Gorka, 1957) Grün *in* Grün and Allemann, 1975. This form is considered the synonym of *B. constans*

Calcicalathina oblongata (Worsley, 1971) Thierstein, 1971. Some authors reported *Calcicalathina erbae* Bergen, 1998 (synonym of *Calcicalathina* sp. A Bergen, 1994 and of

Calcicalathina praeoblongata Aguado et al., 2000) from the base of the Berriasian. *Calcicalathina praeoblongata*, which must be considered as a younger synonym of *C. erbae* Bergen 1984, is described as being smaller than *Calcicalathina oblongata* and having a wider rim. *Calcicalathina erbae* is described as a species of *Calcicalathina* with a low central area. According to the pictures shown (Aguado et al., 2000 fig. 8, plates 29-33; Bergen, 1994 pl. 1, fig. 11a, b; Bergen, 1998 pl. 1, figs 28, 29), we consider these specimens as very overgrown *Rhagodiscus asper* rather than as *Calcicalathina*. In fact, the diagnostic feature of *Calcicalathina* is to possess a high wall and a central area structure which rises above the distal margin of the wall forming a dome-like structure. Bergen (1998) describes *C. erbae* as a species of *Calcicalathina* "with a low central area", which is not consistent with the genus diagnosis. The specimens of *C. praeoblongata* figured by Aguado et al. (2000) have a low wall (better corresponding to the genus *Rhagodiscus*) and central area stuctures which do not rise above the wall. Also, Bergen (1998) states that overgrown specimens of *Rhagodiscus* can be confused with *Calcicalathina erbae*. This may explain the earlier record (Berriasian) of these forms, namely *C. erbae* and *C. praeoblongata*, with respect to true *C. oblongata* (base of Valanginian).

Conusphaera mexicana subsp. *mexicana* (Trejo, 1969)

Conusphaera rothii (Thierstein, 1971) Jakubowski, 1986

Cretarhabdus conicus Bramlette & Martini, 1964

Cretarhabdus inaequalis Crux, 1987

Cruciellipsis cuvillieri (Manivit, 1966) Thierstein, 1971

Cyclagelosphaera margerelii Noël, 1965

Discorhabdus ignotus (Górka, 1957) Perch-Nielsen, 1968. This is considered here as the same species as *D. rotatorius* of some authors (e.g., Erba et al., 2004)

Diadorhombus rectus Worsley, 1971

Diazomatolithus lehmanii Noël, 1965

Diazomatolithus subbeticus Grün, 1975

Ethmorhabdus hauterivianus (Black, 1971) Applegate et al. *in* Covington and Wise, 1987

Eiffellithus windii Applegate and Bergen, 1988

Helenea chiastia Worsley, 1971

Helenea quadrata (Worsley, 1971) Rutledge and Bown *in* Bown et al., 1998

Haqius circumradiatus (Stover, 1966) Roth, 1978. This taxa is found very overgrown in Vergol

Haqius ellipticus (Grün *in* Grün and Allemann, 1975) Bown, 1992 emend. Bown, 2005

Kokia curvata Perch-Nielsen, 1988

Micrantholithus hoschulzii (Reinhardt, 1966) Thierstein, 1971

Micrantholithus obtusus Stradner, 1963

Micrantholithus speetonensis Perch-Nielsen, 1979

Nannoconus bermudezii Brönnimann, 1955

Nannoconus broennimanni Trejo, 1959

Nannoconus bucheri Brönnimann, 1955

Nannoconus colomi Kamptner, 1938

Nannoconus dolomiticus Cita and Pasquare, 1959

Nannoconus globulus subsp. *globulus* Brönnimann, 1955

Nannoconus globulus subsp. *minor* (Brönnimann, 1955) Bralower *in* Bralower et al., 1989

Nannoconus inornatus Rutledge and Bown, 1996

Nannoconus kamptneri subsp. *minor* (Brönnimann, 1955) Bralower *in* Bralower et al., 1989

Nannoconus kamptneri subsp. *kamptneri* Brönnimann, 1955

Nannoconus oviformis Perch-Nielsen, 1988

Nannoconus quadratus (Noël 1959) Deres and Achéritéguy 1980

Nannoconus steinmannii subsp. *steinmannii* Kamptner, 1931

Nannoconus steinmannii subsp. *minor* (Kamptner, 1931) Deres and Achéritéguy, 1980

Nannoconus wintereri Bralower & Thierstein, 1989

Percivalia fenestrata (Worsley, 1971) Wise, 1983

Retecapsa angustiforata Black, 1971

Retecapsa octofenestrata Bralower *in* Bralower et al., 1989

Retecapsa surirella (Deflandre and Fert, 1954) Grün *in* Grün and Allemann, 1975

Rhagodiscus asper (Stradner, 1963) Reinhardt, 1967

Rhagodiscus gallagheri (Rutledge and Bown, 1996)

Rhagodiscus nebulosus (Bralower *in* Bralower et al., 1989)

Rhagodiscus pseudoangustus (Crux, 1987)

Rucinolithus wisei (Thierstein, 1971)

Sollasites horticus (Stradner et al. *in* Stradner and Adamiker, 1966) Cepek and Hay, 1969

Staurolithites crux (Deflandre and Fert, 1954) Caratini, 1963

Staurolithites laffittei Caratini, 1963

Staurolithites mutterlosei Crux, 1989

Tubodiscus frankiae Bown, 2005

Tubodiscus jurapelagicus (Worsley, 1971) Roth, 1973

Tubodiscus verenae Thierstein, 1973

Umbria granulosa Bralower and Thierstein *in* Bralower et al., 1989

Watznaueria barnesiae (Black*in* Black and Barnes, 1959) Perch-Nielsen, 1968

Watznaueria fossacincta (Black, 1971) Bown *in* Bown and Cooper, 1989. This taxa is considered in this work as a morphotype of *W. barnesiae*, according to biometric studies performed by Bornemann and Mutterlose (2006)

Watznaueria biporta (Bukry, 1969)

1463 *Watznaueria britannica* (Stradner, 1963) Reinhardt, 1964

1464 *Watznaueria communis* Reinhardt, 1964

1465 *Watznaueria manivitiae* Bukry, 1973

1466 *Watznaueria ovata* Bukry, 1969

1467 *Zeugrhabdotus diplogrammus* (Deflandre *in* Deflandre and Fert, 1954) Burnett *in* Gale et al.,

1468 1996

1469 *Zeugrhabdotus elegans* (Gartner 1968) Burnett *in* Gale et al. 1996

1470 *Zeugrhabdotus embergeri* (Noël, 1958) Perch-Nielsen, 1984

1471 *Zeugrhabdotus erectus* (Deflandre *in* Deflandre and Fert, 1954) Reinhardt, 1965

1472 *Zeugrhabdotus fissus* Grün and Zweili, 1980

1473 *Zeugrhabdotus trivectis* Bergen, 1994

1474 *Zygolithus xenotus* Stover, 1966

1475

1476 **Figure captions**

1477 Figure 1. Geological setting. Fig.1A. Location map of the Vergol section (Montbrun-les-

1478 Bains, Drôme, France). Fig. 1B. Palaeogeographic map of the Vocontian basin (SE France,

1479 Lower Cretaceous). Fig. 1C. Lithology of the Vergol section; the Berriasian–Valanginian

1480 boundaries *sensu* Blanc et al. (1994) and *sensu* Kenjo (2014, this work) are indicated, see

1481 arrows 1 and 2, respectively; the numbering of beds is made using two letters, “B” and “V”

1482 for “Berriasian” and “Valanginian”, respectively, according to the former position of the

1483 Berriasian–Valanginian boundary *sensu* Blanc et al. (1994); OB: the “Otopeta bundle” that is

1484 composed by 12 calcareous beds (from VGL-B118 to VGL-B129).

1485

1486 Figure 2. Stratigraphic distribution of macrofauna (mainly ammonites) in the Vergol section

1487 and ammonite zonation; Fig. 2A: part A, succession below the slump i.e. from layers VGL-

B95 to V43; Fig. 2B: part B, succession above the slump i.e. from layers VGL-V45 to V69. Layers of sampling and number of specimens are indicated. A question mark is added when identification is doubtful. N = Neocomitidae; O = Olcostephanidae; H = Haploceratidae; L = Lytoceratidae; P = Phylloceratidae; B = Bochianitidae; P = Protancyloceratidae.

Figure 3. Ammonites (Neocomitids) of the Vergol section (collection Kenjo and Reboulet, UCBL-FSL, University of Lyon, France); see appendix A for taxonomy. A, *B. calisto*, UCBL-FSL 485412, VGL-B113, *T. alpillensis* (Sub-)Zone. B, *F. boissieri*, UCBL-FSL 485591, VGL-B125, *T. alpillensis* Zone, "*T.*" *otopeta* Subzone. C, *T. alpillensis*, UCBL-FSL 485603, VGL-B116, *T. alpillensis* Zone, "*T.*" *otopeta* Subzone. D, *T. alpillensis*, UCBL-FSL 485397, VGL-B112, *T. alpillensis* (Sub-)Zone. E, *E. paquieri*, UCBL-FSL 485337, VGL-B121 *T. alpillensis* Zone, "*T.*" *otopeta* Subzone. Scale bars represent 1 cm.

Figure 4. Ammonites (Neocomitids) of the Vergol section (collection Kenjo and Reboulet, UCBL-FSL, University of Lyon, France); see appendix A for taxonomy. A, "*T.*" *otopeta*, UCBL-FSL 485350, VGL-B129, *T. alpillensis* Zone, "*T.*" *otopeta* Subzone. B, "*T.*" *otopeta*, UCBL-FSL 485345, VGL-B127, *T. alpillensis* Zone, "*T.*" *otopeta* Subzone. C, "*T.*" *pertransiens*, UCBL-FSL 485377, VGL-V1b, "*T.*" *pertransiens* Zone, *N. premolicus* Subzone. D, "*T.*" *pertransiens*, UCBL-FSL 485382, VGL-B146, "*T.*" *pertransiens* Zone, *N. premolicus* Subzone. E, "*T.*" *pertransiens*, UCBL-FSL 485380, VGL-V22, "*T.*" *pertransiens* Zone ~~*N. premolicus* Subzone~~. F, "*T.*" *pertransiens*, UCBL-FSL 485379, VGL-B136, "*T.*" *pertransiens* Zone, *N. premolicus* Subzone. G, "*T.*" *pertransiens*, UCBL-FSL 485376, VGL-B148, "*T.*" *pertransiens* Zone, *N. premolicus* Subzone. H, "*T.*" *pertransiens*, UCBL-FSL 485546, VGL-V16, "*T.*" *pertransiens* Zone ~~*N. premolicus* Subzone~~. I, *T.*" *gratianopolitense*,

UCBL-FSL 485386, VGL-B149, "*T.*" *pertransiens* Zone, *N. premolicus* Subzone. Scale bars represent 1 cm.

Figure 5. Ammonites (Neocomitids) of the Vergol section (collection Kenjo and Reboulet, UCBL-FSL, University of Lyon, France); see appendix A for taxonomy. A, *N. neocomiensiformis*, UCBL-FSL 485389, VGL-V43, "*N.*" *neocomiensiformis* Zone, ~~*N. premolicus* Subzone~~. B, *N. neocomiensiformis*, UCBL-FSL 485571, VGL-V68, *N. neocomiensiformis* Zone. C, *K. lucensis*, UCBL-FSL 485440, VGL-V9, "*T.*" *pertransiens* Zone, *N. premolicus* Subzone. D, *K. roubaudiana*, UCBL-FSL 485439, VGL-V31, "*T.*" *pertransiens* Zone, ~~*N. premolicus* Subzone~~. E, *L. superba*, UCBL-FSL 485663, VGL-V64, *N. neocomiensiformis* Zone. F, *S. eucyrta*, UCBL-FSL 485446, VGL-V28, "*T.*" *pertransiens* Zone ~~*N. premolicus* Subzone~~. Scale bars represent 1 cm.

Figure 6. Ammonoids (Olcostephanids, Haploceratids, Phylloceratids, Lytoceratids and Heteromorphs) of the Vergol section (collection Kenjo and Reboulet, UCBL-FSL, University of Lyon, France); see appendix A for taxonomy. A, *O. aff. tenuituberculatus*, UCBL-FSL 485474, VGL-V62, *N. neocomiensiformis* Zone. B, *S. multiforme*, UCBL-FSL 485476, VGL-B112, *T. alpillensis* (Sub-)Zone. C, *N.* (*V.*) *extracornutum*, UCBL-FSL 485468, VGL-V46, ~~"*T.*" *pertransiens*~~ *N. neocomiensiformis* Zone ~~*N. premolicus* Subzone~~. D, *N.* (*V.*) *salinarium*, UCBL-FSL 485463, VGL-V2, "*T.*" *pertransiens* Zone, *N. premolicus* Subzone. E, *L. honnoratianum*, UCBL-FSL 485455, VGL-B121, *T. alpillensis* Zone, "*T.*" *otopeta* Subzone. F, *L. quadrisulcatum*, UCBL-FSL 485449, VGL-V16, "*T.*" *pertransiens* Zone ~~*N. premolicus* Subzone~~. G, *H. silesiacum*, UCBL-FSL 485795, VGL-B103, *T. alpillensis* (Sub-)Zone. H, *P. (S.) semisulcatum*, UCBL-FSL 485458, VGL-V9, "*T.*" *pertransiens* Zone, *N. premolicus* Subzone. I, *P. (H.) tethys*, UCBL-FSL 485774, VGL-V29, "*T.*" *pertransiens* Zone ~~*N.*~~

~~*premolicus* Subzone~~. J, *B. neocomiensis*, UCBL-FSL 485760, VGL-V64, *N. neocomiensiformis* Zone. K, *Protancyloceras* sp. ind., UCBL-FSL 485766, VGL-B141, "*T.*" *pertransiens* Zone, *N. premolicus* Subzone. Scale bars represent 1 cm.

Figure 7. Micrographs of selected calcareous nannofossil species recorded at Vergol with the sample where the specimens have been recorded. White bar = 5 µm. (1) *A. dietzmannii* VGL-V2CM. (2) *B. constans* VGL-V2CM. (3) *C. oblongata* VGL-B146M, the earliest recorded specimen at Vergol. Note the wall which is faint grey in optical microscope, from where rise up a dome-like structure which appears much brighter. (4) *C. oblongata* VGL-V3M. (5) *C. oblongata* VGL-V3M. (6) *C. rothii* VGL-V2CM. (7) *C. cuvillieri* VGL-V12. (8) *C. margerelii* VGL-B108M. (9) *D. lehmanii* VGL-B108M. (10) *D. subbeticus* VGL-B113CM. (11) *D. ignotus* VGL-B150M. (12) *E. windii* VGL-B151. (13) *K. curvata* VGL-B112M. (14) *M. hoschulzii* VGL-V2CM. (15) *M. obtusus* VGL-B112M. (16) *M. speetonensis* VGL-V38M. (17) *M. quadratus* VGL-V2CM. (18) *N. colomii* VGL-B113CM. (19) *N. steinmannii steinmannii* VGL-B108M. (20) *N. globulus globulus* VGL-V34M. (21) *N. kamptneri kamptneri* VGL-V34M. (22) *P. fenestrata* VGL-B112M. (23) *P. fenestrata* VGL-B151M. (24) *R. angustiforata* VGL-V2CM. (25) *R. octofenstrata* VGL-V34M.

Figure 8. Micrographs of selected calcareous nannofossil species recorded at Vergol with the sample where the specimens have been recorded. White bar = 5 µm. (1) *R. surirella* VGL-V34M. (2) *R. achylostaurion* VGL-V12. (3) Large *R. asper* VGL-V1b. (4) Large and overgrown *R. asper* VGL-V1b (closely resembling to *C. erbae* Bergen, 1998 and *C. praeoblongata* Aguado et al., 2000). It is well visible that the central area structure does not rise from the wall (as is in the diagnosis of the genus *Calcicalathina*), but the insertions of the central area grid on the inner part of the wall are visible. (5) *R. dekaenelii* VGL-V1b. (6) *R.*

gallagheri VGL-V42M. (7) *R. nebulosus* VGL-V2CM. (8) *R.* aff. *R. pseudoangustus* VGL-V2CM. (9) *R. laffittei* VGL-V34M. (10) *R. wisei* VGL-V2CM. (11) *S. crux* VGL-V2C. (12) *S. mutterlosei* VGL-V31M. (13) *T. frankiae* VGL-V2CM. (14) *T. frankiae* VGL-V2CM. (15) *T. jurapelagicus* VGL-V3M. (16) *W. barnesiae* VGL-B108M. (17) *W. biporta* VGL-B116M. (18) *W. britannica* VGL-V12. (19) *W. fossacincta* VGL-B108M. (20) *W. manivitiae* VGL-B113CM. (21) *Z. elegans* VGL-V2C. (22) *Z. embergerii* VGL-B113CM. (23) *Z. embergerii* VGL-B113CM. (24) *Z. erectus* VGL-B151. (25) *Z.trivectis* VGL-V3M.

Figure 9. Nannofossil events recorded in the Vergol section. Nannofossil zones are after Thierstein (1971) modified by Bralower et al. (1989).

Figure 10. Comparison of the biostratigraphic and magnetic zonal schemes of Bralower et al. (1989) and Bown et al. (1998) for the interval around the Berriasian–Valanginian boundary.

Figure 11. Comparison of the biostratigraphic zonal schemes of Aguado et al. (2000), Duchamp-Alphonse et al. (2007) and Kenjo (2014; this work) for the interval around the Berriasian–Valanginian boundary.

Figure 12. Principal Component Analysis (PCA) applied to percentages (log values) of calcareous nannofossil taxa. For further explanation, see the text.

Figure 13. Stratigraphical evolution of PCA factorial scores, nannofossil absolute abundance, Shannon diversity index in the Vergol section. The shaded area represents the interval around the Berriasian–Valanginian boundary where major changes occurred in calcareous nannofossil assemblages.

Figure 14. Correlations of lithology and zonal schemes of the Vergol section *sensu* (Kenjo, 2014; this work) *versus* Blanc et al. (1994) and Blanc (1996).

Table 1. Distribution of all the recorded calcareous nannofossil taxa in the Vergol section. The FSL number is shown for each sample.

Table 2. Numerical values for PCA results, absolute abundance and species diversity as calculated in this work.

NB: Tables 1 and 2 are in Supplementary data/material.

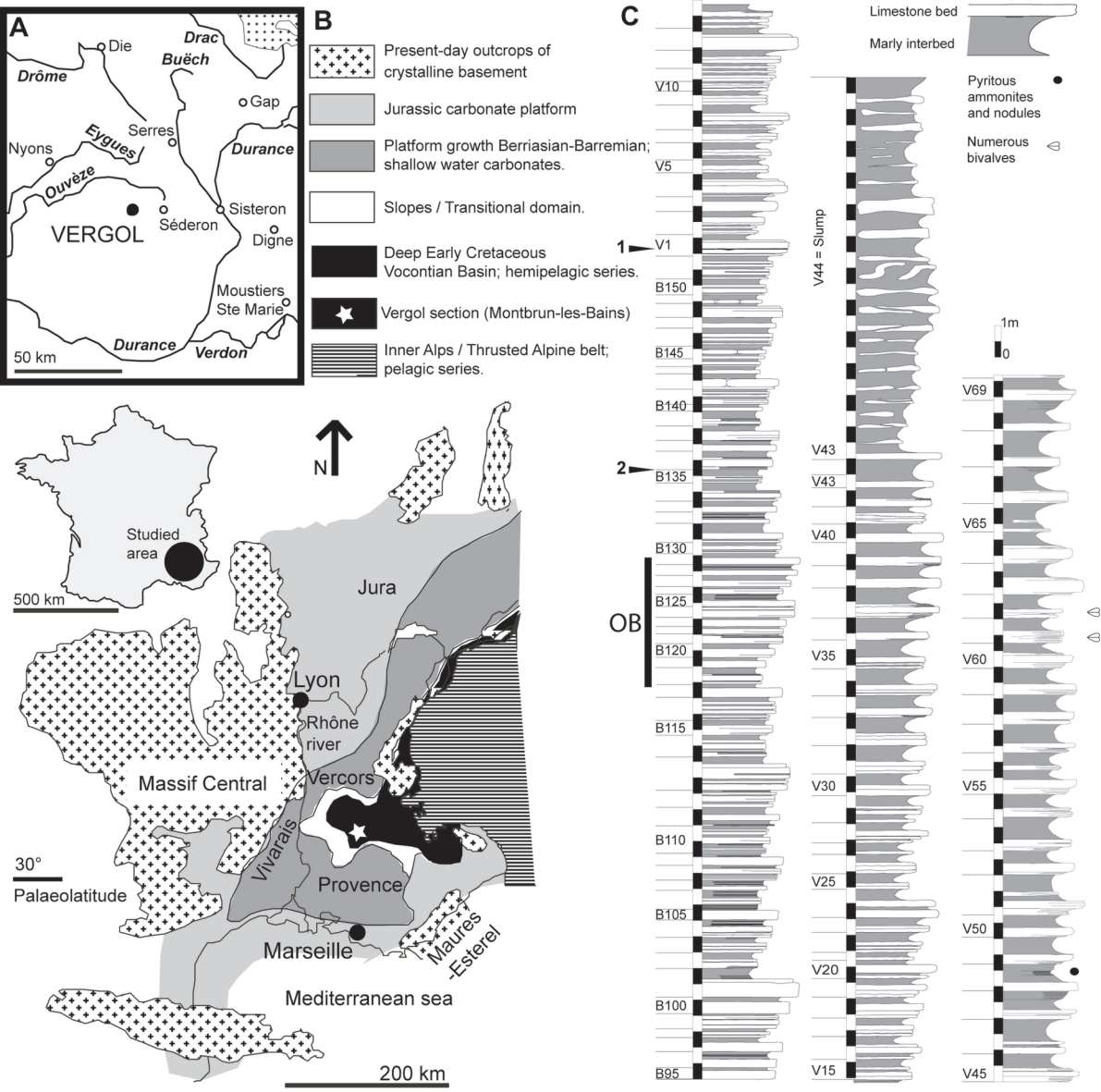

Figure 1 - 2 column fitting image

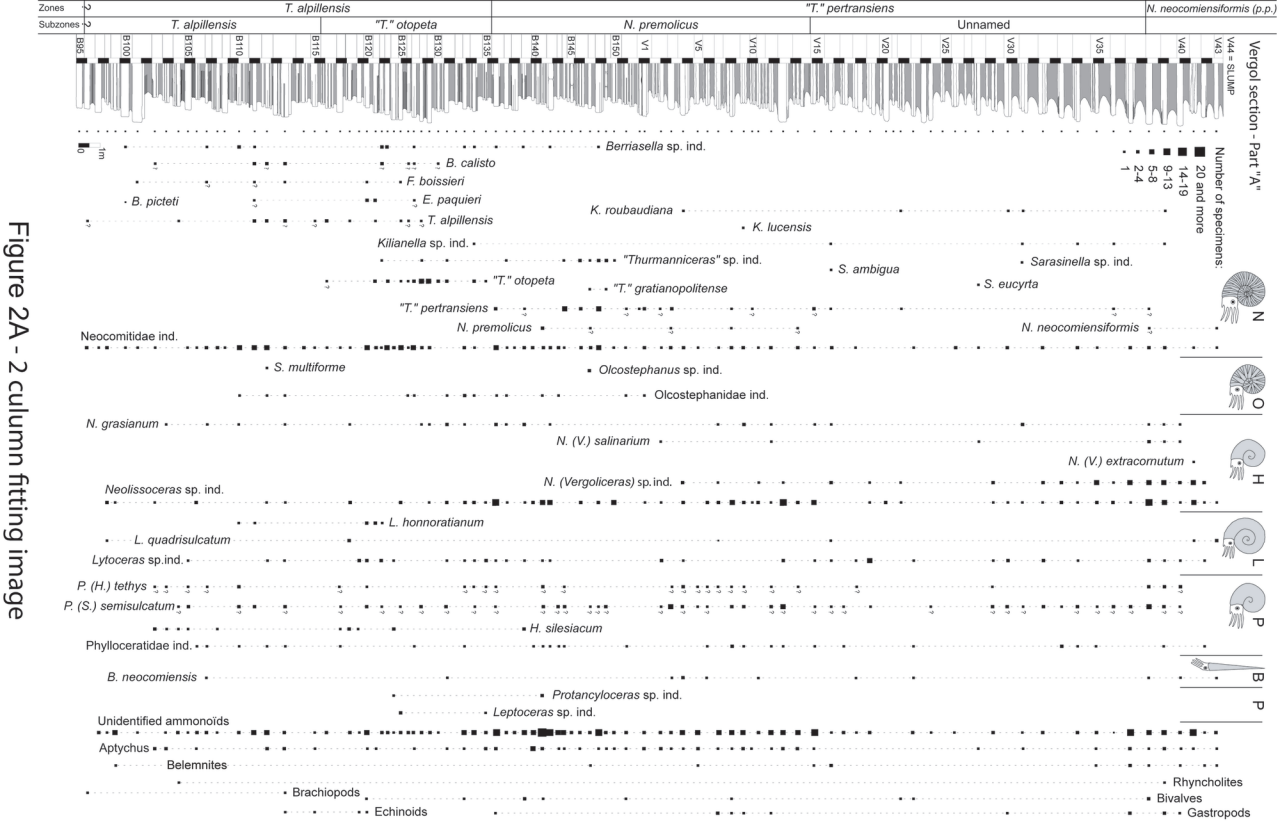

Figure 2A - 2 culumn fitting image

Figure 2B - 2 culumn fitting image

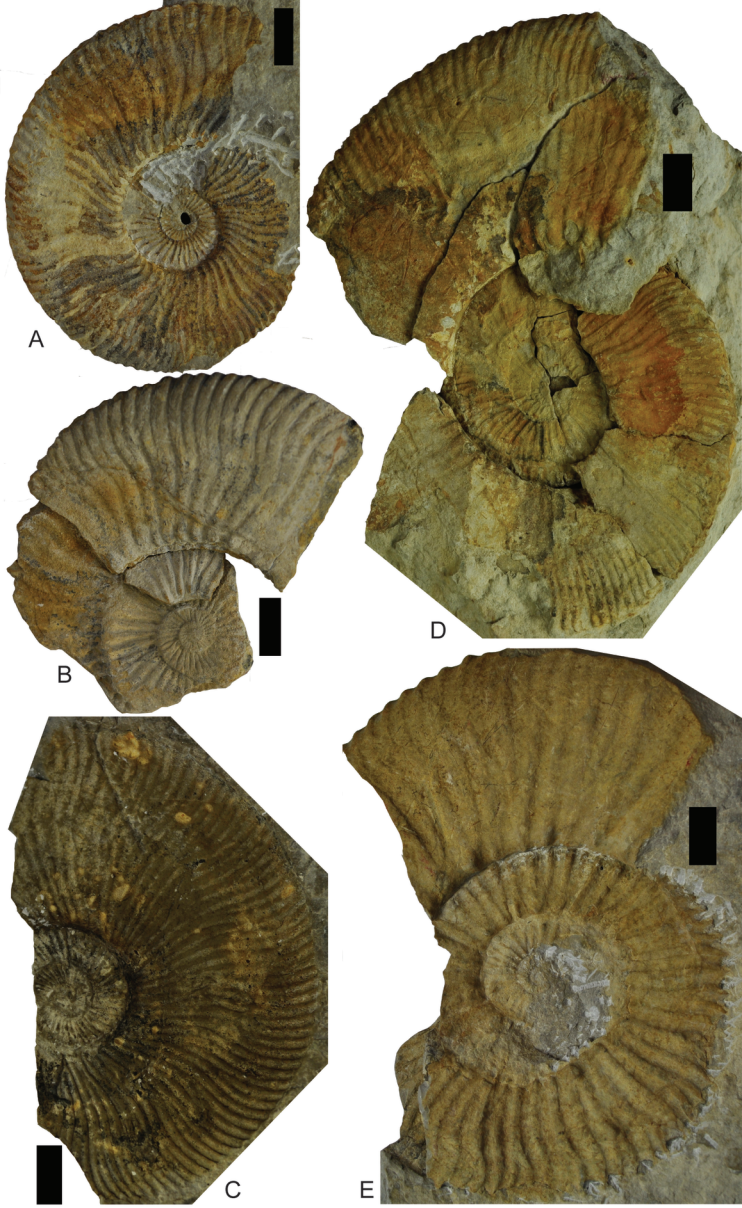

Figure 3 - 2 culumn fitting image

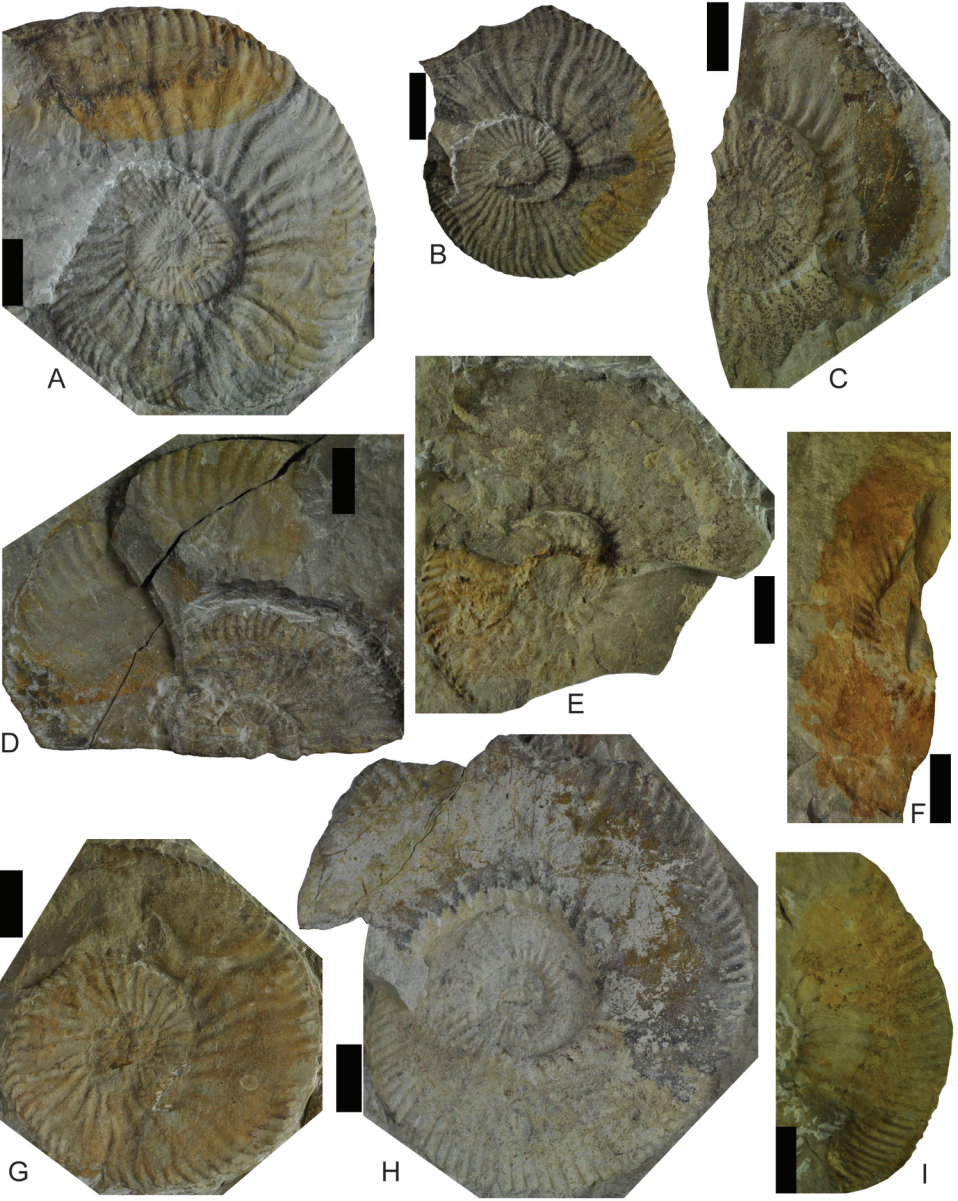

Figure 4 - 2 culumn fitting image

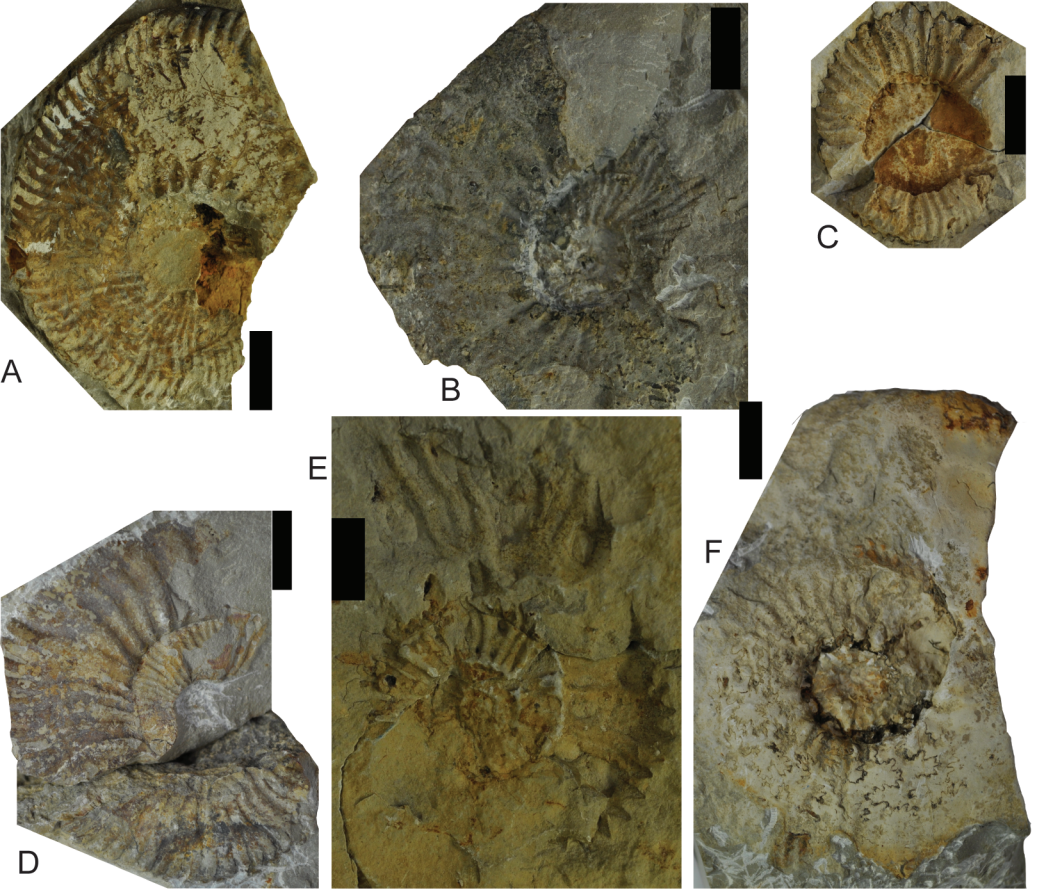

Figure 5 - 2 culumn fitting image

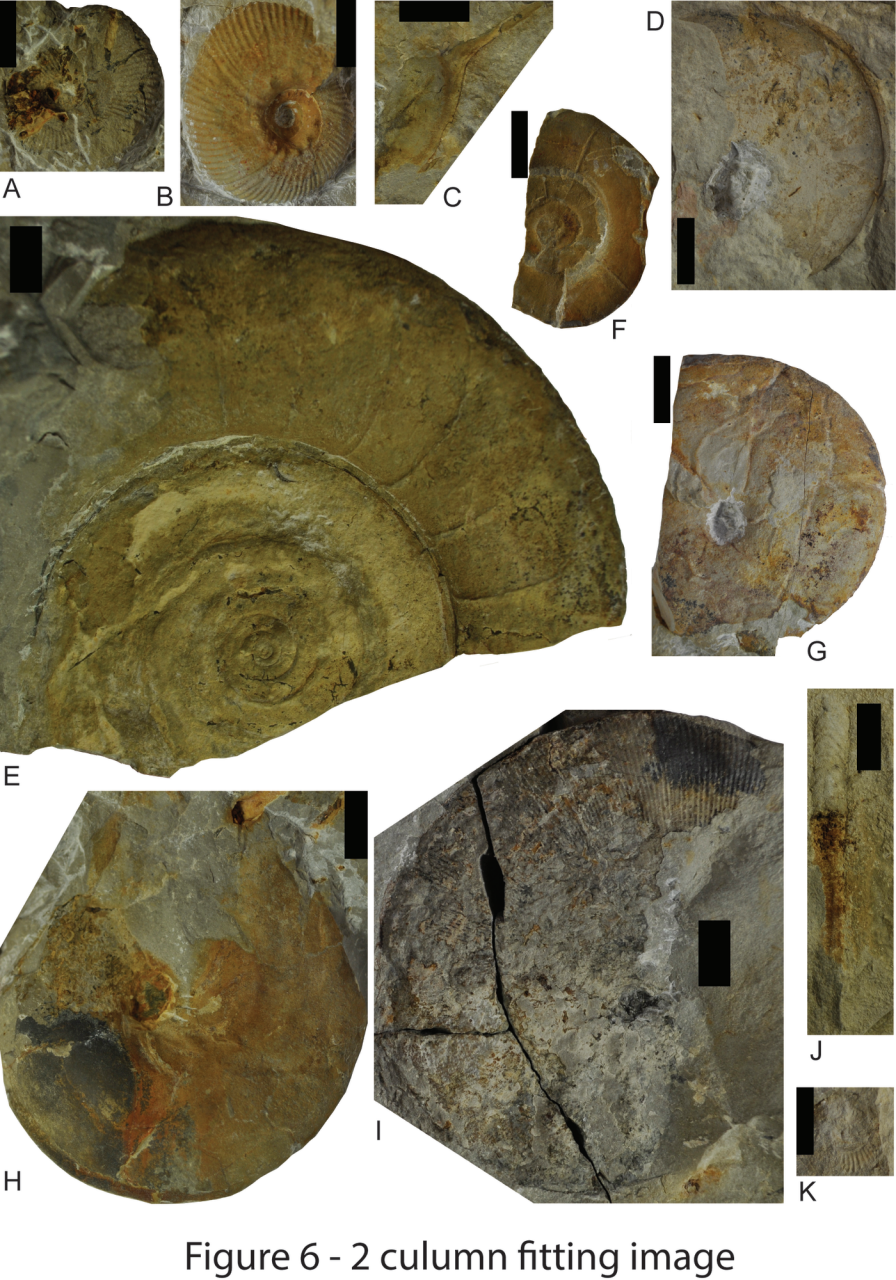

Figure 6 - 2 culumn fitting image

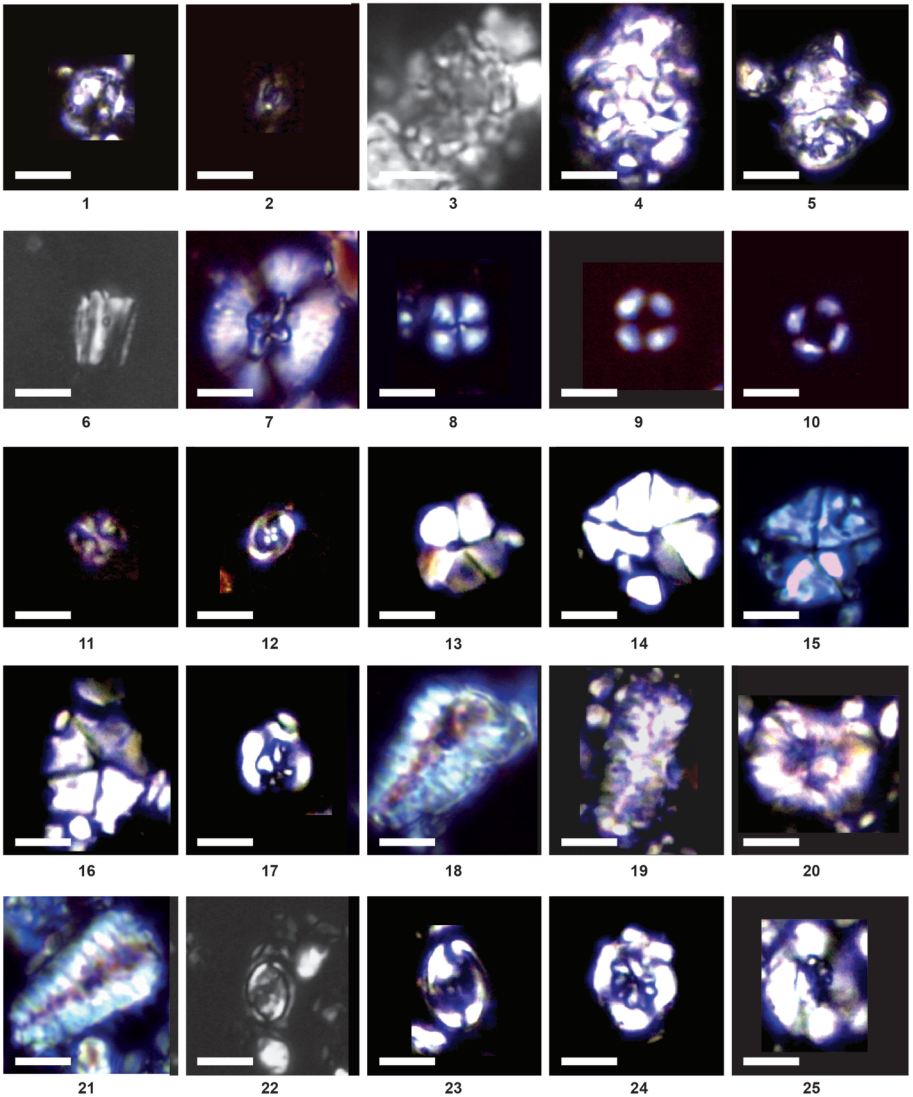

Figure 7

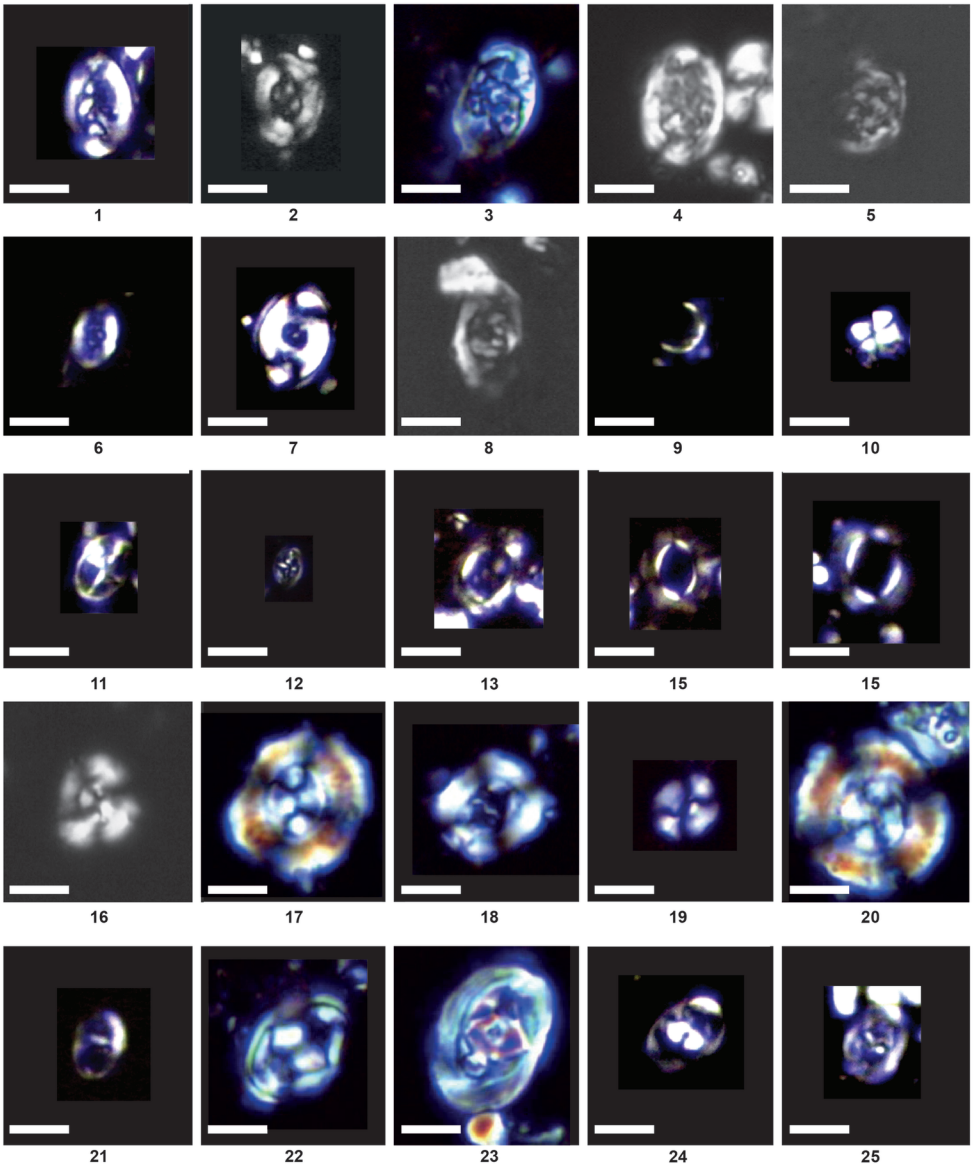

Figure 8

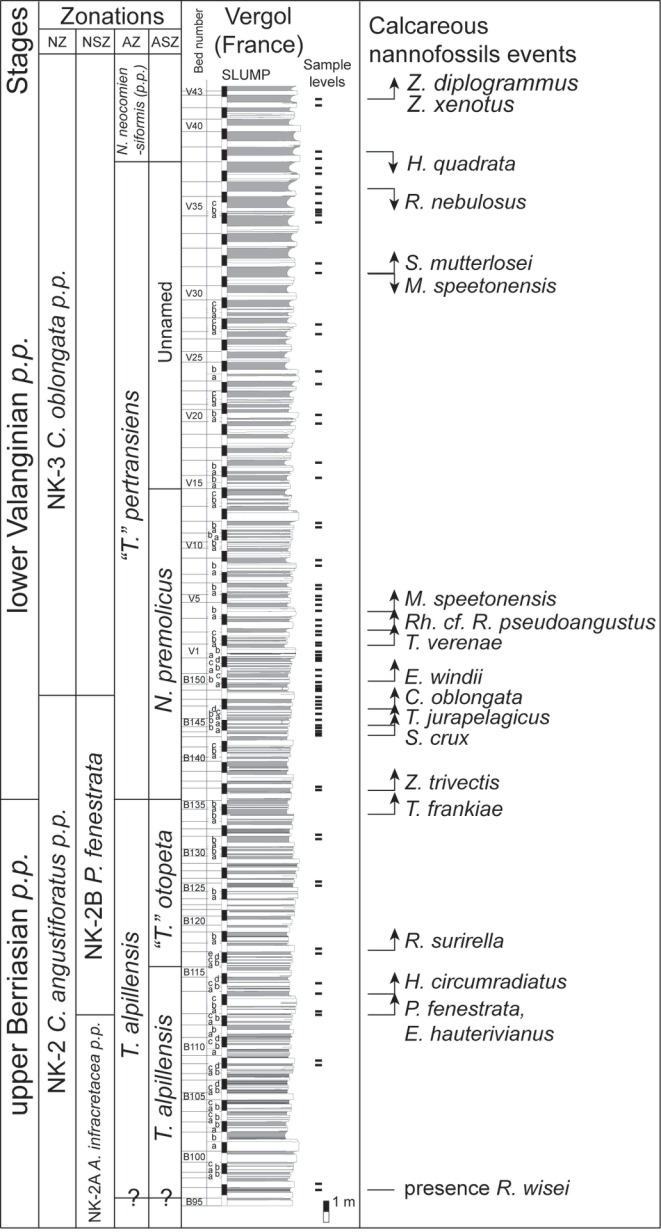

Figure 9 - 2 (1.5?) column fitting image

Figure 10 - 2 (1.5?) column fitting image

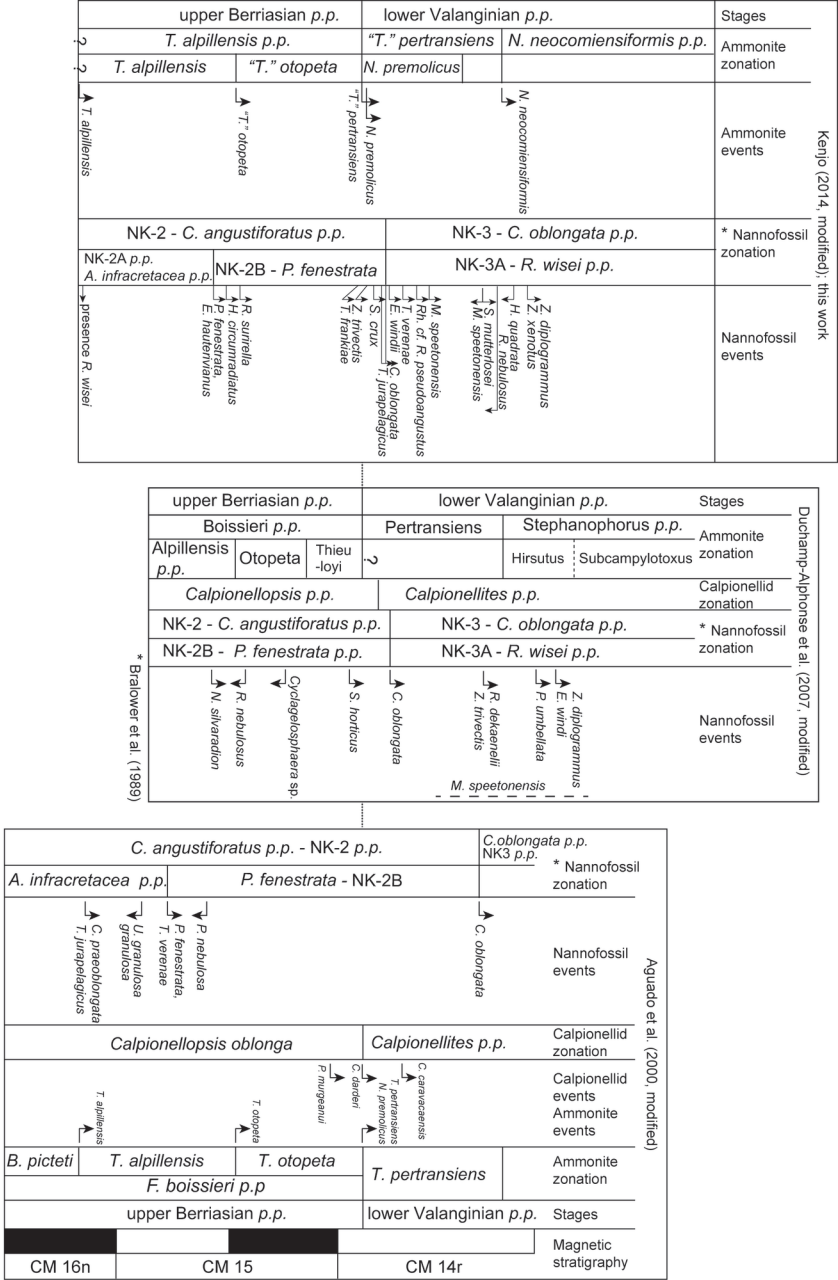

Figure 11 - 2 culumn fitting image

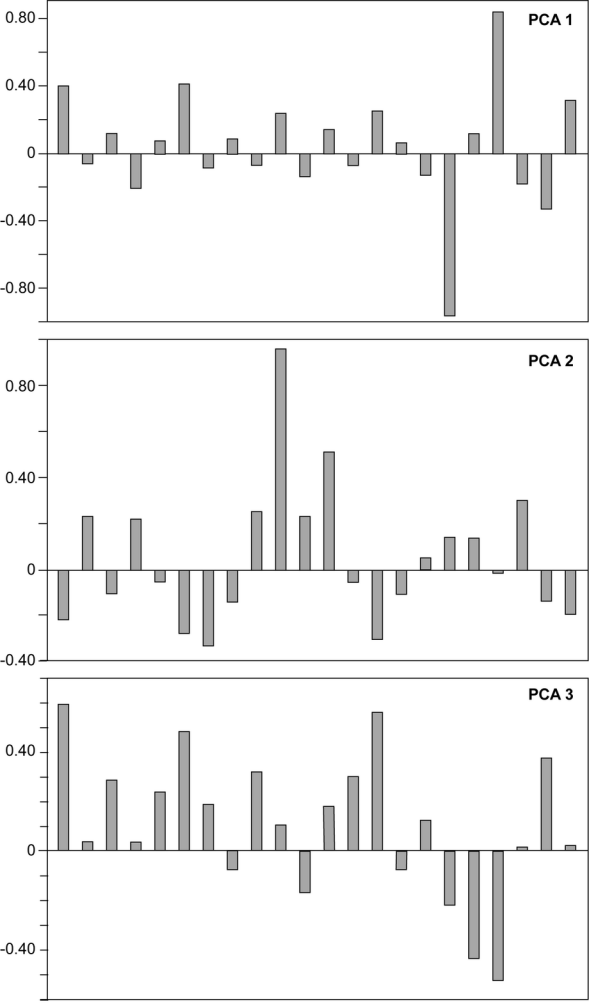

Figure 12 - 2 (1.5?) culumn fitting image

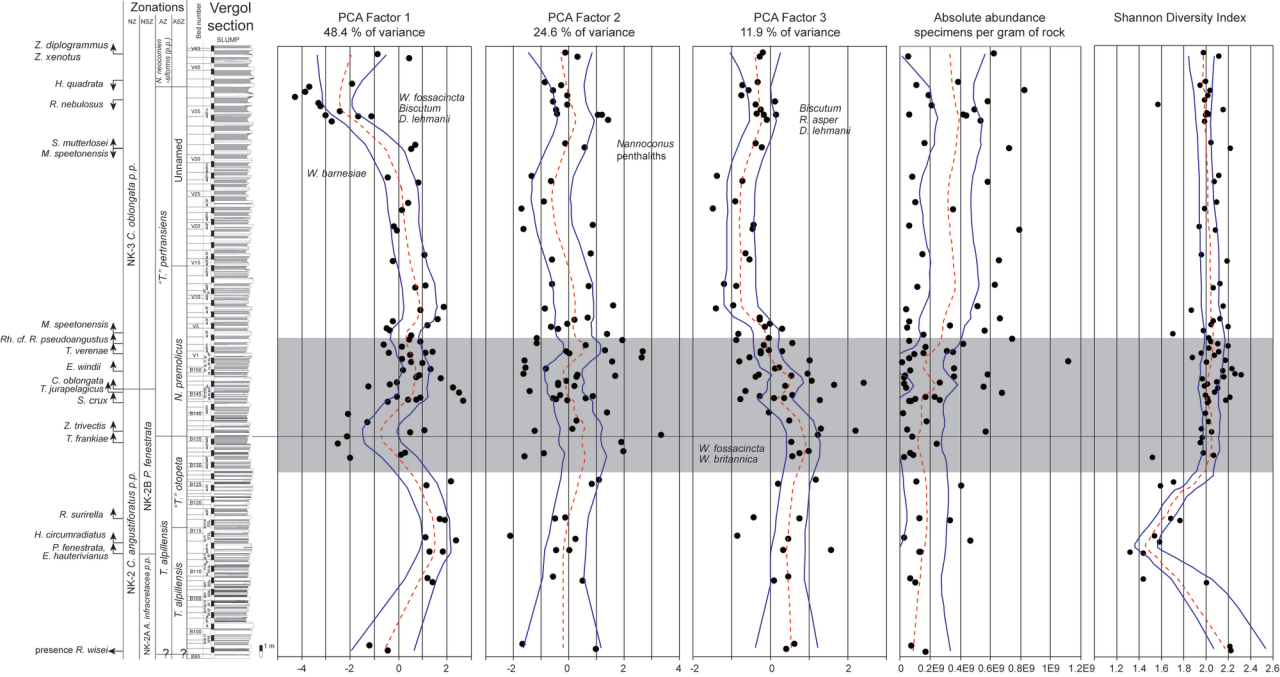

Figure 13 - 2 column fitting image

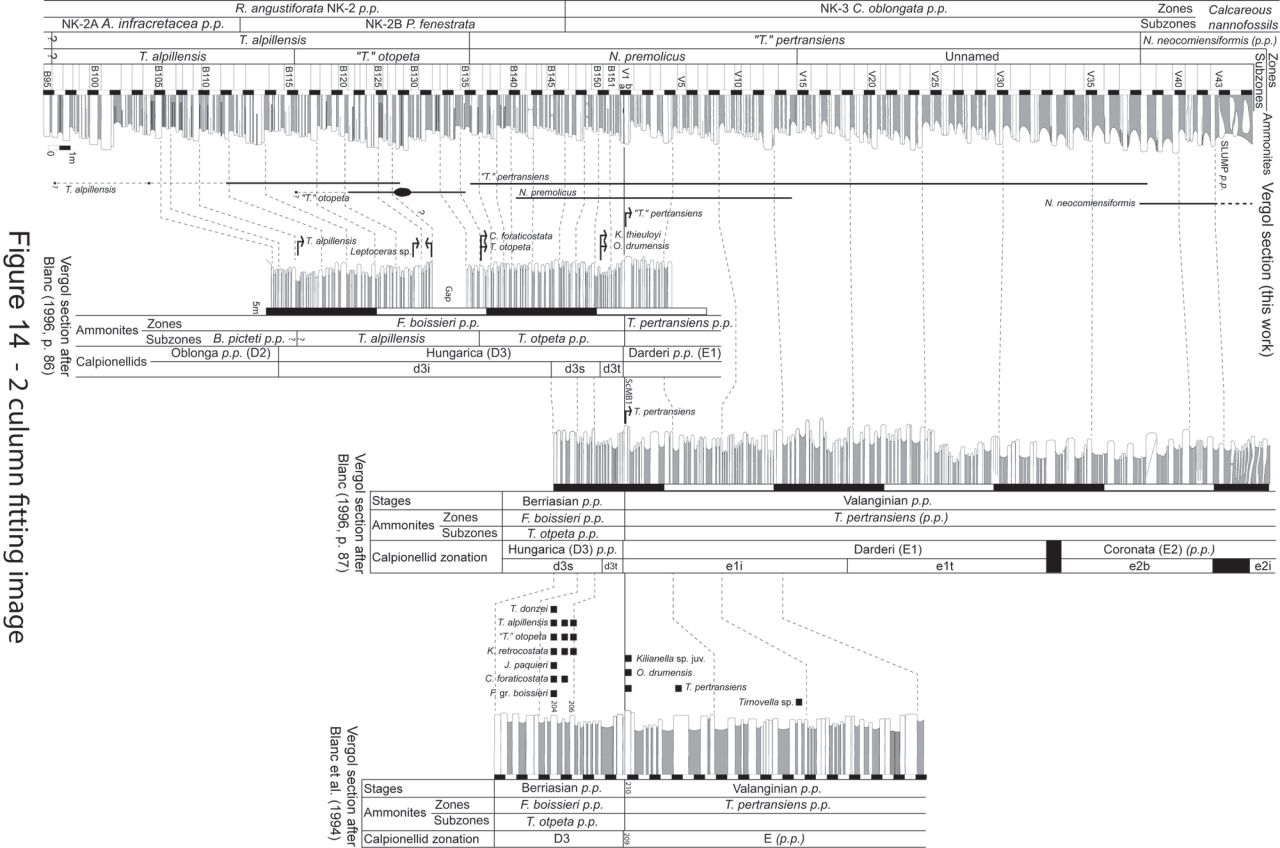

Figure 14 - 2 culumn fitting image

FSL N°	Section	Beds	A. dietzmanni	A. harrisonii	A. infracretacea	B. constans/ellipticum	C. cuvillieri	C. margerelii/rotaclypeata	C. mexicana mexicana	C. mexicana minor	C. rothii	C. oblongata	C. conicus	C. inaequalis	C. aff. striatus	D. ignotus/rotatorius	D. rectus	D. lehmanii	D. subbeticus	E. hauterivianus	E. windii	H. chiastia	H. quadrata	H. circumradiatus	H. ellipticus	K. curvata	M. hoschulzii	M. obtusus	M. speetonensis	N. bermudezii	N. broennimanni	N. bucheri	N. colomi	N. dolomiticus	N. globulus globulus	N. globulus minor	N. inornatus	N. kamptneri minor	N. kamptneri kamptneri	N. oviformis	N. quadratus	N. steinmannii steinmannii	N. steinmannii minor	N. wintereri	P. fenestrata	R. angustiforata	R. octofenestrata	R. surirella	R. asper	R. gallagheri	R. nebulosus	R. lafittei	R. wisei	S. horticus	S. crux	S. lafittei	S. mutterlosei	T. frankia	T. jurapelagicus	T. verenae	U. granulosa	W. barnesiae/fossacincta	W. biporta	W. britannica/communis	W. manivitiae	W. ovata	Z. diplogrammus	Z. elegans	Z. embergeri	Z. erectus	Z. fissus	Z. trivectis	Z. xenotus
766104	Vergol	VGLV42M	.	.	.	•	•	•	•	.	.	•	.	.	.	•	•	•	•	.	.	.	.	.	.	.	•	•	.	.	.	.	.	.	•	.	.	.	•	.	.	•	•	.	.	.	.	.	•	•	.	.	.	.	•	.	.	.	.	.	.	•	•	•	•	•	•	•	•	.	.	•	•
766105	Vergol	VGLV42L	.	.	.	•	•	•	.	.	.	.	•	.	.	•	.	•	•	.	.	.	.	.	.	.	.	•	.	.	.	.	.	.	•	.	.	•	•	.	.	•	•	.	.	.	.	.	.	.	.	.	.	.	•	.	.	.	.	.	.	•	.	•	•	.	.	•	•	.	.	.	.
766106	Vergol	VGLV38M	.	.	.	.	•	•	•	.	.	.	•	•	•	.	.	•	•	.	.	•	•	.	.	.	.	•	.	.	.	.	.	.	•	.	•	.	•	.	.	•	•	.	.	.	.	.	.	.	.	.	•	.	.	.	.	.	.	.	.	•	•	•	•	•	.	.	•	.	.	.	.
766107	Vergol	VGLV38L	•	.	.	•	•	•	•	.	.	.	•	.	.	•	.	•	.	.	.	.	.	.	.	.	.	•	.	.	.	.	.	.	.	.	•	.	.	.	.	•	•	•	.	.	.	.	.	•	.	.	.	•	.	.	.	.	.	.	.	•	.	•	•	•	.	.	•	.	.	.	.
766108	Vergol	VGLV37M	•	.	.	•	•	•	.	.	.	.	.	.	.	•	.	•	•	.	.	.	.	.	.	.	.	.	.	•	.	•	.	.	.	.	•	.	.	.	.	•	•	•	.	.	.	.	.	•	.	.	.	.	.	.	.	.	.	.	.	•	•	•	•	•	.	.	•	.	.	.	.
766109	Vergol	VGLV37L SO	•	.	.	•	•	•	•	.	.	.	.	.	.	•	.	•	.	.	.	.	.	.	.	.	.	•	.	.	.	.	•	.	•	.	•	.	.	.	.	•	•	.	.	.	.	.	.	•	.	.	.	•	.	.	.	.	.	.	.	•	•	•	•	.	.	.	•	.	.	.	.
766110	Vergol	VGLV36M	•	.	.	•	•	•	.	.	.	.	•	•	.	•	.	•	•	.	.	.	.	.	.	.	.	•	.	.	.	.	.	.	.	.	•	.	.	•	.	•	•	.	•	.	•	.	•	•	•	.	•	•	.	•	.	.	.	.	.	•	•	•	•	•	.	.	•	.	.	.	.
766111	Vergol	VGLV36L	.	.	.	•	•	•	.	.	.	.	.	.	.	•	.	•	•	.	.	.	.	.	.	.	.	•	.	.	.	.	.	.	•	.	•	.	.	.	.	•	•	.	.	.	.	.	.	.	.	.	.	.	.	.	.	.	.	.	.	•	•	•	•	•	.	.	•	.	.	.	.
766112	Vergol	VGLV35CM	•	.	.	•	•	•	•	.	.	•	•	.	.	•	.	•	•	.	.	.	.	•	.	.	.	.	.	•	.	.	.	.	•	.	•	.	.	.	.	.	•	.	•	•	•	.	.	.	•	.	•	.	.	.	.	.	.	.	.	•	•	•	•	•	.	.	•	.	.	.	.
766113	Vergol	VGL35CL	•	.	.	•	•	•	•	.	.	.	.	.	.	•	.	•	•	.	.	.	.	.	.	.	.	•	.	.	.	.	.	.	•	.	•	•	.	.	.	•	•	.	•	•	•	.	•	•	.	.	•	.	.	.	.	.	.	.	.	•	•	•	•	•	.	.	•	.	.	.	.
766114	Vergol	VGLV35bM	•	.	.	.	•	•	•	.	.	.	.	•	.	.	.	•	•	.	.	.	•	•	.	.	.	•	.	.	.	.	.	.	.	.	•	.	.	.	.	•	•	•	.	.	.	.	.	.	.	.	.	•	.	.	.	.	.	.	.	•	•	•	•	.	.	.	•	.	.	.	.
766115	Vergol	VGLV35bL	•	.	.	•	•	•	.	.	.	.	.	.	.	•	.	•	•	.	.	•	.	.	.	.	•	•	.	.	.	.	•	•	•	.	•	.	.	.	.	•	•	.	.	•	.	.	.	.	.	.	.	.	.	.	.	.	.	.	.	•	•	•	•	•	.	.	•	.	.	.	.
766116	Vergol	VGLV34M	.	•	•	.	•	•	.	.	.	.	•	.	.	.	.	•	•	.	.	•	•	.	.	.	•	•	.	.	.	.	.	•	•	.	•	.	.	.	.	•	•	.	.	.	.	.	.	.	.	•	.	.	.	.	.	.	.	.	.	•	•	•	•	•	.	.	•	.	.	.	.
766117	Vergol	VGLV32L	.	.	.	•	.	•	.	.	.	.	.	.	.	•	.	•	•	.	.	.	.	.	.	.	.	•	.	.	.	.	.	.	•	.	.	•	•	.	.	•	•	.	.	•	.	.	•	.	.	.	.	•	•	.	.	.	.	.	.	•	.	•	•	.	.	•	•	.	.	.	.
766118	Vergol	VGLV31M	.	.	.	•	•	•	•	.	.	.	.	.	•	.	.	•	•	.	.	.	.	.	.	.	.	•	•	.	.	.	.	.	•	.	.	.	•	.	.	•	•	.	.	.	•	.	•	.	.	.	.	.	•	.	•	.	.	.	.	•	.	•	•	.	.	.	•	.	.	•	.
766119	Vergol	VGLV28CL	.	.	.	•	•	•	•	.	.	.	.	.	.	•	.	•	.	.	.	.	.	.	.	.	.	•	.	.	.	.	.	.	•	.	.	.	•	.	.	.	•	.	.	.	.	.	•	.	.	.	.	•	.	.	.	.	.	.	.	•	.	•	•	.	.	•	•	.	.	.	.
766120	Vergol	VGLV27M	.	.	.	•	.	•	.	.	.	.	.	.	.	•	.	•	•	.	.	.	.	.	.	.	.	•	.	.	.	.	.	.	•	.	.	.	•	.	.	•	•	.	.	•	.	.	•	.	.	.	.	.	•	.	.	.	.	.	.	•	.	•	•	•	.	•	•	.	.	.	.
766121	Vergol	VGLV24BL	.	.	.	•	•	•	•	.	.	.	.	.	•	•	.	•	•	.	.	.	.	.	.	.	.	•	•	.	.	.	.	.	•	.	.	.	•	.	.	.	•	.	.	•	.	.	•	.	.	.	.	.	•	.	.	.	.	.	.	•	.	•	•	.	.	•	•	.	.	.	.
766122	Vergol	VGLV23M	.	.	.	•	•	•	•	.	.	.	.	.	•	•	.	•	•	.	.	.	.	.	.	.	.	•	.	.	.	.	.	.	•	.	.	.	•	.	.	.	•	.	.	•	•	.	•	.	.	.	.	•	•	.	.	.	.	.	.	•	.	•	•	•	.	•	•	.	.	.	.
766123	Vergol	VGLV20BL	.	•	•	•	.	•	•	.	•	.	.	•	•	•	.	•	•	.	.	•	•	•	.	.	.	.	.	•	•	•	.	.	•	.	.	.	•	.	.	.	•	•	.	.	.	.	•	•	•	.	•	.	.	.	.	.	.	.	.	•	.	•	•	•	.	•	•	.	.	.	.
766124	Vergol	VGLV19M	.	.	.	•	•	•	•	.	.	.	.	.	•	•	.	•	•	.	.	.	.	.	.	.	.	.	.	.	.	.	.	.	•	.	.	.	.	.	.	.	•	.	.	•	.	.	•	.	.	.	.	.	•	.	.	.	.	.	.	•	.	•	•	•	.	•	•	.	.	.	.
766125	Vergol	VGLV16M	.	.	.	•	•	•	•	.	.	.	.	.	•	•	.	•	.	.	.	.	.	.	.	.	.	•	.	.	.	.	.	.	•	.	.	.	.	.	.	•	•	.	.	.	•	.	•	.	.	.	.	.	.	.	.	.	.	.	.	•	.	•	•	.	.	•	•	.	.	.	.
766126	Vergol	VGLV15BM	.	.	.	•	•	•	•	.	.	.	•	.	.	•	.	•	•	.	.	.	.	.	.	.	.	•	.	.	•	.	.	.	•	.	.	.	.	.	.	•	•	.	.	•	.	.	•	.	.	.	.	.	•	.	.	.	.	.	.	•	•	•	•	.	.	•	•	•	.	.	.
766127	Vergol	VGLV12BM	.	.	.	•	•	•	•	.	.	.	.	.	.	•	.	•	•	.	.	.	.	.	.	.	.	•	•	.	.	.	.	.	•	.	.	.	.	.	.	.	•	.	.	•	.	.	•	.	.	.	.	.	•	.	.	.	.	.	.	•	.	•	•	.	.	•	•	.	.	.	.
766128	Vergol	VGLV12BL	.	.	.	.	•	•	•	.	.	.	.	.	•	•	.	•	•	.	.	.	.	.	.	.	.	•	•	.	.	.	.	.	•	.	.	.	•	.	.	•	•	.	.	•	.	.	•	.	.	.	.	•	•	.	.	.	.	.	.	•	.	•	•	.	.	.	•	.	.	.	.
766129	Vergol	VGLV8M	.	.	.	.	•	•	•	.	.	.	.	.	.	•	.	•	•	.	.	.	.	.	.	.	.	•	.	.	.	.	.	.	•	.	.	.	•	.	.	•	•	.	.	•	.	.	•	.	.	.	.	.	•	.	.	.	.	.	.	•	.	•	•	•	.	•	•	.	.	.	.
766130	Vergol	VGLV8BL	.	.	.	•	.	•	.	.	.	.	.	.	•	•	.	•	.	.	.	.	.	.	.	.	.	.	.	.	.	.	.	.	•	.	.	.	.	.	.	.	•	.	.	.	.	.	•	.	.	.	.	.	•	.	.	.	.	.	.	•	.	•	•	.	.	•	•	.	.	.	.
766131	Vergol	VGLV6M	.	.	.	•	•	•	.	.	.	.	.	.	.	•	.	•	•	.	.	.	.	.	.	.	.	•	.	.	.	.	.	.	•	.	.	.	•	.	.	•	•	.	.	•	.	.	•	.	.	.	.	.	•	.	.	.	.	.	.	•	•	•	•	.	.	•	•	.	.	.	.
766132	Vergol	VGLV6BL	.	.	.	•	•	•	.	.	•	.	.	.	.	•	.	•	•	.	•	.	.	•	.	.	.	•	.	.	.	.	.	.	•	.	.	•	•	.	.	•	•	.	.	.	•	.	•	.	.	.	.	.	•	.	.	•	.	.	.	•	.	•	•	.	.	•	•	.	.	.	.
766133	Vergol	VGLV5M	.	.	.	•	•	•	•	.	.	.	.	.	.	•	.	•	•	.	.	.	.	.	.	.	.	•	.	.	.	.	.	.	•	.	.	.	.	.	.	•	•	.	.	•	.	.	•	.	.	.	.	.	•	.	.	.	.	.	.	•	.	•	•	•	.	•	•	.	.	.	.
766134	Vergol	VGLV5L	.	.	.	•	•	•	.	.	.	.	.	.	.	•	.	•	•	.	.	.	.	•	.	.	.	•	.	.	.	.	.	.	•	.	.	.	.	.	.	•	•	.	.	•	•	.	•	.	.	.	.	•	.	.	.	.	.	.	.	•	.	•	•	.	.	•	•	•	.	.	.
766135	Vergol	VGLV4BM	.	.	.	•	•	•	•	.	.	.	•	.	.	•	.	•	•	.	.	.	.	•	.	.	.	•	.	.	.	.	.	.	•	.	.	.	•	.	.	•	•	.	•	•	•	.	•	•	.	.	.	•	•	.	.	.	.	.	.	•	.	•	•	•	.	•	•	•	.	.	.
766136	Vergol	VGLV4BL	.	.	.	.	•	•	•	.	•	.	•	.	.	•	.	•	•	.	.	.	.	.	.	.	.	•	•	.	.	.	.	.	•	.	.	.	•	.	.	•	•	.	.	•	•	.	•	.	.	.	.	.	•	.	.	.	.	.	.	•	.	•	•	.	.	•	•	•	.	•	.
766137	Vergol	VGLV3M	.	.	.	•	•	•	•	.	.	•	•	.	.	.	.	•	•	.	.	.	.	.	.	.	.	•	.	.	.	.	.	.	•	.	.	.	•	.	.	•	•	.	•	•	•	.	•	•	.	.	.	.	•	.	.	.	•	•	•	•	.	•	•	•	.	•	•	•	.	•	.
766138	Vergol	VGLV3L	.	.	.	.	•	•	.	.	.	•	.	.	.	.	.	•	.	.	.	.	.	.	.	.	.	•	.	.	.	.	.	.	•	.	.	.	.	.	.	•	•	.	.	.	.	.	•	•	.	.	.	.	.	.	.	.	.	.	.	•	.	•	•	.	.	.	.	.	.	•	.
766139	Vergol	VGLV2CM	.	.	.	•	•	•	•	.	.	.	•	.	.	•	.	•	•	•	.	.	.	.	.	.	.	•	.	.	.	.	.	.	•	.	.	.	•	.	.	•	•	.	•	•	•	.	•	.	.	.	.	•	.	.	.	.	•	•	•	•	.	•	•	•	.	•	.	•	.	.	.
766140	Vergol	VGLV2CL	.	.	.	•	•	•	•	.	.	.	.	.	.	•	.	•	•	.	.	.	•	.	.	.	.	•	.	.	.	.	.	.	•	.	.	.	•	.	.	•	•	.	•	•	.	.	•	.	.	.	.	•	•	.	.	.	.	.	.	•	.	•	•	.	.	•	•	.	.	.	.
766141	Vergol	VGLV2BL	.	.	.	•	•	•	•	.	.	.	.	.	.	•	.	•	•	.	.	.	.	.	.	•	.	•	.	.	.	.	.	.	•	.	.	.	•	.	.	•	•	.	.	•	•	.	•	•	.	.	.	.	•	.	.	.	.	.	.	•	.	•	•	•	.	•	•	.	.	•	.
766142	Vergol	VGLV1BM	.	.	.	•	•	•	.	.	•	•	•	.	.	•	.	•	•	•	•	.	.	.	.	.	.	•	.	.	.	.	.	•	•	.	.	.	.	.	.	•	•	.	•	•	•	.	•	.	.	.	.	•	•	.	.	.	•	•	.	•	.	•	•	.	.	•	•	•	.	.	.
766143	Vergol	VGLV1B-BIS L	.	.	.	•	•	•	•	.	•	.	.	.	.	•	.	•	•	.	.	.	.	•	.	.	.	•	.	.	.	.	•	.	•	.	.	.	•	.	.	•	•	.	.	•	.	.	•	.	.	.	.	.	.	.	.	.	.	.	.	•	.	•	•	•	.	•	•	.	.	•	.
766144	Vergol	VGLV1BL	.	.	.	•	•	•	•	.	.	.	.	.	.	•	.	•	•	.	.	.	.	.	.	.	.	•	.	.	.	.	.	.	•	.	.	.	•	.	.	•	•	.	.	•	•	.	•	.	.	.	.	.	.	.	.	.	.	.	.	•	.	•	•	.	.	•	•	.	.	.	.
766145	Vergol	VGLV1a-L	.	.	.	•	.	•	•	.	.	.	.	.	.	•	.	•	•	.	.	.	.	.	.	.	.	•	.	.	.	.	•	.	•	.	.	.	•	.	.	•	•	.	.	.	.	.	•	•	.	.	.	.	.	.	.	.	.	.	.	•	.	•	•	.	.	•	•	.	.	.	.
766146	Vergol	VGB151M	.	•	.	•	•	•	•	.	.	•	.	.	.	•	.	•	•	•	.	.	•	•	.	.	•	•	.	.	.	.	.	.	•	.	.	.	.	.	.	.	•	.	•	.	•	.	•	•	.	.	.	•	•	•	.	.	.	.	.	•	.	•	•	•	.	•	•	.	.	.	.
766147	Vergol	VGB151L	.	.	.	.	.	•	.	.	.	.	.	.	.	•	.	•	.	.	.	.	.	.	.	.	.	•	.	.	.	.	.	.	•	.	.	.	.	.	.	•	•	.	.	.	.	.	.	.	.	.	.	.	.	.	.	.	.	.	.	•	.	•	.	.	.	.	.	.	.	.	.
766148	Vergol	VGB150M	.	•	.	•	•	•	•	.	.	•	.	.	•	•	.	•	•	.	.	.	.	•	.	.	•	•	.	.	.	.	.	.	•	.	.	.	.	.	.	•	•	.	•	•	•	.	•	•	.	.	.	.	.	.	.	.	.	.	.	•	•	•	•	•	.	•	•	•	.	.	.
766149	Vergol	VGB150L	.	.	.	•	•	•	.	.	.	.	.	.	.	•	.	•	•	•	•	.	.	•	.	.	.	•	.	.	.	.	.	.	•	.	.	.	.	.	.	•	•	.	.	.	•	.	•	.	.	.	.	.	•	.	.	.	.	.	.	•	.	•	•	•	.	•	•	.	.	.	.
766150	Vergol	VGB149M	.	•	.	•	•	•	•	.	.	•	•	.	•	•	.	•	•	•	.	.	•	•	.	.	•	.	.	.	.	.	.	•	•	.	.	.	.	.	.	•	•	.	.	•	•	.	•	•	.	.	.	.	•	•	.	.	•	.	.	•	.	•	•	•	.	•	•	•	.	.	.
766151	Vergol	VGB149L	.	.	.	•	•	•	.	.	.	.	.	.	.	•	.	•	.	.	.	.	.	.	.	.	.	•	.	.	.	.	.	.	•	.	.	.	.	.	.	•	•	.	.	.	.	.	•	.	.	.	.	.	.	.	.	.	.	.	.	•	•	•	•	.	.	•	.	.	.	.	.
766152	Vergol	VGB148M	.	•	•	•	•	•	•	.	.	•	.	.	.	•	.	•	•	•	.	.	.	•	.	.	•	•	.	.	.	.	.	•	•	.	.	.	.	.	.	•	•	.	•	•	•	.	•	•	.	.	.	.	.	•	.	•	.	.	.	•	.	•	•	•	.	•	•	•	.	•	.
766153	Vergol	VGB148L	.	.	.	•	•	•	.	.	.	.	.	.	.	•	.	•	•	.	.	.	.	•	.	.	.	.	.	.	.	.	.	.	•	.	.	•	.	.	.	•	•	.	.	•	•	.	•	.	.	.	•	.	.	.	.	.	.	.	.	•	.	•	•	.	.	•	.	.	.	•	.
766154	Vergol	VGB147M	.	.	.	•	•	•	•	.	.	.	.	.	.	•	.	•	•	.	.	.	.	•	.	.	.	•	.	.	.	.	.	.	•	.	.	.	•	.	.	•	•	.	•	•	•	.	•	.	.	.	.	•	•	.	.	.	.	.	.	•	.	•	•	•	.	•	•	.	.	•	.
766155	Vergol	VGB147L	.	.	.	•	.	•	•	.	.	.	.	.	.	.	.	•	.	.	.	.	.	.	.	.	•	.	.	.	.	.	.	.	•	.	.	.	.	.	.	.	•	.	.	.	•	.	•	.	.	.	.	.	.	.	.	.	.	.	.	•	.	•	•	•	.	•	.	.	.	.	.
766156	Vergol	VGB146M	.	.	.	•	•	•	•	.	•	•	•	.	.	•	.	•	•	.	.	.	.	•	.	.	.	•	.	.	.	.	.	.	•	.	•	.	.	.	.	•	•	.	•	•	•	.	•	•	.	.	.	•	•	•	.	.	•	.	.	•	•	•	•	•	.	•	•	.	.	•	.
766157	Vergol	VGB146cL	.	.	.	•	•	•	•	.	.	.	.	.	.	•	.	•	•	.	.	.	.	.	.	.	.	•	.	.	.	.	.	.	•	.	.	.	.	.	.	•	•	.	.	.	•	.	•	•	.	.	.	.	•	.	.	.	.	.	.	•	.	•	•	.	.	•	•	.	.	.	.
766158	Vergol	VGB145M	.	.	.	•	•	•	•	.	.	.	.	.	.	•	.	•	•	•	.	.	.	.	.	.	.	•	.	.	.	.	.	.	•	.	.	.	.	.	.	.	•	.	•	•	•	.	•	•	.	.	.	•	.	.	.	.	•	.	.	•	•	•	•	•	.	•	•	•	.	•	.
766159	Vergol	VGB145aL	.	.	.	•	•	•	.	.	.	.	.	.	.	•	.	•	•	.	.	.	.	.	.	.	.	•	.	.	.	.	.	.	•	.	.	.	.	.	.	•	•	.	•	•	•	.	•	•	.	.	.	.	•	.	.	.	.	.	.	•	.	•	•	.	.	•	•	•	.	.	.
766160	Vergol	VGB144M	.	.	.	•	•	•	.	.	.	.	•	.	•	•	.	•	•	.	.	.	.	.	.	.	.	•	.	.	.	.	.	.	•	.	.	.	.	.	.	•	•	.	.	•	•	.	•	•	.	.	.	.	•	.	.	.	.	.	.	•	•	•	•	.	.	•	•	.	.	•	.
766161	Vergol	VGB144aL	.	.	.	•	•	•	•	.	.	.	•	.	.	•	.	•	•	.	.	.	.	•	.	.	.	•	.	.	.	.	.	.	•	.	.	.	.	.	.	•	•	.	.	•	•	.	•	•	.	.	.	.	•	.	.	.	.	.	.	•	.	•	•	.	.	•	•	•	.	.	.
766162	Vergol	VGB143M	.	.	•	•	•	•	.	•	.	.	•	.	.	•	.	•	•	.	.	.	.	•	.	.	•	•	.	•	.	.	•	•	•	.	.	•	•	.	.	•	•	.	.	•	•	•	•	.	.	.	•	.	•	.	.	.	.	.	.	•	.	•	•	•	.	•	•	•	.	•	.
766163	Vergol	VGB143L	.	.	.	•	•	•	.	.	.	.	.	.	•	•	.	•	•	.	.	.	.	.	.	.	•	.	.	.	.	.	•	.	•	.	.	.	.	.	.	•	•	.	.	.	•	.	•	.	.	.	.	.	•	.	.	.	.	.	.	•	.	•	•	•	.	•	•	.	.	.	.
766163a	Vergol	VGB140M	.	•	.	.	•	•	.	.	.	.	•	.	.	•	.	•	.	.	.	•	.	•	.	.	•	.	.	•	.	.	•	•	•	.	.	•	•	.	.	•	•	.	.	•	•	.	.	.	.	.	•	.	.	•	.	.	.	.	•	•	.	•	•	.	.	.	.	.	.	.	.
766163	Vergol	VGB138M	.	.	.	.	•	•	.	.	.	.	.	.	.	.	.	•	•	.	.	•	.	.	.	.	•	.	.	.	.	.	•	.	•	.	.	•	•	.	.	•	•	.	.	•	•	.	•	.	.	.	.	.	.	.	.	.	.	.	.	•	.	•	•	•	.	.	.	•	•	.	.
766164	Vergol	VGB137L	.	.	.	•	•	•	•	.	.	.	•	.	.	•	.	•	•	.	.	.	.	.	.	.	•	.	.	.	.	.	.	.	•	.	.	.	.	.	.	•	•	.	.	•	•	.	•	•	.	.	.	.	.	.	.	.	.	.	.	•	.	•	•	•	.	.	.	.	.	.	.
766165	Vergol	VGB136M	.	.	•	•	•	•	•	.	.	.	.	.	.	•	.	•	•	•	.	.	.	•	.	.	.	•	.	.	.	.	.	.	•	.	.	.	.	.	.	•	•	.	•	•	•	.	•	•	.	.	•	•	.	.	.	.	.	.	.	•	•	•	•	•	.	•	•	•	.	•	.
766165a	Vergol	VGB135M	.	.	.	.	•	•	.	.	.	.	.	.	.	.	.	•	.	.	.	•	.	•	.	.	•	.	.	•	.	.	•	.	•	.	.	•	•	.	.	•	•	.	.	.	.	.	.	•	.	.	.	.	.	.	.	.	.	.	.	•	.	.	•	.	.	.	•	.	.	.	.
766165b	Vergol	VGB134M	.	.	.	.	•	•	.	.	•	.	.	.	.	.	.	•	•	.	.	•	.	.	.	.	•	.	.	•	.	.	•	.	•	.	.	•	•	.	.	•	•	.	.	.	•	.	•	•	.	.	.	.	.	.	.	•	.	.	.	•	•	.	•	•	.	.	•	.	.	.	.
766165c	Vergol	VGB132M	.	.	.	•	•	•	.	.	.	.	.	.	.	.	.	.	.	.	.	•	•	•	.	.	•	.	.	.	.	.	•	.	•	.	.	•	•	.	.	•	•	.	.	.	•	.	.	.	.	.	.	.	.	.	.	.	.	.	.	•	•	•	•	•	.	.	•	.	•	.	.
766166	Vergol	VGB132L	.	.	.	•	•	•	.	.	•	.	.	.	.	•	.	•	.	.	.	.	.	.	.	.	.	•	.	.	.	.	•	.	•	.	.	.	.	.	.	•	•	.	.	.	•	.	•	.	.	.	.	.	.	.	.	.	.	.	.	•	.	•	•	•	.	•	.	.	.	.	.
766167	Vergol	VGB131M	.	.	.	•	•	•	•	.	.	.	•	.	•	•	.	•	•	•	.	.	.	•	.	.	.	•	.	.	.	.	.	.	•	.	•	.	.	.	.	•	•	.	•	•	•	.	.	•	.	.	.	•	.	.	.	.	.	.	.	•	.	•	•	•	.	.	•	•	.	.	.
766168	Vergol	VGB126L	.	.	.	•	•	•	.	.	.	.	.	.	.	•	.	•	.	.	.	.	.	.	.	.	.	•	.	.	.	.	•	.	•	.	.	.	.	.	.	•	•	.	.	.	•	.	•	.	.	.	.	.	.	.	.	.	.	.	.	•	.	.	•	.	.	.	•	.	.	.	.
766169	Vergol	VGB125M	.	.	.	•	•	•	•	.	.	.	.	.	.	•	.	•	•	•	.	.	.	•	.	.	.	•	.	.	.	.	•	.	•	.	.	.	.	.	.	•	•	.	.	•	•	.	•	.	.	.	.	.	.	.	.	.	.	.	.	•	•	•	•	•	.	•	•	•	.	.	.
766170	Vergol	VGB117L	.	.	.	•	.	•	.	.	.	.	.	.	.	•	.	•	•	.	.	.	.	.	.	.	.	•	.	.	.	.	•	.	•	.	.	.	.	.	.	•	•	.	.	.	•	•	•	.	.	.	.	.	.	.	.	.	.	.	.	•	.	•	•	•	.	.	.	.	.	.	.
766171	Vergol	VGB116M	.	.	.	•	•	•	•	.	.	.	.	.	.	•	.	•	•	.	.	.	.	.	.	.	•	.	.	.	.	.	.	•	•	.	.	.	.	.	.	•	•	.	.	.	•	.	•	.	.	.	.	.	.	.	.	.	.	.	.	•	.	•	•	•	.	•	•	.	.	.	.
766172	Vergol	VGB114L	.	.	•	•	.	•	.	.	.	.	.	.	.	•	.	•	•	.	.	.	.	.	.	.	.	.	.	.	.	.	•	.	.	.	.	.	.	.	.	•	•	.	.	.	•	.	.	.	.	.	•	.	.	.	.	.	.	.	.	•	.	.	•	.	.	.	.	.	.	.	.
766173	Vergol	VGB113CM	.	•	.	•	•	•	.	.	.	.	.	.	.	•	.	•	•	.	.	.	•	•	.	.	.	•	.	.	.	.	•	•	•	.	.	.	.	.	.	•	•	.	•	•	•	.	•	•	•	.	.	.	.	.	.	.	.	.	.	•	•	•	•	•	.	•	•	.	.	.	.
766174	Vergol	VGB113aL	.	.	.	•	.	•	.	.	.	.	.	.	•	•	.	•	•	.	.	.	.	.	.	.	•	.	.	.	.	.	•	.	•	.	.	.	.	.	.	•	•	.	•	.	.	.	•	.	.	.	.	.	.	.	.	.	.	.	.	•	.	•	•	•	.	.	•	.	.	.	.
766175	Vergol	VGB112M	.	.	•	•	•	•	.	.	.	.	.	.	.	•	.	•	•	•	.	.	•	.	.	.	•	.	.	.	.	.	.	.	•	.	.	.	.	.	.	•	•	.	•	.	•	.	•	.	.	.	•	.	.	.	.	.	.	.	.	•	.	•	•	•	.	•	•	.	.	.	.
766176	Vergol	VGB109L	.	.	•	•	•	•	.	.	.	.	.	.	.	•	.	•	.	.	.	.	.	.	.	.	.	•	.	.	.	.	•	.	•	.	.	.	.	.	.	•	•	.	.	•	•	.	•	.	.	.	•	.	.	.	.	.	.	.	.	•	.	•	•	.	.	•	•	.	.	.	.
766177	Vergol	VGB108M	.	.	.	•	•	•	•	.	.	.	.	.	.	•	.	•	•	.	.	.	.	.	.	.	.	.	.	.	.	.	•	.	•	.	.	.	.	.	.	•	•	.	.	•	.	.	•	.	.	.	.	.	.	.	.	.	.	.	.	•	.	.	•	•	.	.	.	.	.	.	.
766178	Vergol	VGB97L	.	.	.	•	•	•	•	.	.	.	.	.	.	•	.	•	•	.	.	.	.	.	.	.	.	.	.	.	.	.	.	.	•	.	.	.	.	.	.	.	•	.	.	.	•	.	•	•	.	.	.	•	.	.	.	.	.	.	.	•	•	•	•	•	.	.	•	.	.	.	.
766179	Vergol	VGB96M	.	.	•	•	•	•	.	.	.	.	.	.	.	•	.	•	•	.	.	.	.	.	.	•	.	•	.	.	.	.	•	.	•	.	.	.	.	.	.	•	•	•	.	.	•	.	•	•	.	.	•	•	.	.	.	.	.	.	.	•	•	•	•	•	.	•	•	.	.	.	.

presence •
absence .

FSL N°	Beds	Height	PC1	PC2	PC3	Absolute abundance	Shannon index
766104	VGLV42M	52.4	-0.88876	-0.16341	-0.23431	612275892.35	1.98
766105	VGLV42L	52.1	0.40784	0.27441	-0.30588	51974566.73	2.11
766106	VGLV38M	49.9	-1.9623	-0.93438	-0.35984	378689937.51	2.00
766107	VGLV38L	49.6	-3.7149	-0.33023	-0.74866	106467776.50	1.95
766108	VGLV37M	49.2	-3.8977	-0.60758	-0.5981	815617563.21	2.04
766109	VGLV37L SO	48.7	-4.2917	-0.11727	-0.78242	188780478.11	2.01
766110	VGLV36M	48.2	-3.332	-0.62923	0.093401	571593058.64	1.99
766111	VGLV36L	47.9	-3.2505	-0.093962	-0.39868	207254082.03	1.57
766112	VGLV35CM	47.5	-2.4327	-0.50204	-0.2781	487144301.60	2.15
766113	VGL35CL	47.1	-3.0428	-0.48372	-0.37294	57163606.18	2.01
766114	VGLV35bM	47.05	-1.1546	1.1601	-0.20246	416396103.90	2.02
766115	VGLV35bL	47	-1.6756	1.0008	0.11902	436215817.51	2.00
766116	VGLV34M	46.55	-2.7876	1.3495	-0.11216	530310228.51	1.99
766117	VGLV32L	44.6	0.67638	-0.19063	-0.41348	158540290.12	2.04
766118	VGLV31M	44.2	0.4876	0.53482	-0.24213	711935180.58	2.21
766119	VGLV28CL	41.7	-0.46897	-1.4063	-1.4179	76680477.56	2.11
766120	VGLV27M	41.25	0.79659	-0.69001	-0.75384	575885115.95	2.08
766121	VGLV24BL	39.5	0.3632	-0.95008	-0.94396	100765563.72	2.09
766122	VGLV23M	38.9	0.11034	-1.769	-1.5035	347590004.67	1.99
766123	VGLV20BL	37.45	-0.23236	0.8031	-0.45179	60320420.83	1.94
766124	VGLV19M	37.1	-0.079354	-1.6751	-0.49789	781600598.35	2.09
766125	VGLV16M	35	1.0291	0.72761	-0.68006	144993894.99	1.96
766126	VGLV15BM	34.45	-0.25887	-0.66184	-0.57159	650474029.66	2.19
766127	VGLV12BM	32.3	1.0855	-0.67087	-1.2223	619421998.43	2.12
766128	VGLV12BL	32.15	0.65636	0.67806	-0.9177	110630713.29	2.08
766129	VGLV8M	30.5	1.8611	1.5415	-0.98388	505698531.67	2.15
766130	VGLV8BL	30.2	0.86981	-0.91457	-1.4268	35552632.51	1.87
766131	VGLV6M	29.4	1.6012	0.631	-0.30884	656049195.98	2.12
766132	VGLV6BL	29.2	-0.26369	0.13943	-0.29947	60053107.14	2.07
766133	VGLV5M	28.85	1.1836	-0.11725	-0.043246	323336076.48	2.05
766134	VGLV5L	28.6	-0.52721	-0.68171	-0.18006	45815608.59	2.20
766135	VGLV4BM	28.4	-0.37479	-0.42457	0.27768	552936910.80	1.98
766136	VGLV4BL	28	0.47688	1.3435	-0.86753	155865371.17	1.70
766137	VGLV3M	27.65	0.42686	-1.202	-0.059808	736651447.55	2.02
766138	VGLV3L	27.5	0.88578	1.8744	-0.9112	62070748.16	2.04
766139	VGLV2CM	27.2	-0.63838	-1.2099	0.53627	416875439.21	
766140	VGLV2CL	27	0.11484	0.5374	-0.18907	167063656.11	2.11
766141	VGLV2BL	26.6	1.3855	1.2651	-0.077402	305245496.64	2.20
766142	VGLV1BM	26.5	-0.45128	-0.14975	0.28497	345525807.22	2.02
766143	VGLV1B-BIS L	26.45	1.0823	2.6233	-0.26701	154546488.91	2.11
766144	VGLV1BL	26.3	0.4507	-0.039556	-0.28315	89477593.21	1.96
766145	VGLV1a-L	26	0.095732	2.5804	-0.5562	60584553.51	2.08
766146	VGB151M	25.7	0.49776	-1.6628	0.98515	1103129228.13	1.88
766147	VGB151L	25.6	0.97157	1.5219	-0.83419	11537019.41	2.17
766148	VGB150M	25.1	1.2805	-1.6141	0.19345	355073938.41	2.00
766149	VGB150L	24.95	0.17283	-0.88622	0.086065	66899076.48	2.23
766150	VGB149M	24.55	0.83432	-1.6877	0.93609	571092634.58	2.14
766151	VGB149L	24.5	0.73259	0.25308	-0.33069	32435173.24	2.26
766152	VGB148M	24.4	0.71151	1.6388	0.51409	356403388.80	2.31
766153	VGB148L	24.3	1.7033	0.20623	-0.39497	24368552.47	2.15
766154	VGB147M	23.9	-0.099431	-0.13578	1.0376	260261008.17	1.97
766155	VGB147L	23.75	-0.4087	-0.43332	2.3806	26019296.61	2.10
766156	VGB146M	23.55	-1.2814	-0.44396	1.6143	548774362.07	2.01
766157	VGB146cL	23.45	2.2359	0.1505	0.36316	39870752.13	1.99
766158	VGB145M	23	2.477	-1.4766	-0.66355	665062702.62	2.11
766159	VGB145aL	22.65	-0.10042	-0.35232	0.53419	169200628.23	2.08
766160	VGB144M	22.6	0.87602	0.82649	-0.30087	223771326.71	2.00
766161	VGB144aL	22.45	0.38199	0.56869	0.33933	95977916.73	2.21
766162	VGB143Mb	22.4	-0.46837	-0.099021	1.2423	58857142.86	2.01
766162	VGB143M	22.4	0.71901	-0.62499	0.073419	260448754.28	2.18
766163	VGB143L	22.3	2.6414	-0.51588	-0.80128	70944936.77	2.01
766163a	VGB140M	21.2	-2.1028	1.3326	-0.059431	20824701.97	1.99
766163	VGB138M	20.5	-1.3357	0.23537	0.46249	171280575.54	2.01
766164	VGB137L	19.8	1.0582	0.063054	1.2862	47182230.52	1.95
766165	VGB136M	19.6	0.45256	-1.2942	2.1816	560819565.92	2.06
766165a	VGB135M	19.2	-2.1645	3.2834	1.1873	81856253.54	1.97
766165b	VGB134M	18.6	-2.5421	1.8457	0.50541	242016806.72	1.92
766165c	VGB132M	17.8	0.26031	1.9184	0.96108	64487133.02	1.98
766166	VGB132L	17.6	0.054453	-0.9556	0.71205	82415778.81	2.07
766167	VGB131M	17.4	-2.0494	-1.6728	0.52919	27304421.77	1.51
766168	VGB126L	15.3	2.1523	1.0326	1.1508	108320155.79	1.70
766169	VGB125M	15	1.1311	0.77353	0.15909	400252945.38	1.59
766170	VGB117L	12.1	1.6825	-0.19546	-0.46698	122601015.46	1.68
766171	VGB116M	12	1.8943	-0.55412	0.719	328325264.92	1.77
766172	VGB114L	10.5	1.0863	-2.1682	-0.89335	22719841.10	1.52
766173	VGB113CM	10.2	2.3311	0.19391	0.43687	462919221.19	1.58
766174	VGB113aL	9.25	1.2438	-0.027582	0.29168	125105351.88	1.31
766175	VGB112M	9.2	1.7901	-0.51305	1.5305	132603717.16	1.42
766176	VGB109L	6.9	1.1883	-0.63981	0.44175	66189175.63	1.42
766177	VGB108M	6.55	1.3749	0.45694	0.058989	96879653.39	2.00
766178	VGB97L	1.1	-1.2501	-1.7121	0.59468	69385118.39	2.21
766179	VGB96M	0.6	-0.45411	0.91482	0.38912	164951133.29	2.22